Gestion des messages de sécurité dans les réseaux VANET.

Younes Bouchaala

université PARIS-SACLAY

NNT : 2017SACLV101

Thèse de doctorat

UNIVERSITÉ DE VERSAILLES ST-QUENTIN-EN-YVELINES

université PARIS-SACLAY

Handling Safety Messages in Vehicular Ad-Hoc Networks (VANETs)

Thèse de doctorat de l'Université Paris-Saclay
préparée à l'UVSQ

École doctorale n°580 Sciences et Technologies de L'information et de la Communication (STIC)
Spécialité de doctorat : Réseaux, Information et Communications

Thèse présentée et soutenue à Paris, le 21 décembre 2017, par

Younes BOUCHAALA

Composition du Jury :

M. Guy FAYOLLE DR, Inria Rocquencourt (– Unité de recherche)	Président
Mme. Selma BOUMERDASSI MDC, CNAM (– Unité de recherche)	Rapporteur
M. Sidi-Mohammed SENOUCI Professeur, uB (– Unité de recherche)	Rapporteur
M. Marcelo DIAS DE AMORIM DR, CNRS (– Unité de recherche)	Examinateur
Mme. Samia BOUZEFRANE MDC, CNAM (– Unité de recherche)	Examinatrice
M. Samir TOHME Professeur, UVSQ (– Unité de recherche)	Examinateur
M. Paul MUHLETHALER DR, Inria Paris (– Unité de recherche)	Directeur de thèse
Mme. Oyunchimeg SHAGDAR Encadrante, Institut VEDECOM (– Unité de recherche)	Co-Directrice de thèse
M. Nadjib Achir MDR, Paris 13 (– Unité de recherche)	Invité

université PARIS-SACLAY
ÉCOLE DOCTORALE
Sciences et technologies de l'information et de la communication (STIC)

Titre : Gestion des messages de sécurité dans les réseaux VANET.

Mots clés : VANET, MAC, CSMA, CAM, DENM.

Résumé : Les exigences de Qualité de Service (QoS) des applications VANET varient selon la nature et le type de l'application. Par conséquent, un protocole de communication VANET doit pouvoir répondre aux diverses exigences de QoS selon le type du trafic. Dans VANET, le canal de transmission est partagé par tous les véhicules en utilisant une même fréquence radio. Une mauvaise exploitation du canal peut donc conduire à des collisions et peut aussi engendrer un gaspillage de la bande passante. Un protocole MAC doit être alors conçu pour partager le canal entre les différents nœuds d'une manière efficace et équitable.

Dans cette thèse nous présentons les contributions suivantes :

1- Analyse et amélioration de la diffusion dans la norme IEEE 802.11.
2- Optimisation de la technique CSMA pour des réseaux 1D et 2D.
3- Développement d'un algorithme CSMA de transmission adaptatif qui met à jour le taux de détection de la porteuse en fonction d'une valeur de référence.
4- Étude du gain obtenu par l'utilisation d'antennes directionnelles pour Aloha, Aloha non-slotté, et CSMA.

Title : Handling Safety Messages in Vehicular Ad-Hoc Networks (VANETs)

Keywords : VANET, MAC, CSMA, CAM, DENM.

Abstract : Quality of Service (QoS) requirements for VANET applications vary depending on the nature and type of the application. Therefore, a communication protocol in VANETs must be able to meet various QoS requirements according to the type of traffic. In VANET, the transmission channel is shared by all the vehicles using the same radio frequency. A poor exploitation of the channel can therefore lead to collisions and wasted bandwidth. A MAC protocol must therefore be designed to share the channel between the different nodes in an efficient and fair way.

In this thesis we present the following contributions:

1- Analysis and improvement of diffusion in the IEEE 802.11 standard.
2- Optimization of the CSMA technique for 1D and 2D networks.
3- Design of an adaptive transmission algorithm that updates the Carrier Sense threshold to reach a target value.
4- Study the gain obtained by the use of directional antennas for Aloha, non-slotted Aloha, and CSMA.

Université Paris-Saclay
Espace Technologique / Immeuble Discovery
Route de l'Orme aux Merisiers RD 128 / 91190 Saint-Aubin, France

Acknowledgments

First of all, I would like to thank Mrs Selma Boumerdassi and Mr Sidi Mohammed Senouci for kindly accepting to review my thesis. Also, my thanks go to the members of the jury for the interest they showed in my research: Mr Guy Fayolle, Mr Marcelo Dias De Amorim, Mrs Samia Bouzefrane, and Mr Samir Tohme.

I would never have been able to finish my dissertation without the guidance, help, and support of colleagues, friends and family. I thank all these people who made this thesis possible and an unforgettable experience for me.

I would like to express my deepest sense of gratitude to my advisors, Mr Paul Muhlethaler, Mrs Oyunchimeg Shagdar, and Mr Nadjib Achir, for their continuous support and their immense encouragement. Their guidance helped me throughout the research and writing of this thesis.

I have been honored to work with the members of Inria-Eva Team and VEDECOM-MOB01 Team. Thank you for the pleasant working atmosphere you created.

I want to address my kind regards to the many freinds that I have made at Inria as well as VEDECOM, for their wonderful company and sincere friendship: thank you Nesrine, Ines, Mohamed, Marios, Mattia, Amrou, and Ahmed. I am grateful to all of you, for your support as well as the fun times I have shared with you.

I am indebted to Richard James, our English teacher at Inria, for the considerable time and effort he spent correcting my papers and this dissertation.

Finally, I must take this opportunity to express my heartfelt gratitude to my parents. Words cannot express how grateful I am for your support, encouragement, and kind wishes. Their love and their prayers have sustained me over the years.

Abstract

Road crashes and the damage they entail represent a serious issue and are one of the main causes of death. Some statistics have shown that the majority of road accidents are due to human error and that 60% of these accidents could have been avoided if the driver had been warned at least 0.5 sec beforehand. In this context, Vehicular Ad hoc NETworks, known as VANETs, are deployed to reduce the risk of road accidents as well as to improve passenger comfort by allowing vehicles to exchange different kinds of data between the vehicles themselves and potentially between the vehicles and the roadside infrastructure. The data exchanged between vehicles ranges widely from road safety messages and traffic management to infotainment. Nowadays, safety applications are receiving a great deal of attention from researchers as well as from automobile manufacturers. In this thesis, we particularly focus on safety-critical applications, designed to provide driver assistance in dangerous situations and to avoid accidents in highway environments.

Safety-critical applications in VANETs use two different kinds of messages: Co-operative Awareness Message (CAMs) and Decentralized Environmental Notification Messages (DENMs). CAMs are periodically broadcast by vehicles to indicate their speed and position. These messages are generally not forwarded. DENMs are sent when a hazardous event occurs. These messages are often forwarded to warn vehicles over a wider area. CAMs and DENMs must be delivered with strict requirements regarding end-to-end delay and packet loss ratio. One of the main difficulties with VANETs is the great mobility of the nodes and the huge variability in the density of vehicles. On the one hand, recent studies tend to prove that the existing IEEE 802.11p standard can not cope with the varying density of vehicles. On the other hand, alternatives to the CSMA scheme of IEEE 802.11p, such as TDMA protocols, are difficult to achieve in VANETs because they require a central coordination which is difficult in dynamic networks. Thus the approach adopted in this thesis is to adapt and enhance existing techniques in the IEEE 802.11p protocol and in the management of safety messages.

We first introduce Vehicular Ad-hoc NETworks (VANETs) in the second chapter of this thesis. After a short introduction to these networks, we propose a definition and describe their architecture. We discuss VANETs' general characteristics and their applications. VANETs represent a complex technology combining a large variety of

techniques. Numerous projects have been devoted to VANETs to help the design and the development of this technology. We present the most important ones. Standardization is also a key issue in VANETs. We present the status of existing standards devoted to VANETs in Japan, Europe and the United States.

In the third chapter of this thesis, we describe the exact problem that we will tackle and we review the state of the art concerning congestion control which is at the heart of the studies presented in this thesis. We present the different tracks that are possible to control the load in highly dynamic networks such as VANETs. We discuss the results already obtained in this field in the academic and standardization world.

In the fourth chapter we focus on the analysis of the performance of IEEE 802.11p broadcast. In networks, broadcast transmissions are not usually acknowledged and thus the reliability of these transmissions is questionable. This is even more so in IEEE 802.11p where the communication is wireless. In this chapter, we retain a basic model where there is no spatial reuse and we only compute the percentage of successful transmissions for one node. We present various ways to improve broadcast in VANETs: acknowledgment by a random neighbor, blind retransmissions, and we propose the corresponding analytical models. We obtain several results concerning the delivery ratio of the IEEE 802.11p broadcast transmissions and we recommend optimal strategies. We also study the effect of the QoS extension of IEEE 802.11p and propose an analytical model for this QoS scheme. We analyze the effect of the parameters of this scheme on the network performance. As soon as two or more nodes transmit simultaneously there is a collision and the packet is lost. The results show that performance strongly depends on the carrier sense threshold and this leads to furthering our studies with a model which allows spatial reuse.

In the fifth chapter,we build a model of spatial CSMA which is well suited to modeling large networks such as VANETs where the extension of the network can be large and thus where simultaneous transmissions are mandatory. In these networks, spatial reuse is an absolute necessity. Moreover, we consider safety applications and thus the transmissions are usually in broadcast mode and mostly useful for the neighboring nodes. The model we use in this chapter considers random nodes (i.e., Poisson Point Processes PPP) and transmissions from one node to a neighbor which is at the average distance between a node and its nearest neighbor. We study the density of successful transmissions i.e., the number of successful transmissions per unit of space. We propose a simple model of spatial CSMA based on a selection process called the Matern process. We show that we can simply derive the density of successful transmissions with this model. We observe that this density greatly depends on the carrier sense detection threshold which is the main tunable parameter of spatial CSMA. We compute the density of successful transmissions in the network and optimize it with respect to the carrier sense detection threshold. We observe that the optimal carrier sense detection threshold depends not only on all the physical characteristics of the network itself but also to a large extent on node density. We then compare spatial CSMA and Aloha (slotted and non-slotted) with our models. We also study the optimization of Aloha to ensure a maximum density of successful transmissions. We

show that spatial CSMA, when the protocol is optimized, outperforms both slotted and non-slotted Aloha, but this result does not remain true if CSMA is not optimized with respect to node density. Moreover Aloha has the very peculiar property that its optimization only depends on physical parameters (capture threshold, power decay) and not on node density. In other words, Aloha (slotted and non-slotted) perfectly scales with node density, in contrast to CSMA. We compare our analytical model with simulation results. The analytical models of Aloha perfectly match the simulation results. The analytical model of spatial CSMA allows a good understanding of the main behavior of the protocol but since CSMA is much more complex to analyze, we find the approximations that the model had to use in the simulation results.

The sixth chapter is devoted to dynamically adapting spatial CSMA. We first study this problem using the model we developed in Chapter 5. The crux of our scheme relies on the following observation: in spatial CSMA when the system is optimized with a carrier threshold adapted to the density of nodes, the average probability of transmission is constant. In other words, a node's opportunity to transmit must remain constant when we vary node density. One consequence is that the average access delay must remain constant. Thus we propose an algorithm which adapts the carrier sense detection threshold to the density of nodes. A first scheme operates in a similar way to TCP: the carrier detection threshold is doubled when the average delay is too large and it is divided by 1.1 when the average delay is too small. With our analytical model, we show that this stabilization must insure a fast convergence to an operating point of the network that is close to optimal performance. We also show that if we can trust the computation of the average delay and if we suppose that we know the exact values of the network parameters we can in principle accelerate the convergence towards the optimized density of successful transmissions. We show that if the network parameters (fading, decay factor, capture threshold) are not accurately estimated, our scheme continues to achieve an operation point close to the optimal. We finally perform real experiments using ITS communication modules to test the proposed algorithm under real conditions. We show that the algorithm shows good adaptive capacity to the variation of the channel load, and outperforms the non-controlled system.

The seventh chapter is devoted to the evaluation of the gain that can be obtained using directional antennas. In highways the danger comes from downstream vehicles and thus safety messages must only be sent to downstream vehicles. Such a modification of the Vehicular Adhoc NETwork (VANET) can easily be obtained if the vehicles use directional antennas. This modification of the medium access protocol leads to a significant improvement of the performance since the overall interference is reduced. Using the model we have previously derived, we conduct a quantitative study of the improvement when we change the directional antennas with unidirectional antennas on the vehicles. We conduct these evaluation for Aloha (both slotted and non-slotted) and CSMA.

Chapter eight summarizes the results obtained and proposes new developments and perspectives related to the studies presented in this thesis.

Key words: Vehicular Adhoc NETworks (VANETs), MAC, CSMA, highway environments, CAMs (Cooperative Awareness Message) and DENMs (Decentralized Environmental Notification Messages), delivery ratio, density of successful transmissions.

Thesis Publications

Journal Papers

- **Younes Bouchaala**, Paul Muhlethaler, Oyunchimeg Shagdard, *Analysis of broadcast strategies and network parameters in IEEE 802.11p VANETs using simple analytical models*, IJERT 2016

Conference Papers

- **Younes Bouchaala**, Paul Muhlethaler, Oyunchimeg Shagdard, *Analysis of broadcast strategies and network parameters in IEEE 802.11p VANETs using simple analytical models*, The 4th International Conference on Performance Evaluation and Modeling in Wired and Wireless Networks (PEMWN), Nov 2015, Hammamet, Tunisia.
- Nadjib Achir, **Younes Bouchaala**, Paul Muhlethaler, and Oyunchimeg Shagdar, *Comparison of Spatial Aloha and CSMA using Simple Stochastic Geometry Models for 1D and 2D Networks*, ICT 2016 16-19th May Thessaloniki Greece.
- Nadjib Achir, **Younes Bouchaala**, Paul Muhlethaler, and Oyunchimeg Shagdar, *Optimisation of spatial CSMA using a simple stochastic geometry model for 1D and 2D networks*, IWCMC 2016 September 5-9th, 2016, Paphos, Cyprus
- Paul Muhlethaler, **Younes Bouchaala**, Oyunchimeg Shagdar and Nadjib Achir *A simple Stochastic Geometry Model to test a simple adaptive CSMA Protocol: Application for VANETs*, PEMWN 2016. Nov 22-24 2016, Paris.
- **Younes Bouchaala**, Paul Muhlethaler, Oyunchimeg Shagdar and Nadjib Achir *Optimized Spatial CSMA for VANETs: A Comparative Study using a Simple Stochastic Model and Simulation Results*, 14th Annual IEEE Consumer Communications and Networking Conference (CCNC 2017). 8-11 january 2017. Las Vegas.
- **Younes Bouchaala**, Paul Muhlethaler and Nadjib Achir , *Analysis of the IEEE 802.11 EDCF scheme for broadcast traffic: Application for VANETs*, Wireless Days 2017 29-31 March, Porto, Portugal

- **Younes Bouchaala**, Paul Muhlethaler, Oyunchimeg Shagdar, Nadjib Achir *'Evaluating the Gain of Directional Antennas inLinear VANETs using Stochastic Geometry* PEMWN 2017 28-30 November, Paris , France

Submitted Conference Papers

- **Younes Bouchaala**, Oyunchimeg Shagdar, Paul Muhlethaler and Nadjib Achir, *A Simple Adaptive Physical Carrier Sense Protocol for Congestion Control in VANETs*, 16th Annual IEEE Wireless Communications and Networking Conference (WCNC 2018). 18-15 April. Barcelona Spain.

Contents

List of Figures

List of Tables

Chapter 1

General Introduction

1.1 Background and motivation

The continuing increase in road traffic accidents worldwide has motivated the development of Intelligent Transportation Systems (ITS) and other applications to improve road safety and driving comfort. A communication network, called a Vehicular Adhoc NETwork (VANET), in which the vehicles are equipped with wireless devices, has been developed to make these applications feasible. Recently, VANETs have attracted a lot of attention in the research community and in automobile industries due to their promising applications. Nevertheless, VANETs have their own specificities: high node mobility with constrained movements and the mobile nodes have ample energy and computing power (i.e., storage and processing) [8]. In a VANET, communications can either be Vehicle-to-Vehicle (V2V) or Vehicle-to-Infrastructure (V2I) [1]. Based on these two types of communications, VANET applications can be divided into the following categories: safety services, traffic management and user-oriented services [2, 3]. Safety services have special requirements in terms of quality of service. In fact, bounded transmission delays as well as low access delays are mandatory in order to offer the highest possible level of safety. At the same time, user-oriented services need a broad bandwidth. Medium Access Control will play an important role in satisfying these requirements. In VANETs, nodes share a common wireless channel by using the same radio frequencies and therefore an inappropriate use of the channel may lead to collisions and a waste of bandwidth. Hence, sharing the channel is the key issue when we seek to provide a high quality of service. Medium Access Control (MAC) schemes must be designed to share the medium between the different nodes both efficiently and fairly. However, due to the special characteristics

of VANETs, traditional wireless MAC protocols are not suitable, which leads either to adapting these traditional MAC protocols or to designing new mechanisms.

Generally, MAC protocols fall into one of two broad categories: contention-based and contention-free. On the one hand, contention-free MAC protocols try to avoid collisions by assigning access to the channel to only one node in a neighborhood at any given time, but it is difficult to design such protocols since vehicles form a very dynamic network. In VANETs, contention-free protocols have not received support from industry. Most of the work in this field, comes from the academic world. On the other hand, contention-based protocols do not require any predefined schedule, each node will compete for channel access when it needs to transmit, without any guarantee of success. In contention-based protocols, each node can try to access the channel when it has data to transmit, usually using the carrier sensing mechanism [4]. Several neighboring nodes can sense a free channel, and so decide to access and transmit their data at the same time, which generates collisions at the destination nodes.

Safety services consist in the transmission of Cooperative Awareness Messages (CAMs) and Decentralized Environmental Notification Messages (DENMs) in Europe and Basic Safety Messages (BSMs) in the US. These messages are sent periodically by the vehicles and contain their speed and position (CAMs and BSMs); they are broadcast messages and generally only sent at one-hop except for DENMs which are forwarded.

Thus in VANETs, MAC protocols must offer an efficient and reliable broadcast. Moreover, they must also handle frequent topology changes, different spatial densities of nodes and the hidden/exposed node problem. The IEEE 802.11p [19], which is the emerging standard deployed to enable vehicular communication, is a Contention-based MAC protocol, using a priority-based access scheme that employs both Enhanced Distributed Channel Access (EDCA) and Carrier Sense Multiple Access with Collision Avoidance (CSMA/CA) mechanisms [21].

In this thesis we will present an in-depth study of the performance of IEEE 802.11p [19] for broadcast services. We will propose simple modifications to improve the performance of this protocol for safety applications. We study how the QoS extension of the protocol can be used for safety messages. We also investigate how IEEE 802.11p can operate with networks where the density of nodes varies greatly.

1.2 Main contributions

The main contributions of this thesis are summarized below:

1. **Contribution 1: Congestion control in VANETs for safety messages**
   In this part we survey different strategies to cope with congestion in VANETs. The following techniques are described: changing the rate of safety messages when the density of vehicles increases, sending safety messages only under given conditions. We can also adapt the transmission power of the message to the density of vehicles or even tinker with the detection threshold of IEEE 802.11p. This survey considers the important input of ETSI related to this subject.

2. **Contribution 2: Studying and improving the IEEE 802.11p broadcast scheme**
   We study the IEEE 802.11p broadcast scheme in a perfect model where all the nodes are within carrier sense range and where collisions only occur when two transmissions start simultaneously. In this model there is no spatial reuse and no hidden collisions. We build an analytical and Markovian model to study the success rate and the collision rate. We propose simple improvements to the standard technique: the first consists in requesting an acknowledgment from a random neighbor, the second, which is simpler, only consists in blind retransmissions of packets. Such schemes can be analyzed and compared without difficulty.

   In this part we also build a simple analytical model to predict the effect of the EDCF (Extended Decentralized Coordination Function) scheme which is the QoS function of IEEE 802.11. This Markov model allows one to predict the effect of the different Inter Frame Spacings IFSs and the value of the back-off windows.

3. **Contribution 3: Studying and analyzing the performance of spatial CSMA. Application to VANETs and IEEE 802.11p**
   In this part of the thesis we adopt a spatial model of CSMA (and thus of spatial IEEE 802.11p). As seen in the previous contribution, the range of the carrier sense must be limited if we wish to obtain acceptable performance results. In this case, nodes located at a 'reasonable' distance from each other can transmit simultaneously , this is called spatial reuse. At the same time neighboring nodes can successfully receive the transmission from their closest

neighbor, this is the capture effect. This model of neighbor communication is particularly suitable for VANETs and more particularly for safety messages. We propose a simple model for spatial CSMA which makes it possible to compute the probability of node transmissions and the probability of a packet being captured by a node at a distance from the transmitter that is at the average distance to the closest neighbor. This model shows that the carrier detection threshold is a key parameter which allows the performance of the network to be optimized in terms of density of successful transmissions i.e., the mean number of successful transmissions per unit of space. We show that, in our model of local transmissions, the carrier detection threshold must be carefully tuned with respect to the density of nodes in the network and that failing to perform such an adaptation leads to poor network performance.

In the same model of local communication, we compare the performance of spatial CSMA to the performance of slotted and non-slotted Aloha. We show that, when optimized, spatial CSMA outperforms Aloha (both slotted and non-slotted). However this result is not true if spatial CSMA is not tuned according to the density of nodes. Additionally, a very peculiar property of Aloha is that its optimization only takes into account the parameters of the decay function of the signal in the network and does not depend on the density of nodes.

We have also compared the results of our local communication model for CSMA and Aloha with simulations and we have shown a good matching between the analytical and the simulation results .

4. **Contribution 4: Building a dynamic spatial CSMA. Applications to VANETs**

   We use the spatial CSMA model to analyze dynamic CSMA schemes which adapt the carrier detection threshold to the density of nodes. We still aim at obtaining the greatest density of successful transmissions with our model of local communication i.e., transmission to a node at a distance which is the average distance to the node's closest neighbor. We observe that when the system is optimized to obtain the greatest density of successful transmissions, the average probability of transmission in the spatial CSMA network is constant. This constant depends on the network model: decay factor and capture threshold but not on the density of network nodes. Thus when the system is optimized, the transmission opportunity of spatial CSMA must be constant. Consequently

the average waiting time to send a packet must be constant when we vary the density of the nodes in our random network. It is possible to build a stabilization algorithm which updates the carrier sense detection threshold based on the average access delay. We first propose a scheme that operates in a similar way to TCP: the carrier detection threshold is doubled when the average delay is too large and it is divided by 1.1 when the average delay is too small. With our analytical model we show that this stabilization must insure a fast convergence to an operating point of the network that close to the optimal performance. We also show that if we can precisely determine the average delay, and if we suppose that we know the exact values of the network parameters, we can in principle accelerate the convergence towards the optimized density of successful transmissions. We demonstrate that if the network parameters (fading, decay factor, capture threshold) are not accurately estimated our scheme continues to achieve an operation point close to the optimal. Finally an experimental validation has been set up to test the proposed algorithm under real conditions.

5. **Contribution 5: Using directional antennas**

   On highways the danger comes from the downstream vehicles thus safety message can be sent only downstream. In contribution 5, we use the models we have previously developed to quantify the gain we obtain with the vehicles use directional antennas to transmit safety messages. We show that we can very significantly reduced the interference and thus enhance the percentage of successful reception of safety message.

1.3 Manuscript organization

The present chapter has introduced the context and the motivation of our thesis and has described our contributions. The rest of this manuscript is organized as follows.

1. **Part I: State of the art**
   This part consists of two chapters : Chapters 2 and 3. Chapter 2 is an overview of VANETs and Chapter 3 deals with congestion control for safety messages.

   In Chapter 2, we provide an overview of the special features of VANETs. We then give an insight into inter-vehicle communication standardization and projects that are being developed in the field.

In Chapter 3, we discuss the state of the art in congestion control. We describe the following techniques: changing the rate of safety messages when the density of vehicles increases, sending safety messages only under given conditions. We can also adapt the transmission power of the message to the density of vehicles or even tinker with the detection threshold of IEEE 802.11p. This survey will consider the important input of ETSI related to this subject.

2. **Part II: Analysis and improvement of the IEEE 802.11p broadcast scheme**

   In Chapter 4 of the thesis, we analyze the performance of IEEE 802.11p in terms of successful transmissions and collision rate. We adopt a model in which all the nodes are within radio range of each other. Our Markovian model allows us to compute the stationary probability of the system i.e. the probability of being at a given level of the back-off procedure of IEEE 802.11p. Thus we can obtain the average value of the transmission rate for a given node. We can derive the success and collision rates of a given transmission and then the actual success rate of a safety message which encompasses the probability of this message being successfully transmitted and received. We propose amendments to the IEEE 802.11p scheme in order to improve it. The first improvement consists in requesting an acknowledgment from a random neighbor. The second improvement consists in blindly sending the broadcast messages more than once.

   This corresponds to Contribution 2.

3. **Part III: Spatial CSMA in our local communication model. Applications to VANETs**

   This part is divided into two chapters: Chapter 5 and Chapter 6. In the previous chapter we study the performance of our CSMA networks in a model where all the nodes are in the same radio range and where a collision only occurs when two nodes transmit simultaneously. While this model allows one to capture the effect of important parameters such as the back-off of IEEE 802.11p and possible retransmission strategies, it must be completed by taking the spatial effect into account. Networks such as VANETs are large networks where nodes must necessarily be, under certain conditions, allowed to transmit simultaneously. Moreover the overall performance of the network is not reflected by the performance only of a given node but the spatial density of transmissions must be taken into account as the main metric. It is self-evident that in VANETs safety

applications and therefore safety packets are of prime importance for neighboring vehicles. Thus, in Chapter 5, we consider our network to be modeled by a random collection of nodes (also called a Poisson Point Process) and we study transmissions between typical nodes. To ease the computation we mostly consider transmission from a node to a neighbor randomly located at an average distance between a node and its closest neighbor in the Poisson Point Process. The sender node may be any node in the network and we aim at optimizing the spatial density of successful transmissions. To obtain a simple model of spatial CSMA we use a simple selection process in the Poisson Point Process called the Matern selection process. We obtain closed formulas for the transmission probability and the probability of success. In our model we show that tuning the carrier sense detection threshold allows us to optimize the spatial density of successful transmissions and this by several factors of magnitude. In Chapter 5 we extensively study this optimization with respect to all the parameters of the model. We observe that the optimal carrier sense detection threshold depends on the network parameters such as the fading, the power decay, the capture threshold but it also greatly depends on the density of nodes in our random Poisson network.

We study the performance of spatial Aloha (slotted and non-slotted) in our local communication model, then we calculate the optimization for the density of successful transmissions. We observe that, when optimized, spatial CSMA significantly out-performs both slotted and non-slotted Aloha. However, this does not remain true if CSMA is not tuned with the node density while a very particular property of Aloha is that its optimization in our model does not depend on node density. In other words spatial Aloha scales with node density whereas CSMA does not.

In Chapter 6, we describe how we improve spatial CSMA and make it automatically scale with node density. We start by using the model built for spatial Aloha in Chapter 5, still considering transmissions at the average distance of the nearest neighbor and we aim to achieve the highest possible density of successful transmissions. We observe that when spatial CSMA is optimized with the carrier-sense detection threshold as a function of node density, the probability of a node transmitting does not depend on the density of nodes in the network. In other words, when the network achieves its highest transmission throughput, the transmission opportunity of nodes does not depend on node density.

Thus, at the optimum state, the access delay of a node should remain constant with node density. This observation allows us one to build a stabilization algorithm which considers the actual access delay and updates the carrier sense detection threshold accordingly. We first use a "TCP-like" technique where the detection threshold is doubled when the access delay is larger than the targeted delay and is divided by 1.1 in the opposite case. We show that if we can accurately determine the actual access delay, we can accelerate the convergence time. Moreover, we show that if this is not the case, and even if the network parameters are not very well estimated, the scheme still proposes a convergence towards an 'acceptable' state with a density of successful transmissions that is not far from the optimum. We propose a second version of the algorithm that uses the channel busy ratio (CBR) as input parameter. We show that the CBR-based algorithm overcomes the *delay*-based algorithm. We finally implement the CBR-based algorithm in ITS communication modules and test it on road in real conditions.

Part III corresponds to Contributions 3 and 4 of the thesis.

4. **Part IV: Using directional antennas**
   On highways the danger comes from the downstream vehicles thus safety message can be sent only downstream. If we use directional antennas to sent message then we can very significantly reduce the interference and thus enhance the percentage of successful reception of safety messages. In chapter 7 we use the models we have developed in the previous part to quantify the gain we obtain with these directional antennas. We show that this gain is very significant ranging from 50% to 100% depending on the propagation and capture conditions.

   Part IV corresponds to Contribution 5 of the thesis.

In Chapter 8, we conclude this thesis by summarizing our main contributions and key results and then present our future work and open research issues regarding safety applications in VANETs.

Part I

State of the Art

Chapter 2

Vehicular Adhoc NETworks: Achitecture, Features and Standardization Activities

Contents

2.1 Introduction

Vehicular Ad-hoc Networks (VANETs) allow communication between vehicles using ad-hoc wireless devices. VANETs were initially designed to increase road safety by allowing the drivers to be more aware of the surrounding vehicles. Nowadays, however, these networks have become an emerging technology due to the variety of their applications in Intelligent Transportation Systems (ITS).

In this chapter we explain more clearly the context of this thesis by giving an overview of VANETs, their architectures and general characteristics. Then, we classify VANET applications according to their requirements and functions. After that, we give an insight into inter-vehicle communication standardization and projects that are currently under development in the field. Finally, we give a brief summary of different standardization activities, together with their shortcomings at the MAC layer level.

2.2 Vehicular networks

2.2.1 Definition and architectures

Vehicular Ad-hoc Networks (VANETs) are a special case of Mobile Ad-hoc Networks (MANETs). In VANETs, vehicles are equipped with wireless communication devices, usually called On Board Units (OBUs), so they can communicate with each other directly without a centralized control. This communication scenario is known as vehicle-to-vehicle (V2V) communication. V2V aims to help drivers to become more aware of the presence of other cars around them. Another possible scenario of communication is vehicle-to-infrastructure (V2I). This allows data to be exchanged between vehicles and Road Side Units (RSUs), connected to specialized road management establishments, in order to provide Traffic Efficiency services to road users. Finally, a more recent communication scenario called vehicle-to-anything (V2X), has become a part of VANETs. This aims to extend communication so that it involves all kinds of road users, such as between a vehicle and a pedestrian. Other communication scenarios, such as Infrastructure-to-Infrastructure (I2I), or pedestrian-to-Infrastructure (X2I), are also possible. Moreover, a vehicle can have direct access to the Internet through Hotspot devices installed along the road. Each vehicle is equipped, in addition to the OBU, with an Application Unit (AU). The OBU is used to exchange information with other OBUs (and/or with RSUs) within a same ad-hoc domain, whereas the AU executes ITS applications that use the communication capabilities of the OBU. Figure 2.1 shows an overview of possible VANET communication scenarios.

2.2.2 General characteristics

VANETs differ from MANETs in certain characteristics that make them unique and not systematically compatible with existing MANET solutions, such as MAC pro-

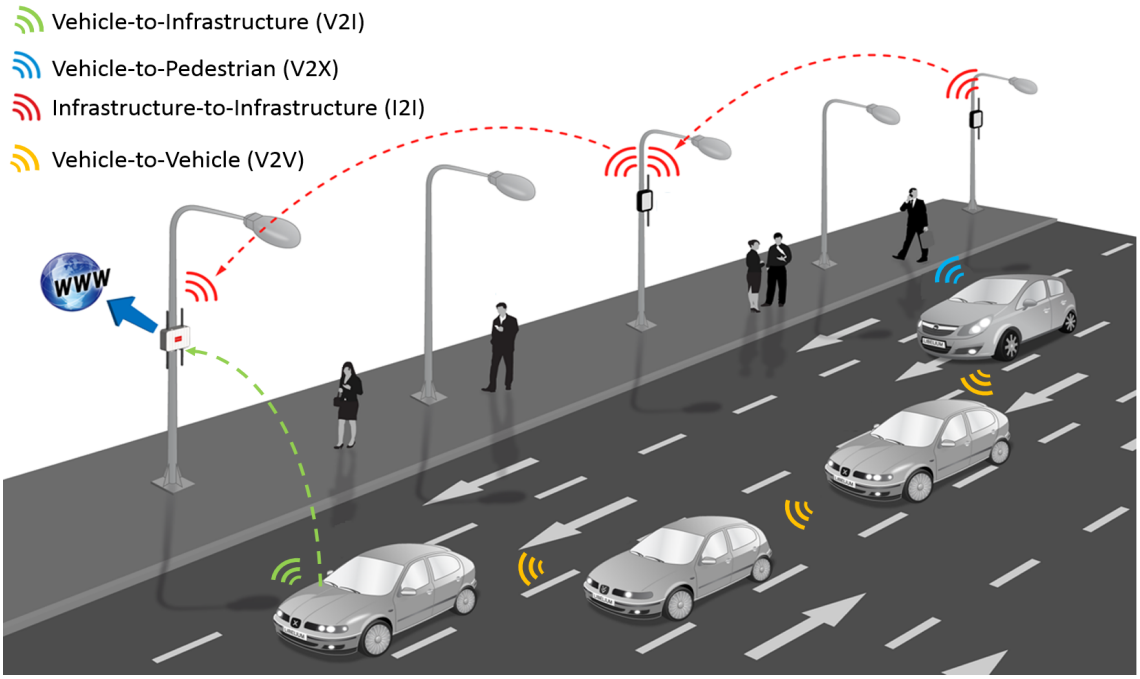

Figure 2.1: An overview of a VANET network

tocols, routing strategies, congestion control algorithms, etc. In the following, we highlight some characteristics related to vehicular networks that should be taken into consideration when proposing a new solution in order to meet the requirements of VANET standards.

- **High node mobility**: VANETs are characterized by having vehicles that change their position and their speed both frequently and rapidly. The speed of the vehicles makes the network topology dynamic, and it also affects the wireless signal, possibly leading to packet loss or high communication delay. Indeed, vehicles may be very densely packed in urban areas, yet may, however, quickly become very sparse when they move towards highways or rural areas. Obviously, the high mobility of the nodes impacts the routing strategy, as well as the communication performance. Thus, deploying adaptive, yet efficient, MAC protocols is a necessity in VANETs.

- **Availability of Geographical position**: Knowing the vehicle's position, as well as the positions of the surrounding neighbors, is important for several geographic protocols in VANETs. Providing an accurate real time three-dimensional position (latitude, longitude and altitude), direction, velocity, and

precise time, allows geographic protocols, such as the GeoNetworking protocol, to route information between vehicles according to their geographical position.

- **Mobility model**:

  A mobility model is an important factor used to evaluate protocol behaviors in vehicular networks. This model should reflect reality (speed variation, traffic lights, crossroads, and traffic-jams) as accurately as possible. Defining a suitable mobility model starts by identifying the environment of the test scenario. Three main environments are conventionally considered:

  - Highway: a main road, especially one connecting major towns or cities, characterized by a high speed with a variable density of vehicles depending on the time of day and the day of the week.
  - City: a large town with several main and secondary roads, characterized by lower speed with a high density of cars during rush hours.
  - Countryside: a geographic area that is located outside towns and cities, characterized by an average speed with a lower density of cars.

- **No energy constraint**: Unlike many MANET setups, VANET nodes have ample energy and computing power for both storage and processing [8]. There is therefore no constraint on energy consumption. In fact, both On Board Units (OBUs) and Road Side Units (RSUs) are directly powered by vehicles and road platforms respectively.

- **Different QoS requirements**: In VANETs, the Quality of Service requirements vary significantly depending on the service.

  For example, real-time applications including services related to road safety and traffic management require guaranteed access to the channel and have strict requirements regarding end-to-end delay and packet loss ratio. On the other hand, Infotainment applications have more flexible requirements on both transmission rates and delay.

In conclusion, VANETs differ from MANETs due to their specific characteristics and requirements which represent a challenge for the design of low-access delay, high-throughput, scalable and robust MAC protocols. Nevertheless, certain other VANET characteristics, such as the ample electrical power and the limited degrees of freedom

in the nodes' movement patterns, can help us to design and develop efficient MAC protocols [9].

2.2.3 VANET applications

Initially, VANET networks were designed to increase traffic safety and efficiency by reducing the risk of road accidents. Nowadays, these networks are used for a wide range of applications which can be divided into the following three categories: safety services, traffic management and user-oriented services.

According to COMe-Safety [34], applications in ITS stations are general services for the ITS user and could be classified under 3 main fields:

- **Traffic Safety**: As mentioned above, this category of VANET applications represents the main objective of inter-vehicular communications. These applications aim to reduce the number of accidents and enhance driver and passenger safety by enabling each vehicle to provide a warning in real time when a critical event is detected. The warning message can be either through a seat vibration, tone or visual display or combinations of these indicators. Figures 2.2 and 2.3 show examples of safety applications that are based on V2V communications. When a potentially hazardous situation is detected, a vehicle can continuously broadcast information about this critical situation to approaching vehicles. Figure 2.3 shows another safety application: when a vehicle breaks suddenly, it broadcasts information about its current status (i.e., position, speed, deceleration, etc.), which is used by the surrounding vehicles to quickly detect the sudden braking.

- **Traffic Efficiency** : Examples of VANET services are not limited to road safety applications, but can be used for other types of applications, especially traffic management. These applications focus on improving traffic flow and route optimization, thus reducing the time spent traveling on the road as well as fuel consumption and air pollutants. Another important consequence of these applications is a reduction in the number of accidents resulting from flow congestion. Figure 2.4 shows a Road Side Unit notifying drivers of the recommended speed according to the current traffic conditions.

- **Value-added services** : Applications in this field aim to provide on-board infotainment, comfort, and convenience to both drivers and passengers. Services

Figure 2.2: Accident detection by using V2V communication.

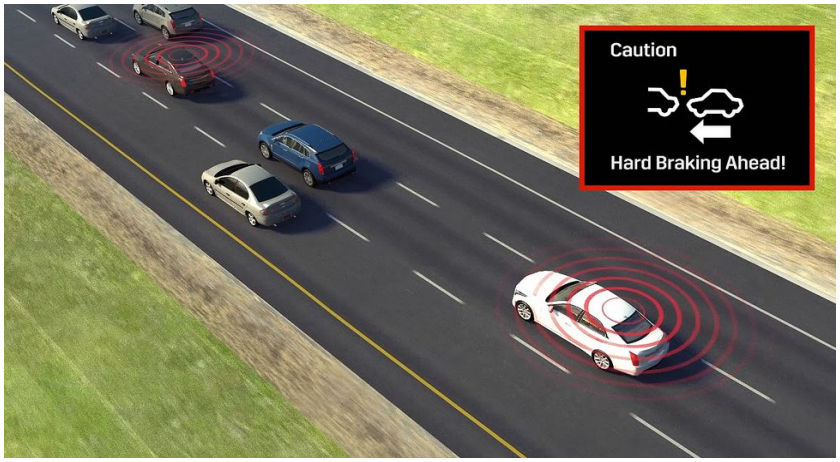

Figure 2.3: Emergency brake warning.

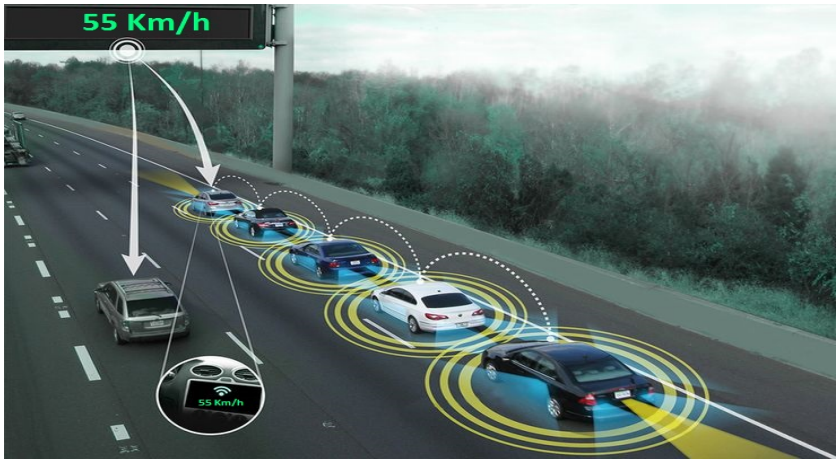

Figure 2.4: Traffic Management service.

in this application type can be Internet access, location free parking places, video streaming sharing, etc. In fact, Internet access can be provided through V2I communications, therefore, business services will be fully available in vehicles [73]. Moreover, and as shown in Figure 2.5, file sharing and video streaming services can be provided through V2V communications [74], making long trips more comfortable and enjoyable. Because this category of applications has different QoS requirements in terms of bandwidth and delay, guaranteeing real-time and reliable communications for delay-sensitive applications without impacting throughput-sensitive applications can be an extremely challenging task. In the next section, we review recent VANET standardization efforts as well as some research projects in the field of VANETs in Europe and beyond.

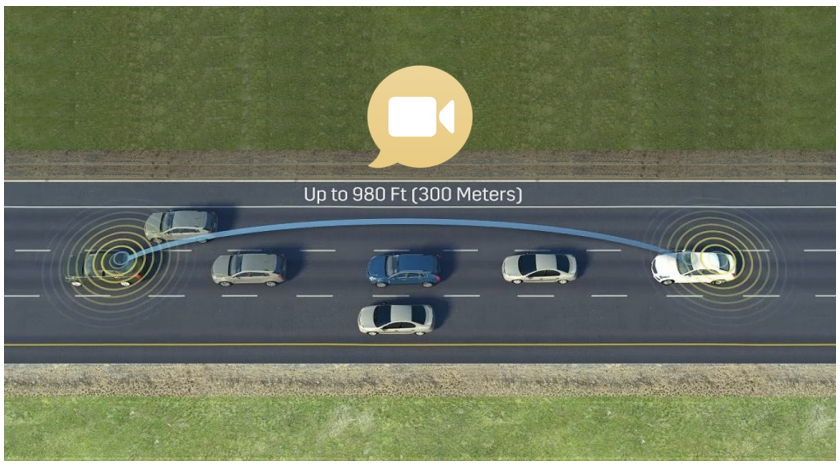

Figure 2.5: V2V communication: video conference application.

2.3 VANET standardization and research projects

2.3.1 Standardization

VANETs were first mentioned and introduced in 2001 in [12], and since then, they have attracted a great deal of attention in research, standardization and development. In this section, we present the recent standardization efforts and related activities in the field of VANETs.

- **Dedicated Short Range Communication**: According to the U.S. Department of Transportation [13], Dedicated Short-Range Communication (DSRC) [11] is a "two-way short-to-medium-range wireless communications capability that

permits very high data transmission critical in communications-based active safety applications". DSRC was initially coined in USA [72] by the United States by the Federal Communication Commission [18] to support vehicular communications. DSRC supports a nominal communication range of [300 - 1000] meters, a data rate of [6 - 27] Mbps, and a vehicular speed up to 190 Km/h.

DSRC is defined in the frequency band of (5.850 GHz to 5.925 GHz) with a total bandwidth of 75 MHz. This band is divided into 7 channels of 10 MHz each, as presented in Figure 2.6. These channels are divided functionally into one control channel and six service channels. The control channel, CCH, is reserved for the transmission of network management messages (resource reservation, topology management) and it is also used to transmit high priority messages (critical messages relating to road safety). The six other channels, SCHs, are dedicated to data transmission for different services.

Beside the U.S, the DSRC standard is also used in other parts of the world such as Europe and Japan. Table 2.1 shows a comparison between different regional standards for DSRC [14]. More details about regional standards for DSRC can be found in [15–17].

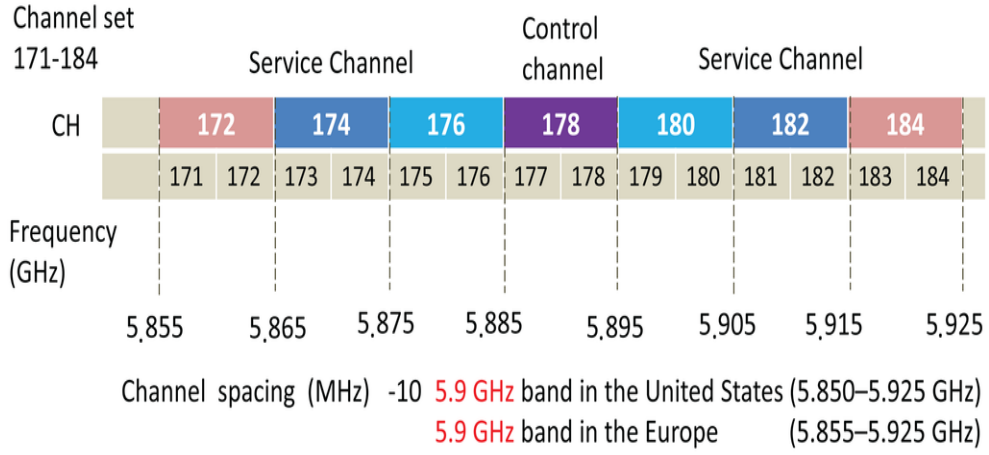

Figure 2.6: 802.11p, WAVE, DSRC frequency spectrum.

- **IEEE 802.11p**: The IEEE 802.11p [19] standard has been proposed by the Task Group of the IEEE "to add wireless access in vehicular environments (WAVE), a vehicular communication system". IEEE 802.11p defines enhancements to the classical IEEE 802.11 [20] standard required to support Intelli-

Table 2.1: Regional standards for DSRC

Features	Japan	Europe	North America
Duplex	Half-duplex(OBU) Full-duplex(RSU)	Half	Half
Radio frequency	5.8 GHz	5.8 GHz	5.8-5.9 GHz
Bandwidth	80 MHz	20 MHz	75 MHz
Channels	7	4	7
Channel Separation	5 MHz	5 MHz	10 MHz
Data rate	Down/Uplink: 1 or 4 Mbps	Down-link: 500 Kbps Up-link: 250 Kbps	Down/Uplink: 6-27 Mbps
Coverage(m)	30	15-20	1000
Modulation	RSU: 2-ASK OBU: 4-PSK	RSU: 2-ASK OBU: 2-PSK	OFDM

gent Transport Systems (ITS) applications. IEEE 802.11p uses Enhanced Distributed Channel Access (EDCA) functionality derived from the IEEE 802.11e standard to improve the QoS [21]. The EDCA allows safety messages with high priority level to have a better chance to be transmitted before other less important messages. Prioritization is achieved by varying the Arbitration Inter-Frame Spaces (AIFS), as well as the Contention Windows (CWs). This adaptation increases the probability of successful medium access which is important for real time communication. The channel access time is equally divided into repeating synchronization intervals of 100 ms [22]. Each synchronization interval is divided into control channel intervals (CCHI) of 50ms each, and service channel intervals (SCHI) of 50ms each, as shown in Figure 2.7.

During a CCHI interval, each vehicle tunes its control channel whether to send and/or receive high priority safety messages, or, to attribute a specific service to a specific channel. The standard also defines a $4\mu s$ Guard Interval, used for radio switching, at the start of each channel interval. Communication between the vehicles requires synchronization. This can be achieved via the coordinated universal time (UTC) provided by the built-in GPS vehicle.

The IEEE 1609.4 standard defines multichannel MAC operations for the IEEE 802.11p in order to support competitive applications [54]. However, if the IEEE 802.11p chipset installed in the communication module (On Board Unit, or,

Road Side Unit) supports two physical antennas, the need to have a channel switching system will no longer be necessary. In this case, the first antenna is tuned to the CCH, and the second one is tuned to the SCH. Thus, each vehicle will therefore be able to broadcast safety messages throughout the 50 ms of the CCHI without needing a Guard Interval.

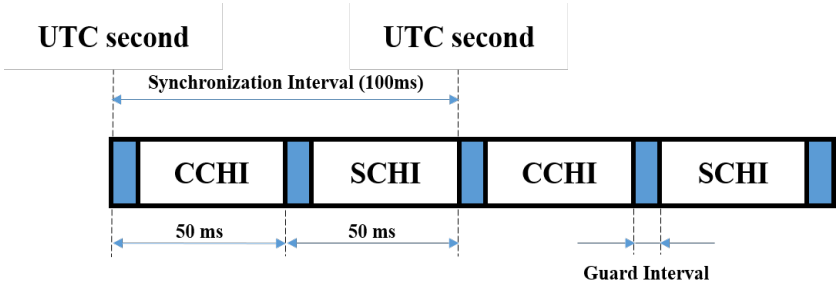

Figure 2.7: Channel access time in the IEEE 802.11p standard

- **Wireless Access in Vehicular Environment WAVE**: WAVE is a vehicular communication system used by IEEE 802.11 devices to operate in the DSRC band. Figure 2.8 shows the IEEE 802.11p DSRC/WAVE protocol stack. It incorporates a number of protocols in conjunction with the family of the IEEE 1609 standards [24]. These protocols include the IEEE 1609.1 WAVE resource manager, the IEEE 1609.2 WAVE security services for applications and management messages, the IEEE 1609.3 WAVE networking services, and the IEEE 1609.4 WAVE multi-channel operation.

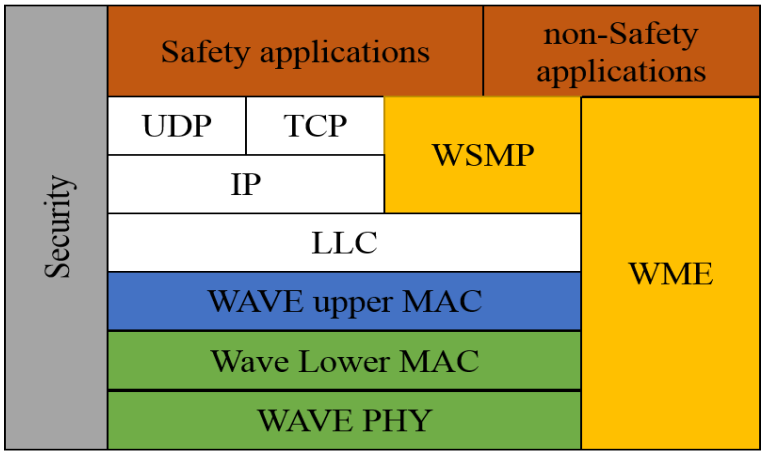

Figure 2.8: The IEEE 802.11p DSRC/WAVE Protocol stack

- **ISO:TC204/WG16-CALM**: The International Organization for Standardization (ISO) proposes a comprehensive mobile network architecture called Communications Access for Land Mobiles (CALM) [25]. CALM uses a wide range of wireless access technologies including 2G/3G/LTE, wireless broadband access (e.g., WiMAX), and IEEE 802.11, to provide broadcast, unicast, and multicast communications between mobile nodes, between mobile nodes and the infrastructure, and between fixed infrastructures [28]. A fundamental ability of the CALM concept is to support media-independent handovers between the various access technologies. This means that mobile nodes are not limited to a single access technology and are able to make an optimal decision to use the most appropriate access technology for message delivery. Moreover, in order to support vehicular ad hoc networking, CALM M5 [26] has been developed based on IEEE 802.11p, for V2V and for V2I communications. CALM M5 is intended for real-time road safety applications requiring bounded access channel delays and low communication overhead. A dedicated frequency band is allocated to such applications, while another frequency band is allocated to non-safety applications with more relaxed latency requirements [29].

- **ETSI TC ITS**: ETSI [42] has established a technical committee TC ITS (Intelligent Transportation System), in order to develop standards and specifications for the use of communication technologies in transport systems [31]. TC ITS is organized into five working groups: WG1 (for User Application requirements), WG2 (for Architecture and cross layer issues), WG3 (for Transport and Networks), WG4 (for Media and related issues), and WG5 (for Security). ETSI TC ITS has also converged in harmonization with ISO TC204 WG16 towards the ITS communication architecture, known as the ITS station architecture [32,33].

2.3.2 Related projects

Several European, American and Japanese research projects are currently focusing on vehicular communications. FleetNet [46] is an European project that aims to develop a wireless multi-hop ad hoc network for inter-vehicle communication to improve the driver's and passenger's safety and comfort. PReVENT [61] is a European automotive industry activity co-funded by the European Commission to contribute to road safety by developing and demonstrating preventive safety applications and technologies. SAFESPOT [43] is an integrated research project co-funded by the European

Commission Information Society Technologies. It aims to create dynamic cooperative networks where the vehicles and the road infrastructure communicate to share information gathered on board and at the roadside to enhance the drivers' perception of the vehicle's surroundings.

The Car2Car Communication Consortium (C2C-CC) is a non-profit organization [47] launched by the European vehicle manufacturers and supported by the automobile industry. ETSI, ISO/TC, and the C2C-CC cooperates together to develop the specifications of the European ITS standards. Several other research projects have been created on national and international scales to develop and prepare the deployment of efficient vehicular communication protocols. Figure 2.9 shows some projects that have been funded by the European Union, or the governments of the USA and Japan. These include COMeSafety [40], GeoNET [36], SEVECOM [38], CarTALK [39], coopers [35], euroFOT [62], PRE-DRIVEC2X [63] and evita [37] which are sponsored by the European Union, Advanced Highway Technologies in the USA and the Advanced Safety Vehicle Program (ASV) sponsored by the government of Japan which are presented in [67].

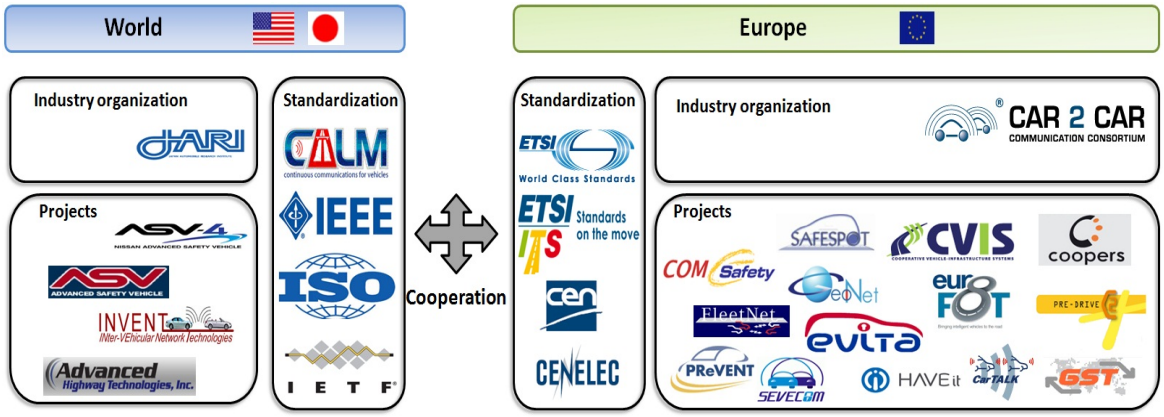

Figure 2.9: Overview of ITS activities in Europe and the rest of the world

2.3.3 Summary and discussion

Several research activities and standardization efforts have been established in Europe, the USA, and Japan, to develop efficient vehicular communication systems [67]. Moreover, many standardization organizations, such as ETSI ITS, IEEE [66], ISO [65] and IETF [45], are cooperating together on an international level with the aim of es-

tablishing a collaborative convergence towards a first deployment of the well expected Intelligent Transportation Systems (ITS) (see Figure 2.9).

Despite all these efforts, some open issues are still present and need to be studied by the standardization organizations.

Firstly, safety applications have strict QoS requirements in terms of delay and loss rate that cannot always be guaranteed by the IEEE 802.11p under its current state, particularly in heavy traffic conditions [91]. Indeed, when safety messages are transmitted in broadcast mode on the control channel, no acknowledgment messages are sent-back to confirm the reception. Moreover, no RTS[1]/CTS[2] exchange is used. This increases the collision probability in the presence of hidden terminals. Furthermore, the Virtual Carrier Sensing (VCS) mechanism is not applied in broadcast communications. Furthermore, employing the EDCA [20] technique leads to potential collisions between messages that have the same Access Category (AC).

Secondly, in the WAVE standard, a single DSRC radio can switch between the control channel, used to boradcast safety messages, and the service channels, used for unicast communications. However, due to the use of static time intervals, the DSRC radio cannot handle both safety and non-safety messages with a high degree of reliability in dense scenarios. To meet the safety application requirements and ensure reliable safety messages transmission, maximizing the control channel interval (CCHI) and minimizing the service channel interval (SCHI) may be needed. In addition, due to the overhead latency of the channel switching process, safety messages could be lost while the radio is busy switching channels. Thus, retransmissions may be needed to ensure reliable transmission.

Moreover, the main IEEE 802.11p MAC layer is based on the CSMA/CA[3] protocol to organize the channel access. However, it is well-known that the CSMA/CA system cannot handle packet collisions in broadcast communications. Thus, the CSMA/CA system, under its current state, does not guarantee bounded channel access delays in dense scenarios. Therefore, the inherent QoS safety applications requirements are not satisfied.

These issues are very important in VANETs since the reliability of the ITS safety applications depends directly on the performances of the MAC layer.

[1]Request To Send

[2]Clear To Send

[3]Carrier Sense Multiple Access with Collision Avoidance

2.4 Conclusion

Research in Vehicular Ad hoc Networks (VANETs) has attracted increasing interest over recent years thanks to its promise to improve road safety by using vehicular communications. However, a challenging problem when designing communication protocols in VANETs is coping with high vehicle density, which causes frequent changes in the channel load and leads to frequent loss in communication. In this chapter, we have described features of VANETs and their different types of vehicular communications. We classified vehicular applications into three main categories based on their improvement of safety on the road and their requirements in terms of delays and throughput. Moreover, we presented research and standardization activities in the field, and we identified their shortcomings focusing particularly on the QoS at the MAC layer.

The next chapter presents the problematic of radio channel congestion, as well as the different congestion control strategies and algorithms.

Chapter 3

Congestion Control in Vehicular AdHoc NETworks

Contents

3.1 Introduction

In VANETs, vehicle-to-vehicle (V2V) communication is used to support vehicular safety and traffic efficiency, and it is important that each node of the network can send its packets to its neighbors in a reliable way and with low latency. However, due to the limited channel resources reserved for the IEEE 802.11p, which is commonly considered as the default radio communication technology for VANETs, a high rate

of safety messages exchanged between network entities can easily lead to a channel congestion issue.

In this chapter we review the root cause of this channel congestion issue in VANETs, as well as its effects on the communication performances. We then survey the fundamental congestion control strategies and techniques. Finally, we give a global summary of the Decentralized Congestion Control (DCC) mechanism standardized by ETSI.

3.2 Channel Congestion in CSMA Networks

3.2.1 CSMA Medium Access Control

In classical IEEE 802.11 wireless networks, all the nodes are constantly competing to communicate with an access point which usually serves as a gateway to the Internet or another resource. Since the Carrier Sense Multiple Access (CSMA) technique is the main core of the IEEE 802.11 technology, only one packet can be transmitted at a time. However, in VANETs, as the concept of a central node is less relevant and the spatial extension of the network has increased considerably, simultaneous transmissions are therefore necessarily present. This property could lead to unbounded packet collisions and transmission delays, which is undesirable for demanding networks like VANETs.

3.2.1.1 MAC Back-off algorithm and IEEE 802.11p Broadcasting Mode

MAC Back-off algorithm: Carrier Sense Multiple Access with Collision Avoidance (CSMA/CA) is the main core of the IEEE 802.11p MAC method, where nodes listen to the wireless channel and make sure it is free before sending their packets. If the carrier sensing indicates a free channel for a predefined period of time, the node vehicle is allowed to send its data. Otherwise, if the carrier sensing indicates a busy channel, the node vehicle must defer the transmission by choosing a random back-off time in order to reduce the probability of packet collision. This back-off time is determined by an integer randomly chosen from a uniform distribution between 0 and CW, where CW refers to the size of the contention window. As long as the channel is detected to be busy, the back-off countdown is frozen and the transmission is deferred. The back-off timer is decremented if the channel has been detected to be

idle for a duration of a DCF[1] Interframe Space (DIFS). When the back-off countdown expires, transmission begins.

IEEE 802.11p Broadcasting Mode: In unicast communications, any message transmitted by the sender must be acknowledged by the receiver, otherwise the transmission will be considered unsuccessful, the back-off window size is therefore doubled (up to a maximum value), and the transmission procedure is relaunched. However, acknowledgments are not used in broadcast mode given the number of collisions they can cause, and therefore, each packet is transmitted only once, using the minimal value of the back-off counter. Systematically using the minimal value of the contention window has an impact on the performances of the MAC layer that has been widely studied in the context of WLANs. For example, Bianchi showed in [128] that the optimal value of the minimum back-off window is a function of the number of contending nodes. This means that mechanically using the minimal value of the contention window is not suitable for networks with highly variable node density. Moreover, the RTS/CTS[2] handshake mechanism, as well as the BEB [3] mechanism are not supported in the broadcast mode which increases the likeliness of packet collisions.

3.2.1.2 CSMA and Carrier Sensing

Sensing the channel to make sure it is free before any MAC layer transmission is the main foundation of the channel access method CSMA described in the IEEE 802.11 standard. Carrier sensing can be either virtual or physical. Virtual carrier sensing is based on Network Allocation Vector (NAV) which is a MAC layer mechanism that reserves the medium for data transmission using two flow control frames: Request to Send (RTS) and Clear to Send (CTS). Every time a node wants to transmit a frame, it must perform a RTS/CTS handshake exchange prior to the normal data transmission. The sender first sends an RTS message, and the destination replies with a CTS. Only upon reception of a CTS is the node allowed to start the transmission.

Virtual carrier sensing helps to prevent collisions from occurring in classical CSMA/CA systems where all nodes compete to create a point-to-point communication with a central access point. However, this technique can not be applied for VANETs and similar

[1]DCF: Distributed Coordination Function is a sharing access method to the medium based on the CSMA/CA protocol

[2]Request to Send / Clear to Send

[3]Binary Exponential Backoff

distributed networks where there is no central access point, and most traffic needs to be broadcasted to disseminate the information as widely as possible.

On the other hand, physical carrier sensing is based on Clear Channel Assessment (CCA) which is a part of the Physical Medium Dependent (PMD) and Physical Layer Convergence Protocol (PLCP). CCA is independent of the communication mode and it is used to determine whether the channel is idle or not.

CCA is also used to determine whether or not the received signal strength indicator (RSSI) exceeds a predefined threshold needed for a node to detect and decode incoming 802.11 transmissions.

Initially, these principles were developed and optimized for short-range communications. As long as the channel load is moderate, they work well for both unicast and broadcast communications. However, in more recent wireless networks, such as Wireless Sensor Networks (WSNs) and VANETs, channel load could easily could easly become over loaded. Moreover, the overall throughput largely depends on the amount of spatial reuse, which itself depends on the state of the network. Therefore, the carrier sensing and the CCA threshold can easily influence the channel load.

3.2.2 Communication Performance in High Channel Load Scenarios

3.2.2.1 Impact of Channel Load on Packet transmission

We begin our study by evaluating the default non-controlled CSMA system as specified by IEEE 802.11. The simulation tool is the ns-3 Network Simulator and the simulation setup follows the ETSI recommendations for congestion control evaluation [75]. The scenario consists of vehicles distributed on a section of a highway 1000 meters long and 18 meters wide. The highway contains three lanes, each 3 meters wide, with traffic moving in both directions.

The communication parameters are listed in Table 3.1.

The simulation time is equal to 50 seconds, and the computation duration varies between 1 and 40 minutes according to the scenario simulated. Node density varies between 66 and 606 nodes according to four scenarios : Sparse, Medium, Dense, and Extreme. The inter-vehicle distance is 100, 45, 20, and 10 meters respectively, (see Table 6.2).

We start the evaluation of the default IEEE 802.11 CSMA system by defining two performance metrics: the Packet Delivery Ratio (PDR), and the Inter Packet Arrival

Table 3.1: non-controlled CSMA System : communication parameters

Parameters	Value
Channel Bandwidth	10 Mhz
Transmission Power	23 dBm
Energy Detection Threshold	-95 dBm
Carrier Sense Threshold	-85 dBm
Propagation Model	Log-distance
CAM generation rate	10 Hz
CAM size	437 Bytes

Table 3.2: Scenarios density

Scenario	Inter-vehicle distance (m)	Node density (Nodes/Km)
Sparse	100	66
Medium	45	138
Dense	20	303
Extreme	10	606

Time ($IPAT$). PDR refers to the ratio of the number of packets received over the number of packets generated. PDR is measured at individual nodes targeting safety messages ($CAMs$) transmitted by each neighbor node. $IPAT$ refers to the time gap between consecutive CAM messages.

The Packet Delivery Ratio (PDR): Figure 3.1 plots the average packet delivery ratio (PDR) of the different scenarios while considering different transmission ranges: from 10 to 500 meters. The horizontal axis represents the distance in meters between the transmitters and the receivers, while the vertical axis represents the PDR. We observe that the default CSMA system shows an excellent PDR for the Sparse scenario. Almost 100% of the generated packets are received by the receivers, even for nodes at 400 meters from each other. It is unsurprising that such high performances are obtained given the number of simulated nodes and the inter-vehicle distance (66 nodes with 100 meters of inter-vehicle distance).

The channel congestion effect becomes noticeable starting from the Medium scenario, with 138 simulated vehicles, the PDR is equal to 90% for a close distance

of 45 meters. This value degrades continually with the increase in the transmission distance. For example, it is equal to 70% for a communication distance of 400 meters.

The impact of channel congestion becomes greater with the Dense scenario: with 303 simulated vehicles, the PDR is equal to 52% for an inter-vehicle distance of 25 meters. It then continually degrades with the increase in the transmission distance until reaching 15% for a transmission distance of 400 meters.

For the Extreme scenario, with 606 simulated vehicles, the PDR shows very poor performances: 24% for an inter-vehicle distance of 10 meters, and it becomes even worse with larger distances: 9% of PDR for a transmission distance of 400 meters.

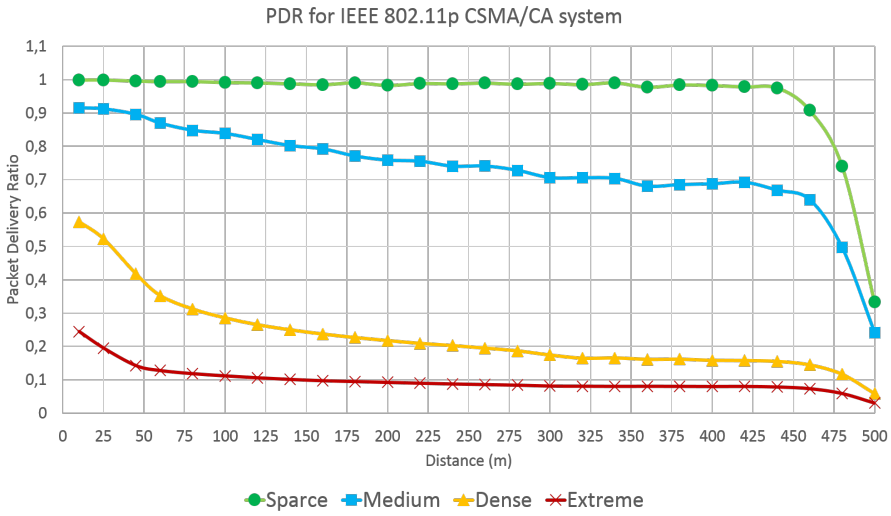

Figure 3.1: Packet delivery ratio and transmission range in IEEE 802.11p CSMA/CA.

The Inter Packet Arrival Time ($IPAT$): Figure 3.2 shows the average inter packet arrival time ($IPAT$) of the different scenarios. similarly to the PDR case, the CSMA system performs very well with low node density, especially with the Sparse scenario where the IPAT is less than 0.1 seconds even for large transmission distances. However, for more dense scenarios, such as the Dense and the Extreme scenarios, the time gap between consecutive messages increases with the increasing distance; it exceeds 1 second for certain distances.

Packet Loss: Figure 3.3 plots the average packet loss for the different scenarios while considering a transmission range of between 10 and 400 meters. The horizontal axis represents the simulated scenario, while the vertical axis represents the packet

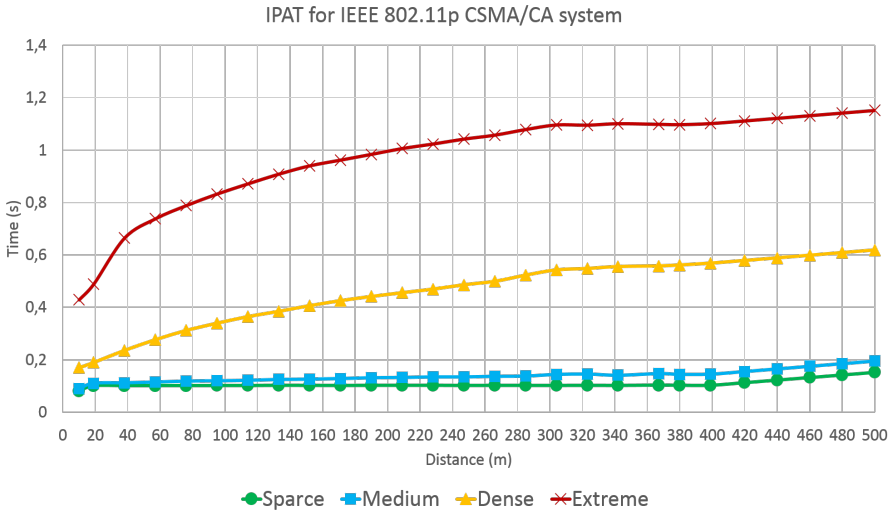

Figure 3.2: Packet delivery ratio and transmission delay in IEEE 802.11p CSMA/CA.

loss percentage. We observe that the packet loss is very high for Dense and Extreme scenarios.

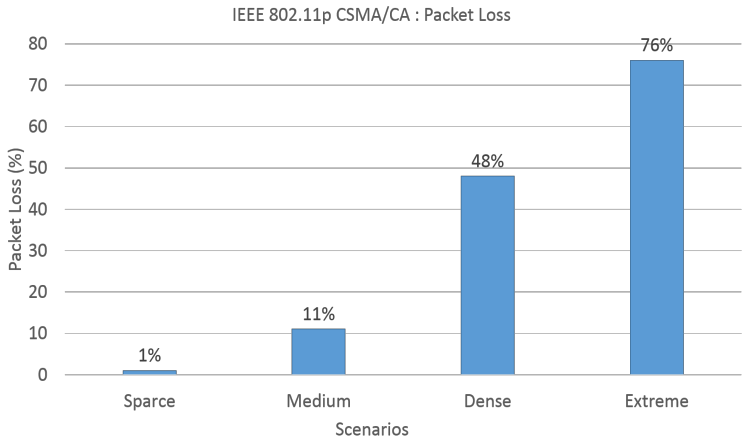

Figure 3.3: Packet delivery ratio and packet loss in IEEE 802.11p CSMA/CA.

The main, but not exhaustive, reasons for packet loss are summarized below :

- **Simultaneous Transmissions:** simultaneous transmissions can occur if tow (or more) nodes have the same backoff counter.
- **Hidden Nodes:** since there is no RTS/CTS handshake mechanism in broadcast mode, the channel cannot be reserved by NAV, the virtual carrier sense parameter, and therefore the hidden terminal problem is more likely to occur.

- **Exposed Nodes:** packet loss can occur whena a node is prevented from sending packets to other nodes because of a neighboring transmitter.

In conclusion, although the evaluation scenario is very simplistic, the results obtained show that the default CSMA system can not simply be applied to VANETs without adapting its parameters to the characteristics of this type of network. In fact, both the PDR and the $IPAT$ are directly impacted by network density, and therefore by the transmission distance, hidden nodes, and transmission collisions.

3.3 Fundamental Congestion Control Mechanisms

The aforementioned considerations show that an increasing channel load leads to packet loss, a decreasing packet delivery ratio, and an increasing transmission delay. Since the safety messages broadcasting operation is performed locally by each node without a central coordination, a decentralized congestion control DCC mechanism is therefore required. The fundamental concept behind the DCC mechanism is that every node should be able to measure the channel load and make some resource utilization decisions in such a way that every node participates in maintaining a moderate overall channel load.

3.3.1 Input and Output Parameters

A DCC algorithm can be perceived as a control loop that, on the one hand, takes input parameters that characterize the target factor: the channel load, and, on the other hand, gives output parameters that decide the local allowed resource utilization.

Input parameters: The input parameters can include the following non-exhaustive list:

- **The Channel Busy Ratio (CBR):** is the most common DCC input parameter. CBR is the ratio of the time the channel is perceived as busy, over the monitoring interval:

$$CBR = T_{busy}/T_{monitor}$$

  A high CBR can be an indicator of a high number of neighboring nodes, or a high transmission rate, or both. The CBR threshold is an important parameter that should be chosen carefully since it determines whether the channel is

perceived as busy or idle. A low CBR threshold allows low signals from distant transmitters to be received, which often results in a highly loaded channel. A low CBR threshold, however, allows a higher resolution of low channel load, and therefore fewer restrictions on the utilization of resources. Thus, the choice of the threshold value must be given careful consideration.

- **Number of nodes:** Another commonly used DCC input parameter is the number of neighboring nodes, which can be determined via the neighbor table in the Networking and Transport layer of the ITS protocol stack. The number of neighboring nodes can also be determined via the Local Dynamic MAP (LDM) at the Facilities layer.

Output parameters: The output parameters can include the following non-exhaustive list:

- **Transmission Rate:** Although receiving fresh signaling messages is clearly important in VANETs, however, a high beaconing rate, especially in dense scenarios, may lead to a high bandwidth utilization and consequently to a congested channel. Therefore, dynamically adjusting the packet generation rate according to the level of the channel load can reduce congestion. Transmission rate-based strategies have the disadvantage of strangling the generation of safety messages which means that the information they contain may become obsolete.

- **Transmission Power:** Safety applications generally send their safety messages with a high transmission range in order to cover as many nodes as possible. However, when the channel is overloaded, the transmission power can be tuned according to the node density and/or the congestion level. Reducing the transmission range reduces the the probability of collisions caused by simultaneous transmissions. Increasing the transmission range increases the transmission distance, but increases the probability of collusions.

- **Carrier Sense:** Unlike transmission Power, which cuts off communication by reducing the transmission range, the carrier sense parameter tunes the perception of the channel and decides whether to receive a packet or not.

3.3.2 DCC Reactive Control

Reactive DCC algorithms usually take the current CBR as an input parameter to determine the appropriate message rate. The most common method is to use a look-up table. See Table 3.3 .

Table 3.3: Example of a Reactive DCC look-up table

State	Index	CBR	Transmission Interval	Message Rate
RELAXED	1	<30%	100 ms	10 Hz
ACTIVE 1	2	30-39%	200 ms	5 Hz
ACTIVE 2	3	40-49%	300 ms	3.33 Hz
ACTIVE 3	4	50-59%	400 ms	2.5 Hz
RESTRICTIVE	5	>60%	500 ms	2 Hz

A Reactive DCC look-up table generally proposes three logical states : RELAXED, ACTIVE, and RESTRICTIVE. In the RELAXED state, the CBR is below a minimum threshold, the channel is considered relatively idle, and the Reactive DCC algorithm imposes no restrictions on the message transmission rate or the message transmission interval. The ACTIVE state represents the state for which the channel load range is optimal, and the transmissions rate and the message rate are moderately limited. In the RESTRICTIVE state, however, the channel is considered overloaded, and the restrictions on the use of the communication resources are greater. The ACTIVE state is further divided into several sub-states (ACTIVE1, ACTIVE2, etc.) for more fine-grained control.

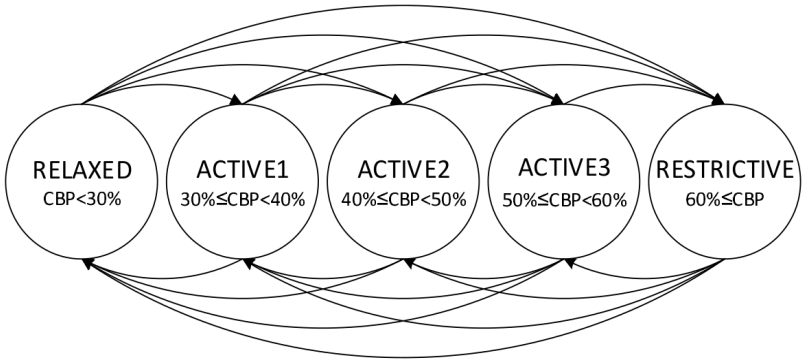

Figure 3.4: Reactive DCC: Logical state machine.

The choice of an output parameter, e.g., the transmission rate $r(t')$ depends on a set of predefined CBR thresholds, and can be specified as follows:

if $CBR(t') > CBR_{restrict}$, then $r(t) = r_{restric}$ for all $t' \in [t-\Delta, t]$

if $CBR(t') > CBR_{restrict}$, then $r(t) = r_{active3}$ for all $t' \in [t-\Delta, t]$

if $CBR(t') > CBR_{active3}$, then $r(t) = r_{active2}$ for all $t' \in [t-\Delta, t]$

if $CBR(t') > CBR_{active2}$, then $r(t) = r_{active1}$ for all $t' \in [t-\Delta, t]$

$r(t) = r_{relaxed}$ otherwise.

Note that the previous example uses the transmission rate as an output parameter, however, this system can be also applied to other output parameters such as power control, coding scheme, and carrier sensing. Furthermore, several active sub-states can be used to extend the state machine so the relation between the current channel load and the transmit instructions can be managed more finely.

3.3.3 DCC Adaptive Control

Unlike the Reactive Control approach where the DCC algorithm reacts directly to the perceived channel load and the behavior of the output parameter is predefined for every possible channel load measurement, the Adaptive Control approach adapts the output parameter, e.g., the the message rate, of each node in such a way that the total channel load converges to a specified target: a $CBRtarget$. By driving the CBR toward a $CBRtarget$, the adaptive control approach ensures that the channel load does not exceed a given limit: the target value.

3.3.3.1 LIMERIC algorithm

The LIMERIC (LInear MEsages Rate Intergrated Control) algorithm [76] is a distributed and adaptive linear rate-control algorithm where each node adapts its message rate in a such way that the total channel load converges to a specified target. The message rate of a node denoted as $j(t)$ is adapted every δ time using the following linear equation :

$$rj(t) = (1-\alpha)rj(t-1) + \beta(CBRtarget - CBRmeasured(t-1))$$

Where $CBRtarget$ denotes the target channel load. α and β are adaption parameters that control stability, fairness and steady state convergence. β is related to a certain default frame duration δ. If a frame duration d different to this is used, β is scaled by δ/d to achieve the same control behavior. For a specific $CBRtarget$ and

a frame duration of d measured in ms, in a steady state, LIMERIC converges to a CBR determined by the following equation :

$$CBRconvergence = CBRtarget(dk\beta)/(\alpha + d + k + \beta)$$

Where k is the number of nodes within the interference range. According to the previous equation, the converged channel load can be adjusted by using different $CBRtarget$ values. In LIMERIC, a message is generated when there are channel resources available with at least one Hz, which is the maximum time between two message generations.

3.3.3.2 Additive Increase Multiplicative Decrease (AIMD) approach

Another well-known approach to congestion control is based on the Additive Increase Multiplicative Decrease (AIMD) [77] algorithm. This algorithm was originally designed to controls TCP's congestion window, which reduces the number of transmitted TCP segments with pending acknowledgments. As long as transmitted segments are successfully acknowledged, the congestion window size increases slowly by an increment α. However, if a transmission fails, the congestion window size decreases with a factor β.

3.4 The ETSI/ISO DCC Framework in the ITS Protocol Stack

Targeting the fact that ITS safety applications require a low communication latency and a high PDR, ETSI specified a framework called the Decentralized Congestion Control (DCC) Framework [76]. DCC is an important component of the ITS station architecture used to maintain network stability, throughput efficiency and fair resource allocation to ITS stations. DCC requires components on several layers of the protocol stack and these components work together to fulfill a set of operational requirements such as providing fair allocation of resources and fair channel access among all ITS stations in the same communication zone, and keeping the channel load caused by periodic messages below a predefined threshold.

Figures 3.5 3.6illustrates the general architecture of an ETSI/ISO ITS station (ITS-S), as well as the distribution of the DCC components on its layers. It is useful to note that, as of today, ETSI DCC remains a set of standards that has been partially

tested in a research context where a lot of attention has been paid to CAM and DENM generation rates, as well as to MAC power-control, on DCC_fac and DCC_acc components respectively. However, to the best of our knowledge, much less work has been done on the other features of the DCC algorithm.

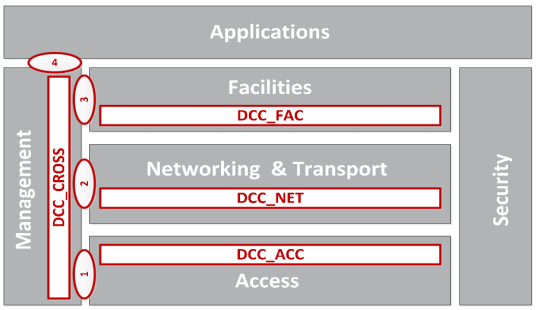

Figure 3.5: ETSI DCC architecture.

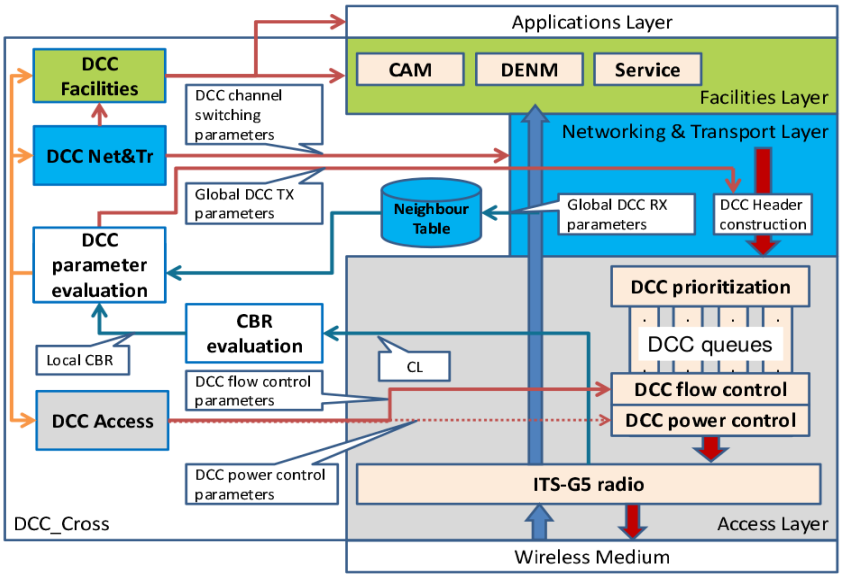

Figure 3.6: ETSI DCC mechanism architecture.

3.5 Conclusion

Decentralized Congestion Control (DCC) mechanisms become necessary in IEEE 802.11 when using broadcast communication in scenarios with a high node density and a high transmission rate. As discussed in Section 3.2.2, a high channel load

directly results in a degradation in performances, especially in packet delivery ratio and transmission delay. This, in turn, reduces the amount of information exchanged between vehicles and limits cooperative awareness.

DCC algorithms limit the individual local use of communication resources with the aim of reducing the overall channel load. Typical DCC approaches have been discussed in Section 3.3 : reactive algorithms use a measured channel load to directly set a fixed output value, e.g., a fixed transmission rate. Adaptive algorithms, however, use a channel load target and adapt the output parameters, usually the transmission rate, based on the difference between the perceived channel load and the desired channel load. Finally, the DCC framework is already a part of specifications in the European Telecommunication Standards Institute (ETSI), and it is expected to be able to manage the channel load in a very efficient and complete way.

The next chapter presents an analysis and improvement of the IEEE 802.11p broadcast in the VANET context.

Part II

Analysis and improvement of the IEEE 802.11p broadcast

Chapter 4

Analysis and improvement of the IEEE 802.11p broadcast

Contents

4.1 Introduction

This chapter proposes and analyzes different broadcast strategies in IEEE 802.11p Vehicular Ad-hoc NETworks (VANETs). The first strategy is the default IEEE 802.11p strategy. Using a model derived from the Bianchi model, we provide the network performance in terms of throughput and success rate. The second strategy is to use an acknowledgment technique similar to the acknowledgment with point-to-point traffic. A node will send its broadcast packet as in the default case, but it requires an acknowledgment from a neighbor node. This node may be a random neighbor or may be selected according to precise rules. We analyze this second strategy in terms of throughput and success rate. Somewhat surprisingly, we show that this second strategy improves the delivery ratio of the transmitted packets but reduces the overall throughput. This means that if the CAM messages (Cooperative Awareness Messages) are broadcasted, the total number of packets actually delivered will be greater with the default strategy than with the improved strategy. We propose a third strategy which consists in using the default strategy for normal packets, but we add random redundant transmissions to ensure greater reliability for very important packets. We show that with this simple technique, not only do we obtain suitable reliability, but we also achieve larger global throughput than with the acknowledgment-oriented technique.
Another contribution of this chapter is to compute network performance in terms of throughput and success rate with respect to the network parameters and to analyze their impact on performances.

At the end of this chapter we analyze the IEEE 802.11p when when use varying inter-frame spacings and collision windows to create different priority classes. We build an analytical model with closed formulas to compute the probability of successful of transmissions for the different classes of traffic.

IEEE 802.11p was proposed as the main communication protocol to offer Wireless Access in Vehicular Environments (WAVE) [24]. IEEE802.11p is required to support Intelligent Transportation Systems (ITS) applications by providing communication between vehicles (V2V), and between vehicles and roadside infrastructure (V2I). Nowadays, one of the main ITS applications expected by vehicle manufacturers is safety applications that rely on the broadcast principle. Therefore, a reliable broadcast scheme is necessary to ensure the reliable reception of critical messages such as priority Cooperative Awareness Messages (CAM) [124] and Decentralized Environmental Notification Messages (DENM) [125]. In the contention-based Medium Access

Control (MAC) of IEEE802.11p, several studies have shown a correlation between an increase in the number of connected vehicles and an increase in packet loss rate. Several approaches to improve the reliability of broadcasting have been proposed in the literature, as reported in Section 4.2.

In this chapter, we propose and analyze two broadcast strategies and we compare them with the default IEEE 802.11p broadcasting method [126], [127]. We propose a mathematical model derived from the Bianchi [128] model to analyze the network performances of the default broadcast service of the IEEE 802.11p protocol in terms of throughput and packet delivery ratio,

The remainder of this chapter is organized as follows. Section 4.2 briefly reviews related work; Section 4.3 describes the proposed system model and the analytical model. We propose three different broadcast techniques. Simulation results are reported in Section 4.4. Section 4.5 describes an analytical model for IEEE 802.11p with priorities and Section 4.6 provides the results of this model. Finally Section 4.7 concludes this chapter.

4.2 Related work

The fundamental Medium Access Control (MAC) technique of the IEEE 802.11 based Wireless Local Area Networks (WLANs) is known as the Distributed Coordination Function (DCF). DCF is a Carrier Sense Multiple Access with Collision Avoidance (CSMA/CA) scheme that assumes all packet losses within a WLAN are due to packet collision. To avoid packet losses, DCF triggers a binary slotted exponential backoff procedure. In the contention-based MAC used in IEEE 802.11, as well as the amendment IEEE 802.11p, packet loss greatly depends on the channel contention, therefore, many studies have been carried out in the literature to evaluate the system throughput for WLANs as well as for Wireless Access in Vehicular Environments. In his performance Analysis of the IEEE 802.11 DCF, Bianchi [128] provided an analytical model to evaluate the throughput performance of both basic access and Request To Send/Clear To Send (RTS/CTS) access mechanisms as well as a combination of the two assuming a finite number of terminals and ideal channel conditions. Bianchi demonstrated the accuracy of his model for predicting the system throughput.

Unfortunately, most IEEE 802.11 DCF performance evaluation studies proposed in the literature cover the unicast transmission mode. There do, however, exist a few studies related to the IEEE 802.11 protocol in broadcast mode. Hafeez et al. [129]

have proposed an analytical study in which they model each terminal as one two-dimensional Markov chain to calculate the probability of successful transmissions of the periodic status messages (CAM), as well as the priority messages (DENM). They show that their model gives accurate results when estimating the recommended throughput level of IEEE 802.11p for each category of messages. Ghahramani et al. [130] start from the assumption that the number of contending vehicles in VANETs varies, enabling them to model the dynamicity of the contending terminals and to add more accuracy to the existing methodology of IEEE 802.11p MAC broadcast mode evaluation. The study in [127] proposes a simple analysis of IEEE 802.11 in broadcast mode. In this Chapter we re-use the results of [127] and we adapt and exploit them in the context of VANETs. Since we also propose to use reliable broadcast, we will use and adapt the study of the point-to-point mode as our broadcast transmissions will require acknowledgments.

4.3 System model

We use models which are very close to the Bianchi model [128]. In these models M is the number of vehicles in the network within the same carrier sense range; λ is the packet arrival rate in a station assumed to be Poisson and the duration of a packet is denoted by T. Moreover we assume that there is no waiting queue. When a packet arrives during the treatment of a packet we assume that it is lost. [1]

The other parameters are related to the IEEE 802.11p protocol. These parameters are : the duration of a mini-slot σ, and the number of back-off slots W. σ should be greater than the sensing delay of the Carrier Sense Multiple Access (CSMA) scheme of the IEEE 802.11p protocol. In usual implementations, σ is of the same order as the sensing delay of CSMA. W is the greatest back-off window that a node can select. In practice, W is set to the maximum duration of the back-off. When IEEE 802.11 uses an acknowledgment to enhance the transmission success rate, another parameter n is required in order to fix the maximum number of retransmissions before a packet is discarded.

All the models derived from the Bianchi model assume that the channel can be modeled as a succession of slots. Each slot may be a mini-slot (of duration σ) or a slot of duration T. The mini-slots are used to represent the time intervals during

[1] A better assumption is to to switch the new packet with the packet in the transmission (which is obsolete) and to discard this obsolete packet. This treatment does not change our analysis

which the channel is idle. There is no activity during these intervals and thus the nodes which are in back-off mode just decrement their back-off counters. When the back-off counter reaches zero, the node transmits its packet. The slot of duration T corresponds to the transmission of a packet. This transmission will succeed if only one node transmits in this slot as there will be a collision if several nodes transmit simultaneously.

The models derived from [128] all introduce τ, the node transmission rate at the beginning of a slot. If no node transmits, this occurs with a probability of $(1-\tau)^M$ thus the current slot will be a mini-slot of duration σ. If at least one node is transmitting, the current slot will be of duration T, which occurs with a probability of $1-(1-\tau)^M$. Thus, the mean duration between two slots will be $(1-(1-\tau)^M)T+(1-\tau)^M\sigma$. This duration is called the duration of a pseudo-slot. It is also possible to compute the throughput t of the system

$$t = \frac{(1-(1-\tau)^M)T}{(1-(1-\tau)^M)T+(1-\tau)^M\sigma}$$

The successful throughput is t_s and is given by

$$t_s = \frac{M\tau(1-\tau)^{M-1}T}{(1-(1-\tau)^M)T+(1-\tau)^M\sigma.} \tag{4.1}$$

and p_s is the probability of successful transmission for a randomly transmitted packet.

$$p_s = \frac{M\tau(1-\tau)^{M-1}}{(1-(1-\tau)^M)} \tag{4.2}$$

Thus, the performance of the network is completely defined if we can compute τ. The models derived from [128] are Markovian models whose states are the value of the back-off counter. When there are retransmissions, the value of the back-off counter is complemented by the number of previous transmissions. The transitions in these models are simple. When the station is in the idle state, the transmission to a back-off state (between 0 and $W-1$) is random with the probability of $1/W$. When the station is in back-off in the state $1 \leq k+1 \leq W$, the transition is towards state k with the probability of $p_e = (1-\tau)^M$, this means that there is no transmission. With probability $1-p_e$ the station with back-off counter $k+1$ remains in the same state. When the back-off counter reaches 0, the state transmission rate to the idle state is 1.

4.3.1 Pure broadcast

We first consider a model without retransmission, which represents the default operation mode of 802.11p. The state diagram of the protocol is presented in Figure 4.1. We denote by b_I the probability that the node is idle and b_i for $0 \leq i \leq W-1$ the

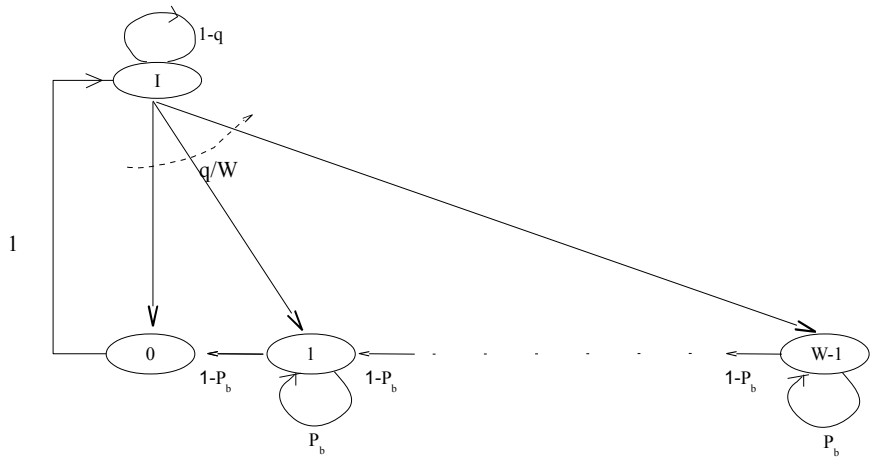

Figure 4.1: State diagram of the IEEE 802.11p simple broadcast scheme with arrival in single buffer with loss.

probability that the node having a pending packet has i mini slots to wait in back-off before the transmission. We can easily write the steady state equation:

$$b_I = b_0 + (1-q)b_I$$

$$b_{W-1} = \frac{b_I(1-q)}{W}$$

$$b_i = (1-P_b)b_{i+1} + \frac{b_I(1-q)}{W} + P_b b_i \text{ for } 0 \leq i \leq W-2.$$

Some easy algebra leads to:

$$qb_I = b_0$$

$$b_{W-k} = \frac{kqb_I}{W(1-P_b)} = \frac{kb_0}{W(1-P_b)} \text{ for } 1 \leq k \leq W-1$$

and the normalization equation can be written as:

$$1 = b_I + \sum_{i=0}^{W-1} b_i = b_0\Big(\frac{1}{q} + 1 + \frac{W-1}{2(1-P_b)}\Big)$$

The resolution of the steady-state of the Markov chain leads to the following equation [127] :

$$b_0 = \tau = \Big(\frac{1}{q} + 1 + \frac{W-1}{2(1-\tau)^M}\Big)^{-1}. \tag{4.3}$$

with:

$$q = 1 - e^{-\lambda((1-(1-\tau)^M)T + (1-\tau)^M\sigma)}. \tag{4.4}$$

where b_0 denotes the probability that the node has a pending packet whose back-off is 0. q denotes the probability of at least one packet arriving during a pseudo-slot. A pseudo slot is a slot of duration equal to the mean duration of a slot on the channel, i.e. σ weighted by the probability of an idle slot plus T weighted by the probability of a transmission slot. Using (4.3) and (4.4) we obtain the following fix-point equation in τ:

$$\tau = \Big(\frac{1}{1 - e^{-\lambda((1-(1-\tau)^M)T + (1-\tau)^M\sigma)}} + 1 + \frac{W-1}{2(1-\tau)^M}\Big)^{-1} \tag{4.5}$$

which can be easily solved numerically. If τ is known via (4.5) then the successful throughput can be easily computed using (4.1).

4.3.2 Broadcast with acknowledgment request

We will also discuss a model with retransmission. The protocol is still broadcast but we will assume that a node requests an acknowledgment from, for example, a random neighbor. If the acknowledgment is sent, the node will transmit another packet. If not, the packet is transmitted again and the collision window is doubled. The collision window reaches 2^nW after n collision. If a packet reaches $n+1$ collisions, the packet is dropped. Thus even if the transmission remains in broadcast mode, the protocol operates as in unicast mode with an acknowledgment. We can apply the model derived in [131] where the collision window doubles until n retransmissions and then remains constant. The resolution of the steady-state of the Markov chain leads to the following equation:

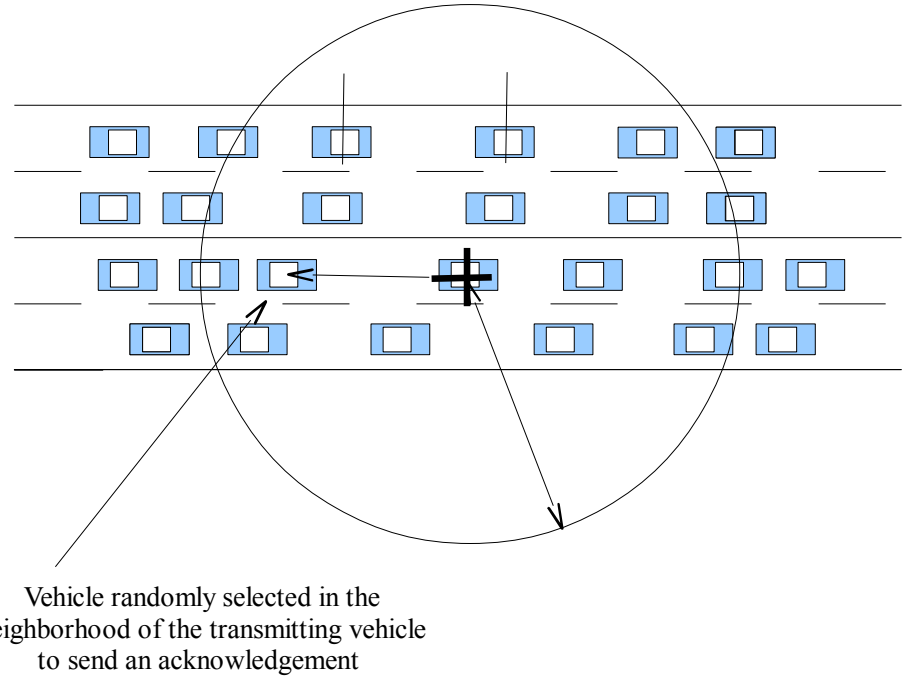

Figure 4.2: A random neighbor is requested to send an acknowledgment.

$$b_0 = \tau = \frac{2(1-2P_{col})q}{q[(W+1)(1-2P_{col}) + WP_{coll}(1-(2P_{coll})^n] + 2(1-q)(1-P_{col})(1-2P_{col})} \quad (4.6)$$

with

$$P_{coll} = 1 - (1-\tau)^{M-1} - (M-1)\tau(1-\tau)^{M-2}. \quad (4.7)$$

where b_0 is again the probability that a node with a pending packet has its back-off reaching 0 and thus starts transmitting. If we use (4.4) and (4.7) in (4.6) we obtain a fix-point equation in τ. The probability of successful transmission for a packet actually sent is:

It is possible to compute the network performance with a similar algorithm. A node still requests an acknowledgment from, for example, a random neighbor but if there is no acknowledgment, the packet is simply retransmitted without any change to the collision window. Equation (4.6) is simply changed into the following equation:

$$\tau = \frac{b_{0,0}}{1 - P_{col}} = \frac{2q}{q(W+1) + 2(1-q)(1-P_{col})} \tag{4.8}$$

As q and P_{col} depends on τ, equation 4.8 is another fix-point equation in τ.

We prove (4.8). The proof is an adaptation of [131]. We use the same notation[2] and use the same transmission state diagram represented in Figure 4.3. The only modification in [131] is in W_i; we have $1 \leq i \leq n$ $W_i = W$ instead of $W_i = 2^i W$.
$b_{i,k}$ denotes the stationary probability that a node waits for a transmission with a back-off counter $k \in [1, W-1]$ for the ith transmission (there have been $i-1$ previous unsuccessful transmission attempts).
We still have $b_{i,0} = P_{col}^i b_{0,0}$ and $b_{n,0} = \frac{P_{col}^n}{1-P_{col}}$. We also have:

$$\begin{aligned} b_I &= (1-q)(1-P_{col}) \sum_{i=0}^{n} b_{i,0} + (1-q) b_I \\ &= \frac{(1-q)(1-P_{col})}{q} \sum_{i=0}^{n} b_{i,0} \\ &= b_{0,0} \frac{1-q}{q}. \end{aligned}$$

For $k \in [1, W]$, the other values of $b_{i,k}$ satisfy the following equations:

$$\begin{aligned} b_{0,k} &= \frac{W-k}{W} \Big(q(1-P_{col}) \sum_{k=0}^{n} b_{i,0} + q b_I \Big) = \frac{W-k}{W} b_{0,0} \\ b_{i,k} &= \frac{W-k}{W} P_{col} \;\; b_{i-1,0} \qquad i \in [1, n-1] \\ b_{n,k} &= \frac{W-k}{W} P_{col} \;\; (b_{n-1,0} + b_{n,0}) \end{aligned}$$

For $i = 0$ we have:

$$\begin{aligned} \sum_{k=1}^{W-1} b_{0,k} &= \sum_{k=1}^{W-1} \frac{W-k}{W} b_{0,0} \\ &= \frac{W-1}{2} b_{0,0} \end{aligned}$$

[2] instead of m used in [131] we use n and instead of P_{eq} we use P_{col} i.e $m->n$ and $P_{eq}->P_{col}$

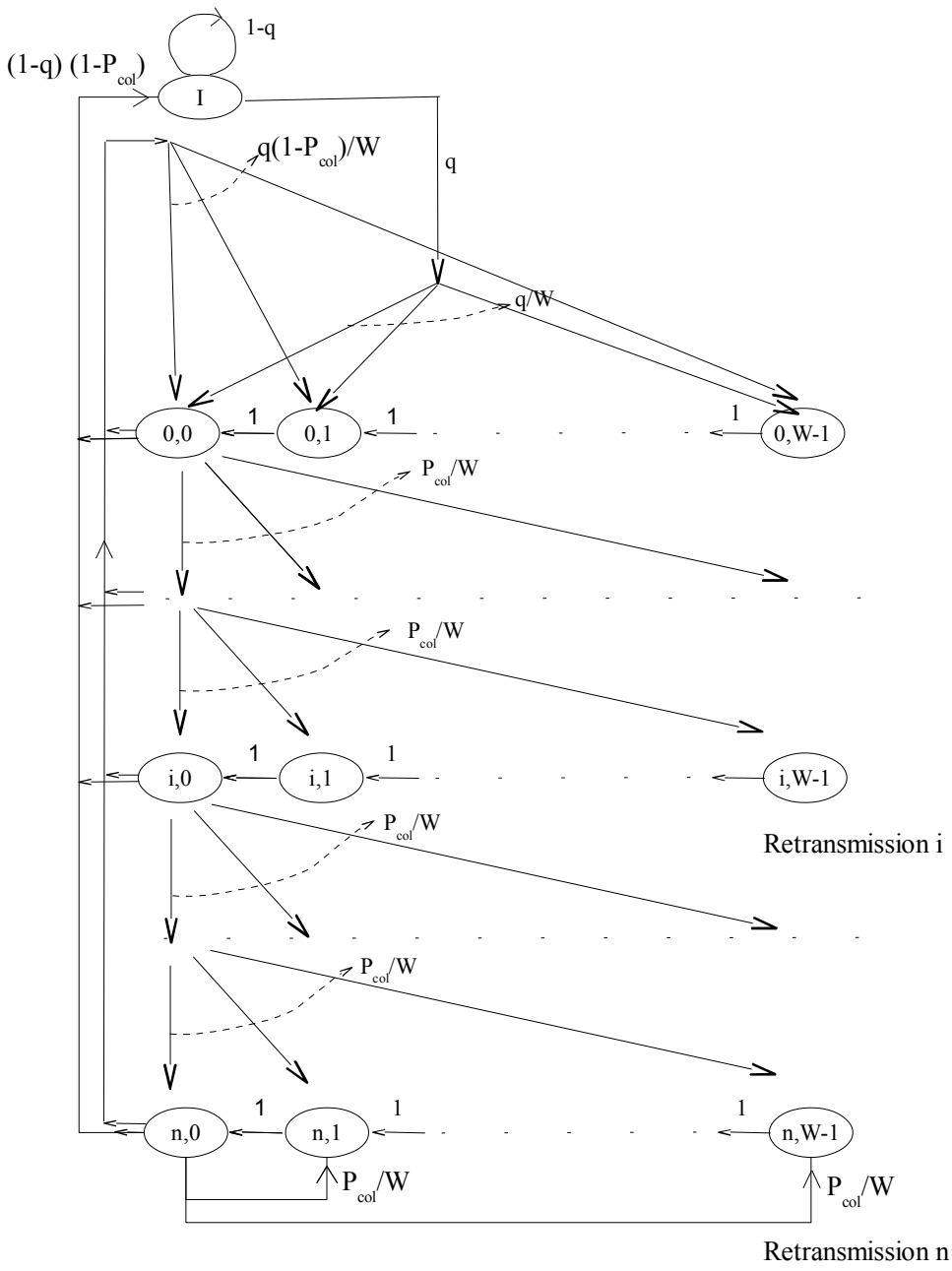

Figure 4.3: State diagram of the back-off scheme with retransmission but with a constant back-off window (no binary exponential back-off).

For $i \in [1, n-1]$ we have:

$$\begin{aligned}\sum_{k=1}^{W-1} b_{i,k} &= \sum_{k=1}^{W-1} \frac{W-k}{W} P_{col} b_{i-1,0} \\ &= \frac{W-1}{2} P_{col} b_{i-1,0} \\ &= \frac{W-1}{2} b_{0,0} P_{col}^{i}\end{aligned}$$

For $i = n$ we have:

$$\begin{aligned}\sum_{k=1}^{W-1} b_{n,k} &= \sum_{k=1}^{W-1} \frac{W-k}{W} P_{col}(b_{n-1,0} + b_{n,0}) \\ &= \frac{W-1}{2} P_{col}(b_{n-1,0} + b_{n,0}) \\ &= \frac{W-1}{2} b_{0,0}\Big(P_{col}^n + \frac{P_{col}^{n+1}}{1-P_{col}}\Big) \\ &= \frac{W-1}{2} \frac{b_{0,0} P_{col}^n}{1-P_{col}}\end{aligned}$$

We also have :

$$\sum_{i=0}^{n} b_{i,0} = \frac{b_{0,0}}{1-P_{col}}$$

After a few simplifications, the normalization condition gives the following fundamental equation:

$$\begin{aligned}1 &= \sum_{i=0}^{n} \sum_{k=0}^{W_i-1} b_{i,k} + b_I \\ &= \frac{b_{0,0}}{2}\Big[W\Big(\sum_{i=0}^{n-1} P_{coll}^i + \frac{P_{coll}^n}{1-P_{col}}\Big) + \frac{1}{1-P_{col}} + \frac{2(1-q)}{q}\Big] \\ &= \frac{b_{0,0}}{2}\Big[W\Big(\sum_{i=0}^{n-1} P_{coll}^i + \frac{P_{coll}^n}{1-P_{col}}\Big) + \frac{1}{1-P_{col}} + \frac{2(1-q)}{q}\Big] \\ &= \frac{b_{0,0}}{2}\Big[\frac{W}{1-P_{col}} + \frac{1}{1-P_{col}} + \frac{2(1-q)}{q}\Big]\end{aligned}$$

Thus we obtain :

$$\frac{b_{0,0}}{1-P_{col}} = \tau = \frac{2q}{q(W+1) + 2(1-q)(1-P_{col})}$$

and that concludes the proof.

4.3.3 Broadcast with n random retransmissions

To improve the probability of successful transmission for a small number of dedicated packets, we propose using random transmissions for these packets. These packets are randomly re-transmitted $n-1$ times, thus, in total, a packet will be transmitted n times. We assume that the number of additional packets due to these retransmissions is negligible and so the station transmission probability is τ given by (4.5). The

probability of successful transmission for a normal packet is t_s which is computed by (4.1). The probability of successful transmission for a packet with n retransmissions is

$$1 - (1 - p_s)^n.$$

4.3.4 Parameters of vehicular networks

We assume that the vehicles are randomly located on nb lanes. In one lane, the mean distance between two vehicles is l. We denote by cs the carrier sense[3], when a node transmits at distance up to cs from the current node the channel is sensed busy, see Figure 4.4. For a distance larger than cs, the channel is sensed idle. Thus, given cs, nb and l we can compute the number of vehicles M within the same carrier sense area.

$$M = \frac{2 \times cs \times nb}{l}. \tag{4.9}$$

We assume that each vehicle periodically sends messages, and even if it is not completely true, we assume that the traffic is Poisson with a mean rate corresponding to the synchronous traffic. The value of M can be used in (4.4), (4.5), (4.6) and (4.8) to compute τ.

In this paper we assume that the M nodes which are within carrier sense range of the current node are those which can create a collision with this node if the current node and another node within this area transmit nearly simultaneously. In this paper we also assume that the transmission from the current node is local [4] so that hidden collisions from nodes outside the carrier sense range are not possible. Thus collisions can only occur when transmissions are simultaneous.

4.4 Results of the models

We use the following figures: the packet inter-arrival time in a node is 100 ms , $\sigma = 77$ bits. The packet size, including the overhead, is $T = 3998$ bits and the data rate is 6

[3] we express the carrier sense in meters but it can also be expressed in Watts or in decibels

[4] for instance the transmission is for the neighbor vehicles

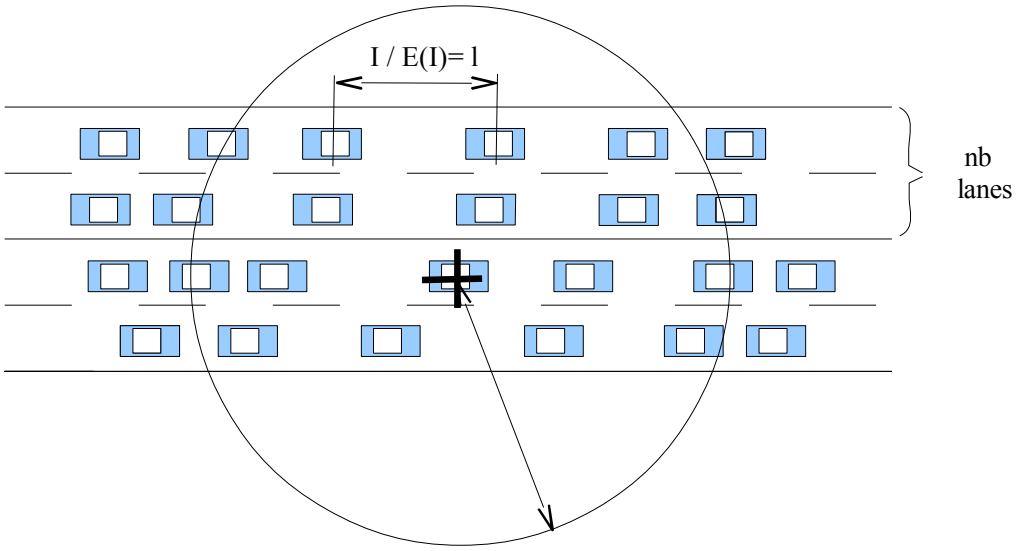

Figure 4.4: Number of vehicles in the carrier sense range of a transmitter.

Mbps thus $\lambda = 1/600000$. We use (if not otherwise defined) $l = 25$ m for the mean distance between two vehicles in a lane. We vary the carrier sense range cs from 300 m to 1400 m.

4.4.1 Effect of the carrier range and the transmission strategy

In this section we vary cs and we study the different transmission strategies.

In Figure 4.5, we present the percentage of success for each broadcast strategy for a transmitted packet. This means that for a transmitted packet we compute the probability that this packet is successfully received. We observe that the acknowledgment procedure has a significant impact on the success rate, especially when the network load is very high.

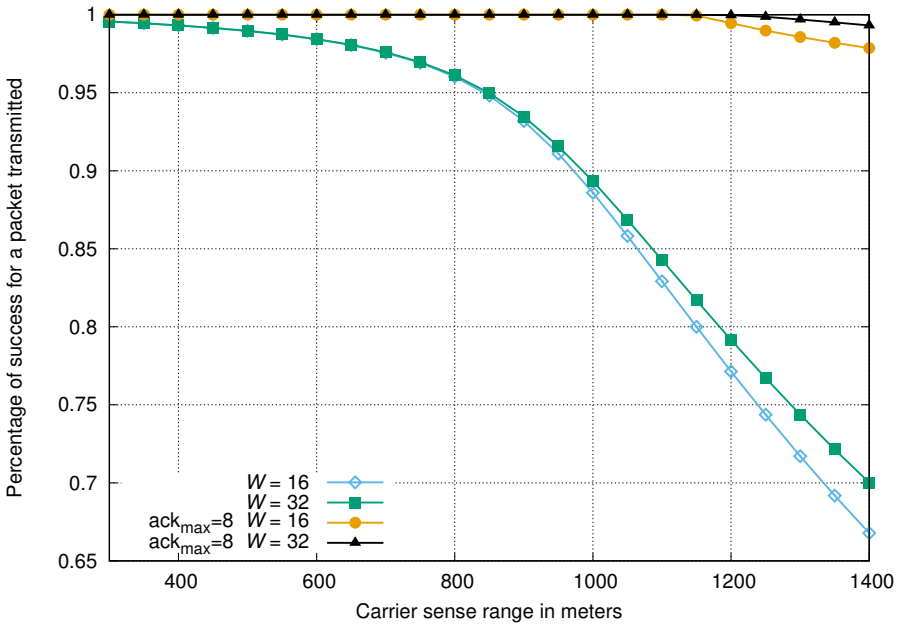

Figure 4.5: Percentage of transmitted packets successfully received.

In Figure 4.6 we present the percentage of successfully transmitted packets. This is the ratio of the number of successfully received packets divided by the number of generated packets. In this ratio we include the loss due to collision and the loss due to the limitation of the total bandwidth. We observe that the techniques using acknowledgments produce a smaller percentage of received packets. This is because managing retransmissions in the techniques using acknowledgments consumes more bandwidth than the others.

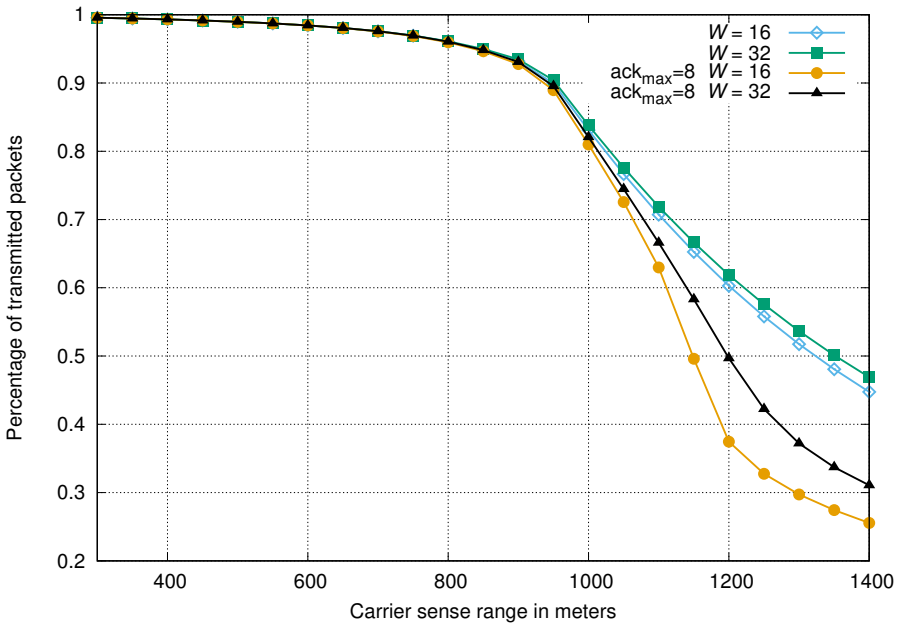

Figure 4.6: Percentage of transmitted packets successfully received versus carrier sense range.

In Figure 4.7 we compare techniques using acknowledgments with and without using the binary exponential back-off. We observe that the percentage of successfully transmitted packets is higher with the binary exponential back-off. This is because this back-off reduces congestion. Without the binary exponential back-off, the model does not compute any stable equilibrium for $cs \geq 1128$ if $W = 16$, for $cs \geq 1179$ if $W = 32$ and for $cs \geq 1304$ if $W = 64$. Actually, we have the same phenomenon with the binary exponential back-off but de-stabilization occurs with larger values of cs. The binary exponential back-off helps reduce congestion when the load increases.

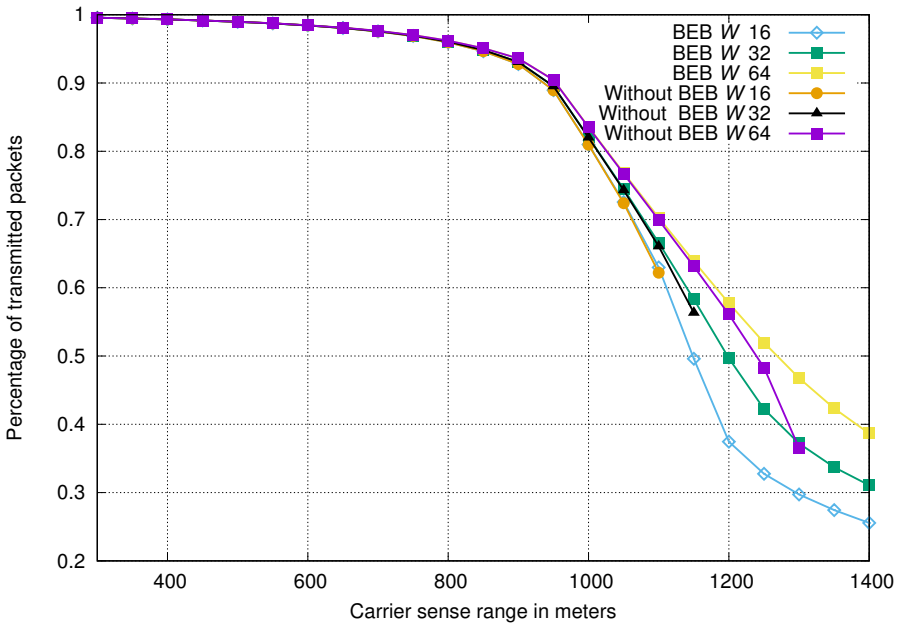

Figure 4.7: Percentage of transmitted packets successfully received versus carrier sense range.

When we have a target for the percentage of successfully transmitted packets, Figures 4.6 and 4.7 can be used to compute the suitable carrier sense range to reach this goal. For instance, if we must satisfy a percentage of successful transmissions greater than 0.95, then we must use a carrier sense range smaller than 800 m.

Figure 4.8 shows the effect of the maximum number of retransmissions on the percentage of successfully transmitted packets. We observe that when n increases, the percentage of successfully transmitted packets also increases, but above a small threshold (n=4) the gain obtained with larger values of n becomes small. Above n=8 there is hardly any advantage in increasing n.

4.4.2 Effect of the distance between the vehicles

In this section, we vary the distance l between the vehicles and we use a simple transmission strategy with a constant back-off window of 32. We consider the following figures cs = 300, 600, 900 or 1200m for the carrier sense range. In Figure 4.9, we observe that for a number of lanes $nb = 6$ and $nb = 8$ the percentage of successfully transmitted packets is low when $cs = 900, 1200$m. Figure 4.9 can also be used to find the suitable network parameters to ensure given performance thresholds.

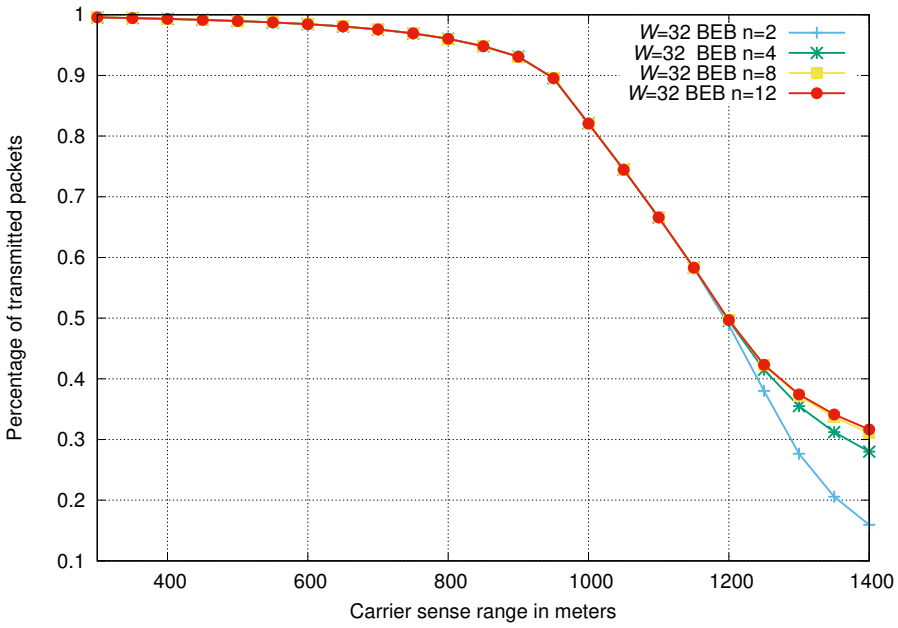

Figure 4.8: Percentage of transmitted packets successfully received versus carrier sense range for various values of n.

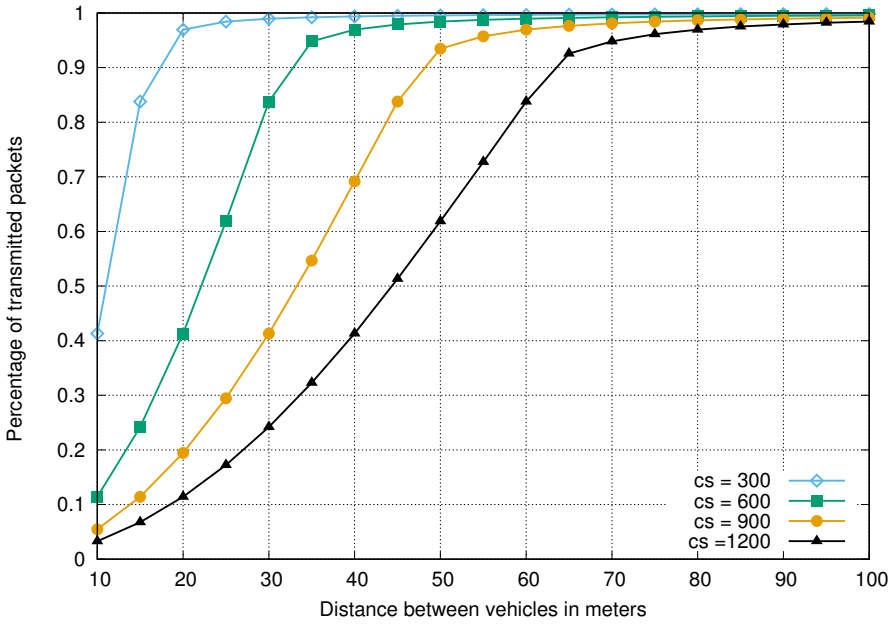

Figure 4.9: Percentage of transmitted packets versus distance between vehicles.

4.4.3 Effect of the number of lanes

In this section, we vary the number of lanes nb. We use a simple transmission strategy with a constant back-off window of 32. We consider the following figures $cs = 300$, 600, 900 and 1200 m for the carrier sense range . In Figure 4.10, we observe that, for $nb = 6$ and $nb = 8$, the percentage of successfully transmitted packets is low when $cs = 900, 1200$ m.

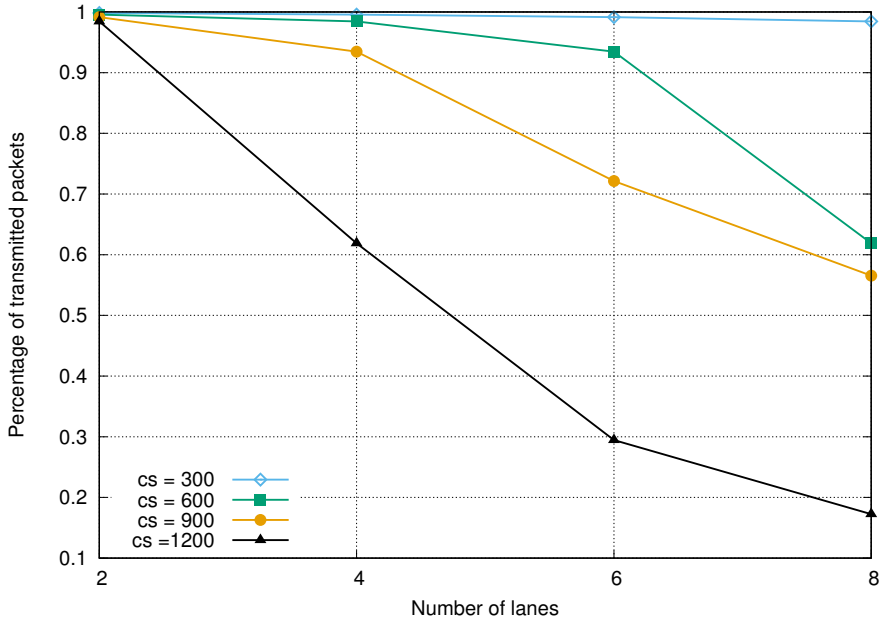

Figure 4.10: Percentage of transmitted packets versus the number of lanes.

In the next section we study how a traffic of high priority (for instance safety messages) can be protected against normal traffic (for instance entertainment traffic). To do so we will use different parameters of the IEEE 802.11p access scheme. We will see that small differences in these parameters can introduce a very significant priority effect.

In the next section we study how IEEE 802.11p can support different classes of priorities.

4.5 System model for the IEEE 802.11p with priorities using different AIFS

The IEEE 802.11p protocol with priority uses different inter frame spacings called AIFSs for Arbitration Inter Frame Spacings to differentiate various classes of traffic. When a node has a pending packet it must first wait for the channel to become idle for a given number A of mini-slots σ before starting to decrement its back-off; this interval of A mini-slots σ is called the AIFS, see Figure 4.11. If the channel becomes busy before this back-off expires, then the node will have to wait for another A mini-slots before starting to decrement its back-off again.

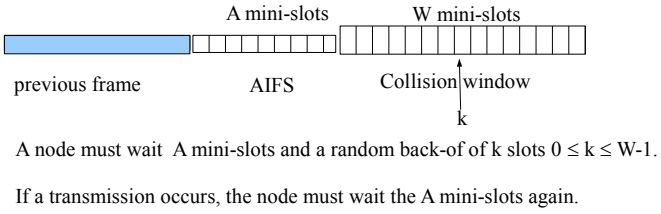

Figure 4.11: Back-off procedure with IEEE 802.11 EDCF scheme.

We first study the steady state of an IEEE 802.11p network which includes the AIFS mechanism.

4.5.1 Steady-state of an IEEE 802.11p with AIFS

The state diagram of IEEE 802.11p with priorities is shown in Figure 4.12.
The state at the top of the diagram represents the probability that the node is idle i.e. without any packet waiting for transmission and we call c_I the probability of the node being in this state at equilibrium.
The A states just below represent the states when the node starts waiting for the AIFS. We denote by c_i for $1 \leq i \leq A$ the probability that the node has waited for i idle slots in the AIFS part of the waiting time before beginning its transmission.
The W states represented horizontally correspond to the back-off states of the node. The state k with $0 \leq k \leq W-1$ represents the state that the node, having already waited for the entire AIFS interval is now in back-off and still has i mini-slots of back-off to wait. We call b_i for $0 \leq k \leq W-1$ the probability that the node

still has k mini-slots to wait before it can access the channel. The states (j, i) $0 \leq j \leq W-1$ $0 \leq i \leq A$ illustrated vertically correspond to the case when a back-off procedure (at stage j) has been interrupted by a transmission and the node has to wait A mini-slots again.

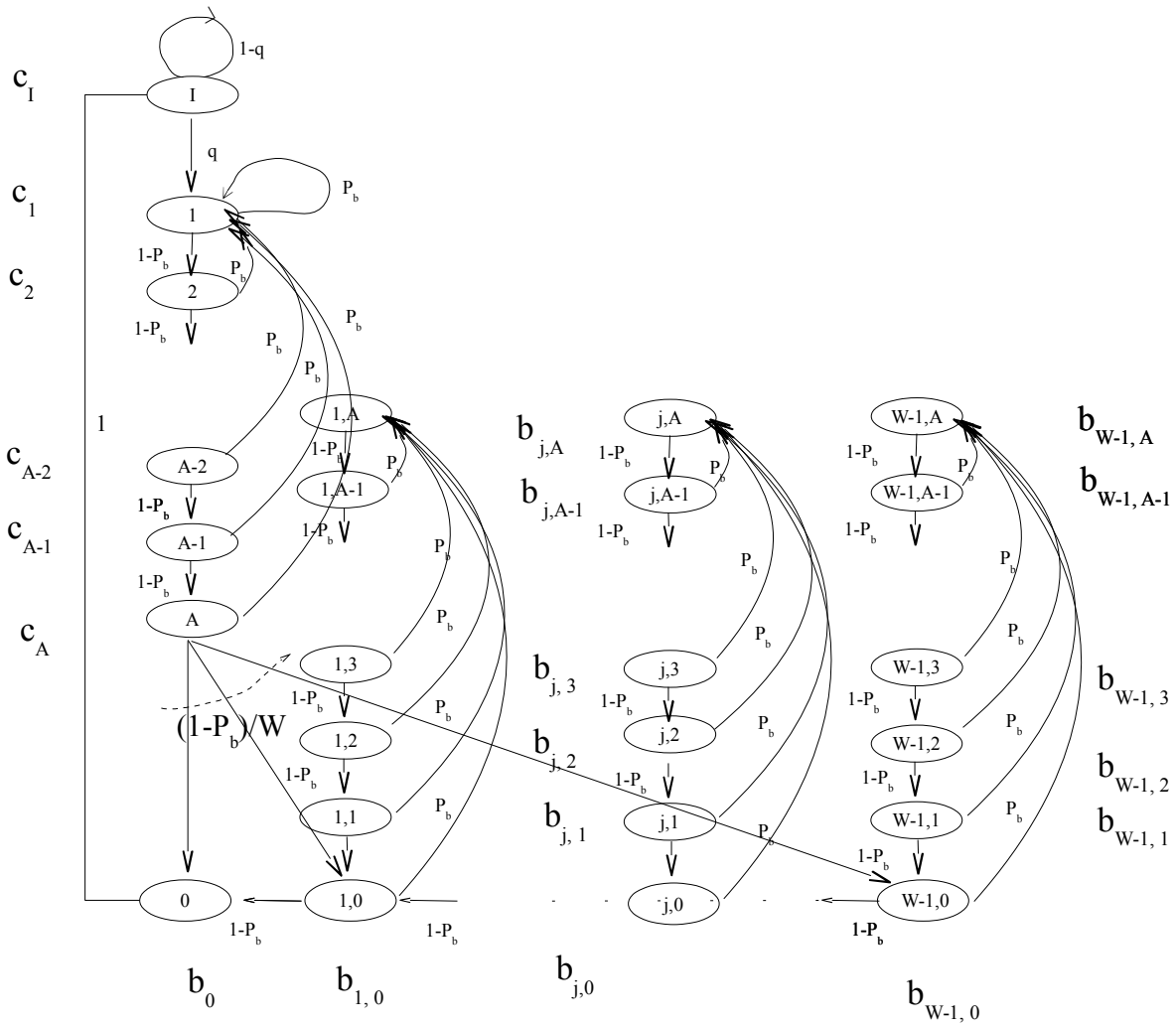

Figure 4.12: State diagram of the back-off scheme with retransmission with AIFS. A contiguous mini-slots must be idle before a transmission can be made and a transmission in one these mini-slots re-starts the whole process.

The transitions are

- when a packet arrives at an idle node, the node starts to wait for the AIFS,
- in the AIFS states, the number of idle slots already sensed increases when the current mini-slot on the channel is idle (with probability $1 - P_b$) and the AIFS

count down must begin again if the transmission of a packet starts in the current mini-slot (with probability P_b),

- in the back-off states, the remaining number of mini-slots that a node must still wait decreases when the current mini-slot on the channel is idle (with probability $1 - P_b$) and the AIFS count down begins again if the transmission of a packet starts in the current mini-slot (with probability P_b),

- when the back-off reaches 0, the pending packet is transmitted and the state of the node becomes the idle state.

We can see all these transitions in Figure 4.12. $c_I, c_1, c_2, \ldots, c_A$, b_0, $b_{i,j}$ $1 \leq i \leq A$, $1 \leq j \leq W-1$ are the steady-state probabilities of the corresponding state. The transitions are shown by arrows and the transition probabilities are indicated, see Figure 4.12.
We analyze the probability flow between state I (probability c_I) and state $(0,0)$ (probability b_0). The equation of the steady state is :

$$(1-q)c_I + b_0 = c_I$$

which is equivalent to

$$qc_I = b_0$$

where q denotes the probability that at least one packet arrives at a node during the mean duration during two observation instants of the Markov chain. The instants at which we observe our Markov chain are at the end of the sensing slots (slots of duration σ) if the channel is empty or after the transmission of a packet (of duration T) if there is a transmission. Thus the mean duration between two instants of observation is $(1-P_b)\sigma + P_bT$ and

$$q = 1 - e^{-\lambda((1-P_b)\sigma + P_bT)}.$$

Writing the equation for the states i for $1 \leq i \leq A$, we obtain:

$$c_i = (1-P_b)^{i-1}c_1 \text{ for } 1 \leq i \leq A.$$

Concerning the states $(W-1, A), (W-1, A-1), \ldots, (W-1, 1), (W-1, 0)$ we have the following equations :

$$b_{W-1,A-i} = (1-P_b)^i b_{W-1,A} \quad 1 \leq i \leq A,$$

and

$$b_{W-1,A} = P_b(b_{W-1,A} + b_{W-1,A-1} \dots b_{W-1,0}),$$

$$b_{W-1,0} = (1 - P_b)b_{W-1,1} + \frac{c_A(1 - P_b)}{W}.$$

Solving these equations, we find:

$$b_{W-1,i} = \frac{P_b}{(1 - P_b)^i}\frac{c_A}{W} \;\; 1 \leq i \leq A,$$

and

$$b_{W-1,0} = \frac{c_A}{W}.$$

Similarly for states $(j, A), (j, A-1), \dots, (j, 1), (j, 0)$ we obtain:

$$b_{W-j,i} = \frac{P_b}{(1 - P_b)^i}\frac{jc_A}{W} \;\; 1 \leq i \leq A, \;\; 1 \leq j \leq W - 1,$$

$$b_{W-j,0} = \frac{jc_A}{W} \;\; 1 \leq j \leq W - 1.$$

We can now compute

$$\sum_{i=0}^{A} b_{j,i} = \frac{1}{(1 - P_b)^A}\frac{jc_A}{W} \;\; 1 \leq j \leq W - 1$$

and thus:

$$\sum_{j=1}^{W-1}\sum_{i=0}^{A} b_{j,i} = \frac{c_A}{(1 - P_b)^A}\frac{W - 1}{2}.$$

$$b_0 = \frac{W - 1}{W}c_A(1 - P_b) + (1 - P_b)\frac{c_A}{W} = (1 - P_b)c_A$$

$$b_0 = (1 - P_b)^A c_1$$

The normalization condition is :

$$\sum_{j=1}^{W-1}\sum_{i=0}^{A} b_{j,i} + b_0 + \sum_{i=1}^{A} c_i + c_I = 1$$

We obtain :

$$c_1\left(\frac{W - 1}{2(1 - P_b)} + (1 - P_b)^A(1 + \frac{1}{q}) + \frac{1 - (1 - P_b)^A}{P_b}\right) = 1$$

and thus :

$$b_0 = \frac{(1-P_b)^A}{\left(\frac{W-1}{2(1-P_b)} + (1-P_b)^A(1+\frac{1}{q}) + \frac{1-(1-P_b)^A}{P_b}\right)} \tag{4.10}$$

This equation is a fixed-point equation in b_0 because $P_b = 1-(1-b_0)^{M-1}$ when there is only one type of node i.e. the same A and W. To check this equation, we observe that when $A = 0$ we obtain the formula which is in [126].
In the next section, we will study two interdependent Markov chains corresponding to coexisting nodes which have different values of A.We now focus on the analysis of a network containing two kinds of nodes that have different AIFSs and operate with different values of A.

4.5.2 Steady-state of the mini-slots observed after the AIFS

We propose to mix nodes using different AIFSs. Although it is possible to build a model with more than two AIFSs, we will present the computation for only two different AIFSs. We consider the traffic with the highest priority with an AIFS A_1 and a collision window W_1 and the low priority traffic with an AIFS $A_2 > A_1$ and a collision window W_2. We set $L_1 = A_2 - A_1$ and $L_2 = min(W_1, W_2) - L_1$.
In Figure 4.13 we show the state to experience i idle mini-slots after an AIFS of A_1 mini-slots. We have a transition rate of $1-p_b$ from state i to state $i+1$ for $i \leq L_1$ and a transition rate of $1-p'_b$ from state i to state $i+1$ for $0 \leq L_1 \leq i \leq L_1 + L_2$. p_b corresponds to the probability of a busy slot when only the high priority traffic can send packets and p'_b (with $p'_b > p_b$ corresponds to the probability of the current mini-slot being busy when both high and low priority traffics can send packets.

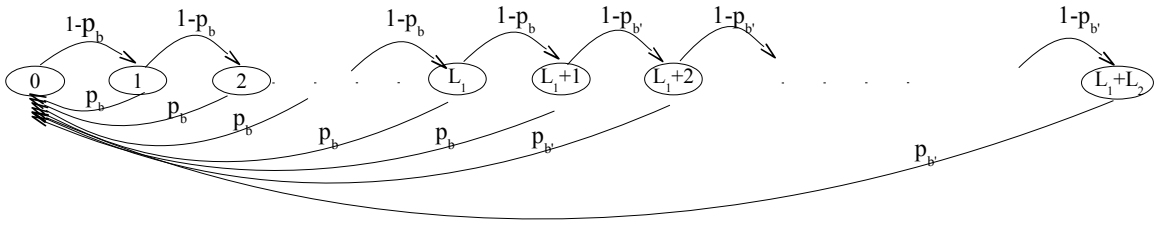

Figure 4.13: State diagram of the state of the channel after the end of a transmission and A_1 mini-slots.

Let d_i with $0 \leq i \leq L_1 + L_2$ be the steady-state probability of state i. We have:

$$d_i = (1-p_b)^i d_0 \text{ with } 0 \leq i \leq L_1 + 1$$

$$d_i = (1-p_b)^{L_1+1}(1-p'_b)^{i-L_i+1}d_0 \text{ with } L_1+2 \leq i \leq L_1+L_2+1$$

Thus the probability of being in the first part of the back-off window (L_1 first mini-slots) is:

$$p_1 = \frac{1-(1-p_b)^{L_1+1}}{p_b}\left(\frac{1-(1-p_b)^{L_1+1}}{p_b} + (1-p_b)^{L_1+1}\frac{1-(1-p'_b)^{L_2+1}}{p'_b}\right)^{-1}.$$

The probability of being in the second part of the back-off windows (L_2 last mini-slots) is:

$$p_2 = (1-p_b)^{L_1+1}\frac{1-(1-p'_b)^{L_2+1}}{p'_b}\left(\frac{1-(1-p_b)^{L_1+1}}{p_b} + (1-p_b)^{L_1+1}\frac{1-(1-p'_b)^{L_2+1}}{p'_b}\right)^{-1}$$

p_1 and p_2 can be used to weight the different back-off situations.

4.6 Results of the model for the IEEE 802.11 with priorities

We use the previous model to compute the effect of the AIFS with two populations of M vehicles and we use the same figures i.e. packet inter-arrival in a node: 100 ms, $\sigma = 77$ bits. The packet size, including the overhead, is $T = 3998$ bits and the data rate is 6 Mbps thus $\lambda = 1/600000$. We use (if not otherwise specified) $l = 25$ m for the mean distance between two vehicles in a lane and we vary the carrier sense range to modify the number M of contending vehicles.

The first type of the M_1vehicles uses an IEEE 802.11 access with an AIFS with A=1 slots and $W = 31$. The second type of the M_2 vehicles uses an IEEE 802.11 access with an AIFS with A=6 slots and $W = 31$. We thus have $2M$ vehicles contending for access.

For the first type of vehicles we call τ_1 the transmission rate in the steady state. For the second type of vehicles we call τ_2 the transmission rate in the steady state. Thus we have equation 4.10 with $b_0 = \tau_1$, $P_b = 1-(1-\tau_1)^{M_1-1}(1-\tau_2)^{M_2-1}$, $A = 1$, $W = 32$ for the first type of vehicles. We have equation 4.10 with $b_0 = \tau_2$ and $P_b = 1-(1-\tau_1)^{M_1-1}(1-\tau_2)^{M_2-1}$, $A = 6$, $W = 32$ for the second type of vehicles. Thus we have two non-linear equations in τ_1 and τ_2 that must be solved numerically. We use Maple to perform this task.

We now use the analysis developed in subsection 4.5.2. The part of the back-off window with only the high traffic contains 5 mini-slots and we still have 26 mini-slots to complete the back-off window. We are not taking into account the last 5 mini-slots of the back-off window where there are only arrivals of low priority traffic.

Thus we have $L_1 = 5$ and $L_2 = 26$, $p_b = 1-(1-\tau_1)^{M_1-1}$ and $p'_b = 1-(1-\tau_1)^{M_1-1}(1-\tau_2)^{M_2-1} = P_b$.

We can compute the success rate for a node of the first kind of vehicles. In the first part of the back-off window the transmission is successful when exactly one high priority vehicle transmits. In the second part of the back-off the transmission is successful when exactly one high priority vehicle transmits and no low priority vehicle transmits. Thus the success rate for the high priority vehicles can be written as

$$succ_1 = p_1 M\tau_1(1-\tau_1)^{M-1} + p_2 M\tau_1(1-\tau_1)^{M-1}(1-\tau_1)^{M-1}$$

For the low priority vehicles the success rate is simply:

$$succ_2 = M\tau_2(1-\tau_2)^{M-1}(1-\tau_1)^{M}$$

The normalized throughput for the high priority vehicles is :

$$thr_1 = \frac{succ_1 T}{P_b T + \sigma(1-P_b)}$$

The normalized throughput for the low priority vehicles is :

$$thr_2 = \frac{succ_2 T}{P_b T + \sigma(1-P_b)}$$

In Figure 4.14, we show the probability of success for the two classes of traffic, i.e., the probability that a transmitted packet is actually received. When the carrier sense range increases, more vehicles are in the same contention area and thus the probability of success tends to decrease. We observe that the EDCF scheme with $A = 1$ and $A = 6$ creates two classes of traffic which have different probabilities of success. However, even when the carrier sense range is large, the difference in success probabilities remains modest: around 15%.

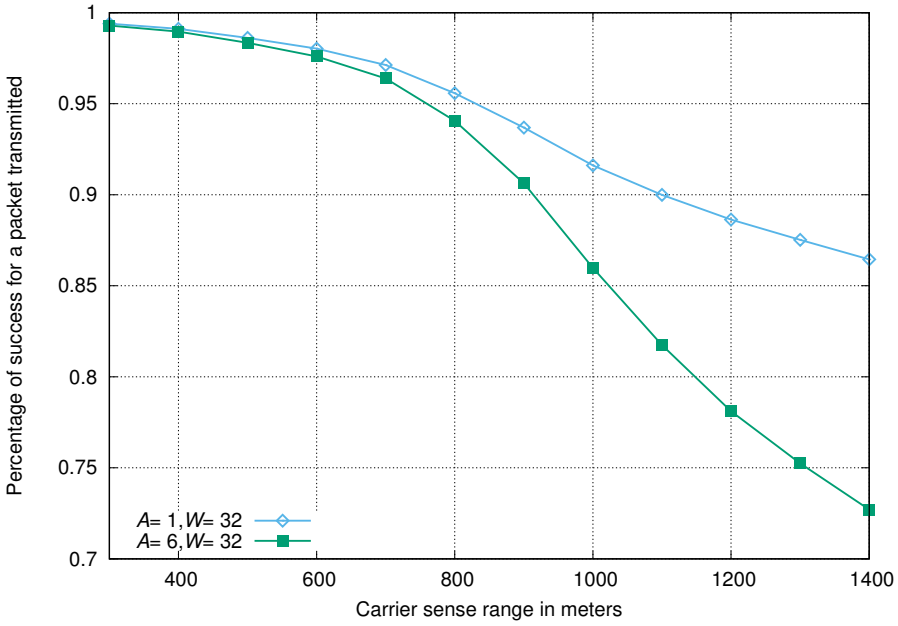

Figure 4.14: Percentage of successful transmissions for both kinds of traffic with different AIFS values.

In Figure 4.15, we show the actual throughput for the two classes of traffic with the EDCF scheme with $A = 1$ and $A = 6$. In contrast to what we note for the probability of success, the EDCF scheme creates two very different classes of traffic. When the carrier sense range increases above 900 m the class of traffic with $A = 1$ continues to increase its throughput whereas the class of traffic with $A = 6$ starts to decrease its throughput. The scheme operates as if the low priority traffic vanishes in order to leave room for the high priority traffic.

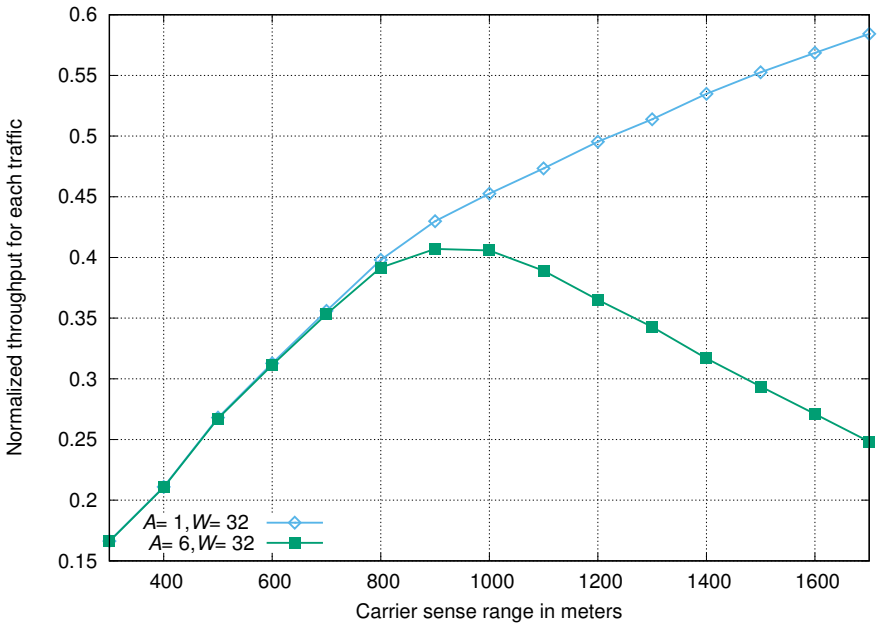

Figure 4.15: Throughput for both kinds of traffic with different AIFS values.

In Figure 4.16, we study the effect of varying the values of A on the performance. We study three cases: two classes of traffic with $A = 1$ and $A = 6$, two classes of traffic with $A = 1$ and $A = 8$ and finally two classes of traffic with $A = 1$ and $A = 10$. Surprisingly, we observe that increasing the difference between the two values of A actually reduces the difference between the success rates. Moreover the average success rate is larger when the difference between the two values of A increases.

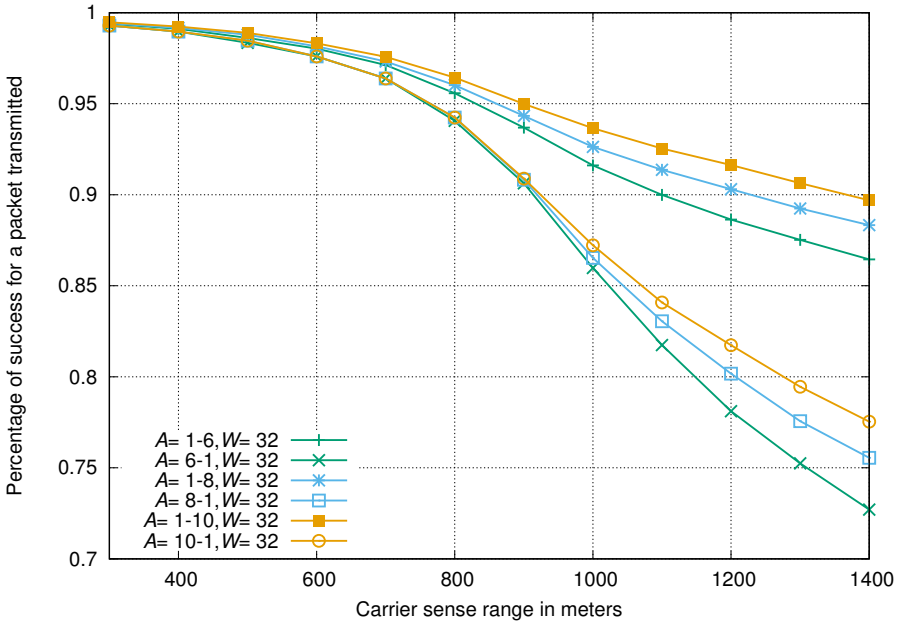

Figure 4.16: Percentage of successful transmissions for both kinds of traffic with different AIFS values. The effect of different values of A. The notation A=1-6 means that we show the performance of a traffic using A=1 while the concurrent trafic uses A =6. Identical remarks for A=1-8 and A=1-10.

In Figure 4.17, we study the effect of varying the values of A on the throughput. We study three cases: two classes of traffic with $A = 1$ and $A = 6$, two classes of traffic with $A = 1$ and $A = 8$ and finally two classes of traffic with $A = 1$ and $A = 10$. This time, the result can be predicted, when the difference between the two values of A increases, the difference between the throughput of the two traffics also tends to increase.

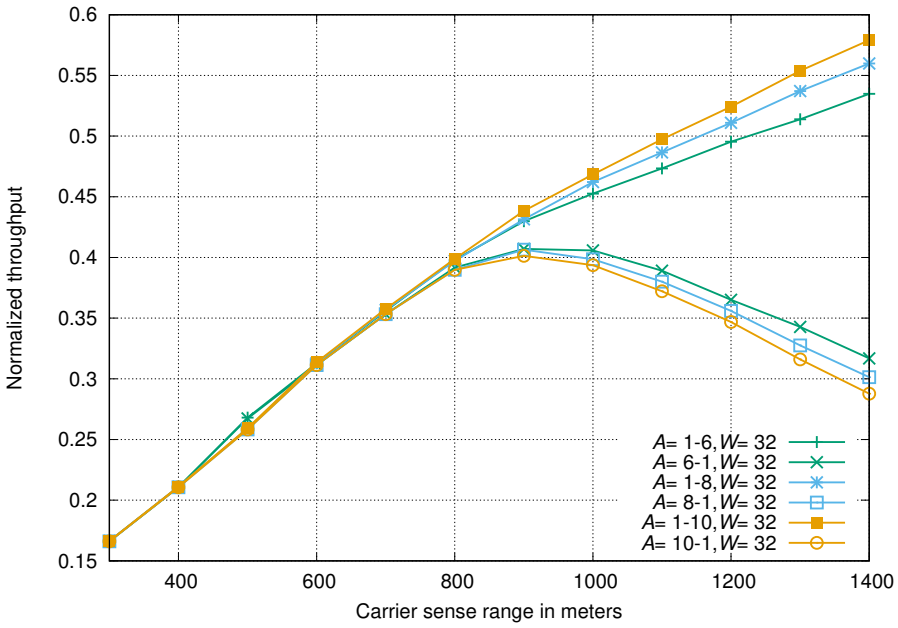

Figure 4.17: Throughput for both kinds of traffic with different AIFS values. The effect of different values of A. The notation A=1-6 means that we show the performance of a traffic using A=1 while the concurrent trafic uses A =6. Identical remarks for A=1-8 and A=1-10.

In Figure 4.18, we compare the effect of varying the values of A and varying the values of W on the percentage of successful transmissions. We set up a network with two types of vehicles, one using $A = 1$ and the other $A = 6$, both with $W = 32$ and another network with two types of vehicles, one using $W = 8$ and the other $W = 64$, both with $A = 1$. We observe that the differentiation obtained by varying the values of A is much greater than that obtained by varying the values of W.

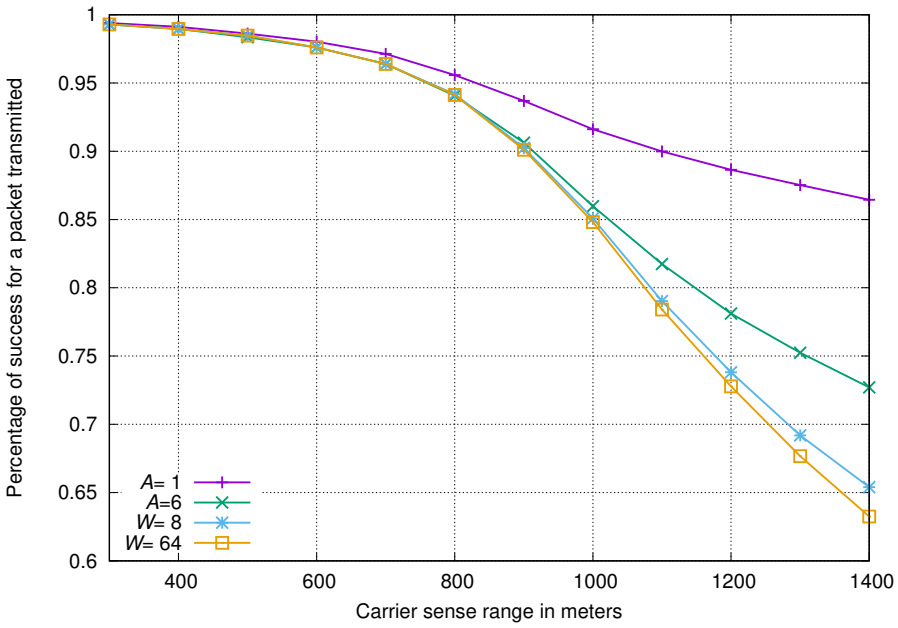

Figure 4.18: Percentage of successful transmissions for both kinds of traffic. Comparison between varying A and varying W

In Figure 4.19, we compare the effect of varying the values of A and varying the values of W on normalized throughput. We compare a network with two types of vehicles, one using $A = 1$ and the other $A = 6$, both with $W = 32$ and another network with two types of vehicles, one using $W = 8$ and the other $W = 64$, both with $A = 1$. We observe that the differentiation obtained by varying the values of A is much greater than that obtained by varying the values of W.

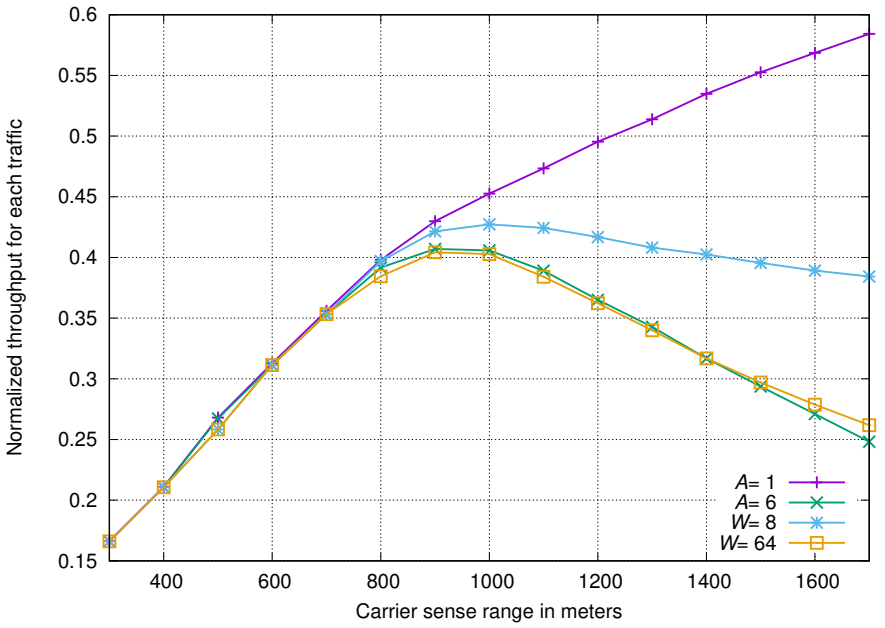

Figure 4.19: Throughput for both kinds of traffic with different AIFS values. Comparison between varying A and varying W

4.7 Conclusion

In this chapter, we have shown that simple models allow network performance of IEEE 802.11p to be analyzed. If we are able to estimate the important parameters of a VANET : packet generation rate, packet length, distance between vehicles, number of lanes, carrier sense range, we can easily evaluate the success rate of a random transmission. We have studied various transmission techniques, both with and without acknowledgments. We have shown that using acknowledgments incurs overhead which degrades the overall performance of the network in terms of packets successfully transmitted, while it improves the success rate of actually transmitted packets. A feasible solution could be to use the simple scheme without any acknowledgment but a few blind transmissions of the same packet could be performed when this packet contains very important information. In this way, we would obtain the same effect as with a transmission with an acknowledgment request.

We have developed an analytical model to study the effect of varying the inter-frame spacing A and the collision window W. We have shown that the differentiation obtained when we vary the inter-frame spacing is very significant and thus can be used to protect urgent traffic against less vital information.

Part III

Model of spatial CSMA. Application to VANETs

Chapter 5

Optimisation of spatial CSMA using a simple stochastic geometry model for 1D and 2D networks

Contents

5.1 Executive summary

In modern wireless networks, especially in Machine-to-Machine (M2M) systems and the Internet of Things (IoT), there are high densities of users and spatial reuse has become an absolute necessity for telecommunication entities. This chapter studies the maximum throughput of Carrier Sense Multiple Access (CSMA) in scenarios with spatial reuse. Instead of running extensive simulations with complex tools which would be somewhat time consuming, we evaluate the spatial throughput of a CSMA network using a simple model which produces closed formulas and gives nearly instantaneous values. This simple model allows us to optimize the network easily and study the influence of the main network parameters. The nodes will be deployed as a Poisson Point Process (PPP) of a one- or two-dimensional space. To model the effect of (CSMA), we give random marks to our nodes and to elect transmitting nodes in the PPP we choose those with the smallest marks in their neighborhood. To describe the signal propagation, we use a signal with power-law decay and we add a random Rayleigh fading. To decide whether or not a transmission is successful, we adopt the Signal-over-Interference Ratio (SIR) model in which a packet is correctly received if its transmission power divided by the interference power is above a capture threshold. We assume that each node in our PPP has a random receiver at a typical distance from the transmitter, i.e., the average distance between a node and its closest neighbor. We also assume that all the network nodes always have a pending packet. With all these assumptions, we analytically study the density of throughput of successful transmissions and we show that it can be optimized with regard to the carrier-sense threshold.

5.2 Introduction

At the end of the twentieth century, the most common wireless networks were WiFi (IEEE 802.11) networks. The dominant architecture of such networks involved an access point where a node, called the access point, generally connected to the Internet, exchanged packets with surrounding nodes. In these networks only one packet was sent at each instant since all the nodes were within carrier sense range of the other nodes and sent their packets one after the other. More recently, great progress in wireless transmission technology has paved the way to much bigger networks with more massive transmission patterns. In these networks, which include military networks, Vehicular Ad Hoc Networks (VANETs), and Wireless Sensor Networks (WSNs), applications require simultaneous transmissions and thus the model with only one access point is no longer valid. The transmissions can be multihop, for instance in military networks or WSNs, and thus the same packet must be forwarded. In this case, and especially when there are long routes, simultaneous transmissions will increase the performance. This phenomenon is known as spatial reuse. In VANETs, extending the networks along roads leads to vast networks where spatial reuse must inevitably be present. The high density of communicating vehicles on a road using IEEE 802.11p - a CSMA-based protocol - justifies the optimization of CSMA in networks with spatial reuse.

However, the access techniques used in these recent networks remain similar to those used in the first Wireless LANs (WLANs) and are based on the well-known Carrier Sense Multiple Access techniques (CSMA). In M2M systems and in the IoT a prominent technology is IEEE 802.15.4, which is also based on CSMA.

Therefore, a deeper understanding of CSMA with spatial reuse is needed and represents the main focus of this chapter. There are two main characteristics to be evaluated in spatial CSMA. The first one is to compute the probability of transmitting when the carrier sense rule is applied. The second one is to compute the probability of the packet being correctly received by a neighbor.

The remainder of this chapter is organized as follows. Section 5.3 briefly reviews related work; Section 5.4 describes the model proposed to study CSMA and develops the corresponding analytical model. The results of the model evaluating the influence of the parameters are reported in Section 5.5. Section 5.6 compares the results of model with those obtained with simulations. Finally Section 5.7 concludes the chapter.

5.3 Related work

The initial studies on CSMA date back to the mid-seventies with the seminal paper by Kleinrock [132]. That paper, together with a great number of papers using the same analytical model framework, analyzed a perfect CSMA where all the nodes are within carrier-sense range of each-other. The framework developed in [132] accurately models the carrier sense access technique but the analysis of the back-off technique remains somewhat fuzzy. In 2000, the paper by Bianchi [128] relating to the IEEE 802.11 access technique took a step further in the modeling of the CSMA backoff technique. However the model still considers a one-hop wireless network, and thus spatial reuse remained beyond the scope of the paper.

The first tentative work which tried to take into account spatial reuse in spatial networks was reported in articles devoted to Aloha such as [165] and [157]. In 1988, Ghez, Verdu and Schwartz introduced a model for slotted Aloha [165] with multi-packet reception capability. To our knowledge this paper was the first quantitative model of a wireless network with spatial reuse. This model was revisited in [157] with a more accurate evaluation of the performance of the network. In [157] Baccelli et al. show that it is possible to accurately compute the probability of successful transmission in an Aloha network with spatial reuse if the distance between the transmitter and the receiver is known. [157] also allows the density of successful transmissions to be computed if the distance between the transmitter and the receiver is known. In Aloha networks, the complete and stateless randomization of the transmitters leads to a particularly simple evaluation of the pattern of the simultaneously transmitting nodes.

In [166] the authors compute the mean number of transmissions with CSMA in a linear random network of vehicles but, in contrast to the present study which takes into account the entire interference, [166] only considers the nearest interferer.

The Matern selection process [168] was first used in [167] to evaluate the pattern of simultaneous transmissions in CSMA. The study in [169] uses a process close to the Matern process to evaluate the interference in CSMA spatial networks but it does not study the throughput of the network, which is the main purpose of this chapter. Finally, the model of [167] was improved by [170], which is the model that is used and extended in this chapter. Apparently, no further improvements in this field have been made in recent years.

Although a few papers [141], [140] have studied the effect of the carrier sense detection

threshold in CSMA protocols, these papers do not explore the spatial effect of the carrier sense detection threshold but rather the probability of capture when all the nodes are at one hop from each other.

5.4 System model

5.4.1 Network nodes

The nodes are randomly deployed according to a Poisson Point Process Φ. We denote by λ the intensity of the process. In this paper we consider a 2D infinite plane, $\mathcal{S} = \mathbb{R}^2$ or a 1D infinite line, $\mathcal{S} = \mathbb{R}$. The 2D model is for Mobile Ad-hoc NETworks (MANETs) or Wireless Sensor Networks (WSNs). The 1D model is more relevant to Vehicular Ad-hoc NETworks (VANETs).

5.4.2 Propagation law, fading and capture model

We suppose that the signal received in a transmission is the result of a random fading F and a power-law in the distance decay $1/r^\beta$ where β is the decay factor and is generally between 3 and 6. In our study, the fading will be Rayleigh, i.e., exponentially distributed with parameter μ and thus is of mean $1/\mu$. Therefore the signal received when the transmitter and the receiver are at distance r from each other is $F/l(r)$[1] with $l(r) = r^\beta$.

We use the well-accepted SIR[2] (Signal over Interference Ratio) with a capture threshold T.

5.4.3 Model for CSMA

Using the model developed in [170], we adopt a Matern selection process to mimic the CSMA selection process. The points X_i in Φ receive a random mark m_i. We also call $F_{i,j}$ the fading for the transmission between X_i and X_j . The idea of the Matern selection is to select the points X_i with the smallest random marks m_i in their

[1]The power received $P = \frac{P_0 F}{l(r)}$ and we set $P_0 = 1$

[2]We omit the thermal noise but it could be easily added, as explained below. An even more realistic model than the SIR based on a graded SIR model using Shannon's law is possible in our framework though with an increased computational cost. This will be discussed below.

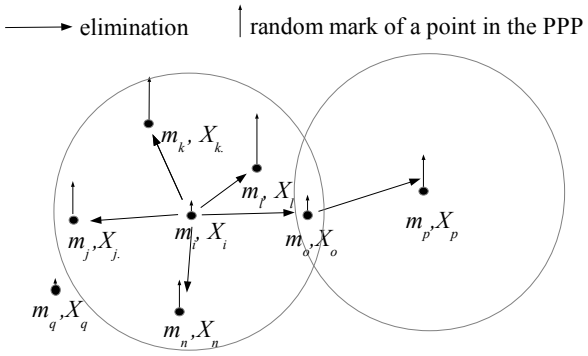

Figure 5.4.1: Matern CSMA selection process and an example of over-elimination.

neighborhood. To define the neighborhood of a point X_i we need to introduce the carrier sense threshold P_{cs}. We define $\mathcal{V}(X_i) = \{X_j \in X_i \ F_{i,j}/l(|X_i - X_j|) > P_{cs}\}$ the neighborhood of X_i. X_i will be selected in the Matern selection process if and only if $\forall X_j \in \mathcal{V}(X_i) \ \ m_i < m_j$. In other words, this means that X_i has the smallest mark m_i in its neighborhood. The Matern selection is illustrated in Figure 5.4.1. Node i has the smallest mark m_i within its neighborhood. Although node q does in fact have a smaller mark, it is not within node i's neighborhood. We should point out that, for the sake of simplicity, here we have not taken into account any Rayleigh fading ($F \equiv 1$) and thus the neighborhood of node i is a disc.

The technique based on marks used by the Matern selection process results in an over-elimination of nodes. When a node is eliminated by a node with a smaller mark, the node which has the smallest back-off in its neighborhood can start transmitting. The nodes which have been eliminated should not further eliminate other nodes. But this over-elimination can occur, as shown in Figure 5.4.1. Node o is eliminated by node i, but node o eliminates node p in the Matern selection process, whereas in a CSMA system, node o is correctly eliminated by node i, but, having being eliminated, node o can not eliminate another node. We do not take this case into account in our model.

We note the medium access indicator of node X_i $e_i = \mathbb{1}_{\{(\forall X_j \in \mathcal{V}(X_i) \ \ m_i < m_j\}})$

Proposition 5.4.1 *The mean number of neighbors of a node is:*

$$\mathcal{N} = \lambda \int_{\mathcal{S}} P\{F \geqslant P_{cs} l(|x|)\} dx.$$

In a 2D network we have :

$$\mathcal{N} = \frac{2\pi\lambda\Gamma(2/\beta)}{\beta(P_{cs}\mu)^{2/\beta}}.$$

In a 1D network we have :

$$\mathcal{N} = \frac{2\lambda\Gamma(1/\beta)}{\beta(P_{cs}\mu)^{1/\beta}}.$$

This result is very simple. Let F_j^0 be the fading between the node at the origin X_i and node X_j

This is just the application of Slivnyak's theorem and Campbell's formula, see [170, 172]

$$\begin{aligned}\mathcal{N} = & \quad E^0\Big[\sum_{X_j\in\phi} \mathbb{1}_{\{()}F_j^0 l(|X_j - X_i|) \geqslant P_{cs}\Big] \\ = & \quad \lambda\int_{\mathcal{S}} P\{F \geqslant P_{cs}l(|x|)\}dx\end{aligned}$$

A straightforward computation provides the explicit value of $\mathcal{N}$ in the 1D and 2D cases.

Proposition 5.4.2 *The probability p that a given node X_0 transmits i.e. $e_0 = 1$ is:*

$$p = \mathbf{E}^0[e_0] = \frac{1 - e^{-\mathcal{N}}}{\mathcal{N}}.$$

Proof: The proof is obtained by computing the probability that a given node X_0 at the origin with a mark $m = t$ is allowed to transmit. The result is then obtained by deconditioning on t. The details of the proof can be found in [170]. ■

Thus p measures the probability of transmission in a CSMA network. If p is close to 1 this means that the carrier sense does not restrain transmissions. In contrast, if p is small, this means that the carrier sense imposes a severe restriction on transmissions.

Proposition 5.4.3 *The probability that X_0 transmits given that there is another node $X_j \in \Phi$ at distance r is p_r with*

$$p_r = p - e^{-P_{cs}\mu l(r)}\big(\frac{1 - e^{-\mathcal{N}}}{\mathcal{N}^2} - \frac{e^{-\mathcal{N}}}{\mathcal{N}}\big)$$

Proof: The proof is the same as that of Proposition 5.4.2. ■

Proposition 5.4.4 *Let us suppose that X_1 and X_2 are two points in Φ such that $|X_1 - X_2| = r$. We suppose that node X_2 is retained by the selection process. The probability that X_1 is also retained is:*

$$h(r) = \frac{\frac{2}{b(r)-\mathcal{N}}\big(\frac{1-e^{-\mathcal{N}}}{\mathcal{N}} - \frac{1-e^{-b(r)}}{b(r)}\big)(1 - e^{-P_{cs}\mu l(r)})}{\frac{1-e^{-\mathcal{N}}}{\mathcal{N}} - e^{-P_{cs}\mu l(r)}\big(\frac{1-e^{-\mathcal{N}}}{\mathcal{N}^2} - \frac{e^{-\mathcal{N}}}{\mathcal{N}}\big)}$$

with

$$b(r) = 2\mathcal{N} - \lambda \int_{\mathcal{S}} e^{-P_{cs}\mu(l(|x|)+l(|r-x|)} dx.$$

In a 2D network, we have:

$$b(r) = 2\mathcal{N} - \lambda \int_0^{\infty} \int_0^{2\pi} e^{-P_{cs}\mu(l(\tau)+l(\sqrt{\tau^2+r^2-2r\tau cos(\theta)}))} d\tau d\theta.$$

In a 1D network, we have:

$$b(r) = 2\mathcal{N} - \lambda \int_{-\infty}^{\infty} e^{-P_{cs}\mu(l(\tau)+l(|r-\tau|))} d\tau$$

Proof: The proof can be found in [170] ■

Proposition 5.4.5 *Given the transmission of a packet, we denote by $p_c(r, P_{cs})$ the probability of this packet being successfully received at distance r in a CSMA system (modeled by a Matern selection process with a carrier sense threshold P_{cs}) and with a capture threshold T. We have:*

$$p_c(r, P_{cs}) \simeq \exp\Big(- \lambda \int_{\mathcal{S}} \frac{h(|x|)}{1 + \frac{l(|x-r|)}{Tl(r)}} dx \Big)$$

In a 2D network, we have:

$$p_c(r, P_{cs}) \simeq \exp\Big(- \lambda \int_0^{\infty} \int_0^{2\pi} \frac{\tau h(\tau)}{1 + \frac{l(\sqrt{\tau^+ r^2 - 2r\tau cos(\theta)})}{Tl(r)}} d\tau d\theta \Big)$$

In a 1D network, we have:

$$p_c(r, P_{cs}) \simeq \exp\Big(- \lambda \int_{-\infty}^{\infty} \frac{h(\tau)}{1 + \frac{l(|r-\tau|)}{Tl(r)}} d\tau \Big)$$

Proof: The idea of the proof is to consider a transmitter at the origin and to compute the probability of successful reception by a receiver at distance r. To do so, we condition by the presence of another transmitting node at distance τ. According to proposition 7.4.6, the density of such nodes is $\lambda h(\tau)$. We approximate the interference by the interference of a Poisson Process of density $\lambda h(\tau)$. The result is obtained by integrating on τ. The details of the proof can be found in [170]. ■

It is easy to add a thermal noise W to the model. The expression of $p_c(r, P_{cs})$ must then be multiplied by $\mathcal{L}_W(\mu T l(r))$ where $\mathcal{L}_W(.)$ is the Laplace Transform of the noise.

In a more advanced model using Shannon's law, we have the average transmission rate for X_0

$$\mathbf{E}^0(\log(1+SIR)|e_0=1) = \int_0^\infty P^0(\log(1+SIR) > t|e_0=1)dt$$
$$= \int_0^\infty p_c(r, P_{cs}, e^t-1)dt$$

with $p_c(r, P_{cs}, x) = p_c(r, P_{cs})$ where T is substituted by x, see [170]. Although more complicated, such an approach seems computationally achievable, and will form the subject of a more extensive study of spatial CSMA.

We resume with the capture model in the SIR model.

Proposition 5.4.6 *The spatial density of successful transmissions is:*

$$\lambda p p_c(r, P_{cs})$$

This spatial density has a 1D and a 2D version and the values of p and $p_c(r, P_{cs})$ are chosen accordingly.

Proof: Proposition 5.4.6 is just the exploitation of Propositions 5.4.2 and 5.4.5. ■

Remark 5.4.7 *We have assume that $P_0 = 1$ i.e. $P = \frac{F}{l(r)}$. Without this assumption the previous computations remain valid if we substitute P_{cs} by $\frac{P_{cs}}{P_0}$ which means that we have similar effects if we tune P_{cs} or P_0. In this thesis we have chosen to discuss the tuning of P_{cs} to preserve the communication of distant vehicles but tuning the carrier sense range or tuning the transmission power (power adaption) will result in the same global effect on the density of successful transmissions.*

5.5 Results of the model

In this section, the model is used to analyze the network performance and the influence of the model's parameters. We study the transmissions for pairs of source-destination nodes at distance r. r is set at $1/\sqrt{\lambda}$ and $1/\lambda$ for 2D and 1D networks respectively. r can be seen as a typical distance in these networks since it is the average distance between a node and its closest neighbor. Thus the transmitters are in the Poisson Point Process and for each transmitter, we create a random receiver at distance r.

5.5.1 Optimizing the density of successful transmissions with the carrier sense threshold P_{cs}

We consider that the parameters of the model λ, T and μ are constant and we vary P_{cs} to maximize the density of successful transmissions. It is easy to show that p is an increasing function of P_{cs}. When the carrier threshold increases, the probability of transmission in CSMA increases. As the carrier threshold increases, transmission becomes easier and thus p increases. This can be verified using the equation of Proposition 5.4.2. In contrast, when P_{cs} increases then $p_c(r, P_{cs})$ decreases. This can been shown using the equation of Proposition 7.4.6. When P_{cs} increases, $h(\tau)$ increases and thus $p_c(r, P_{cs})$ decreases. Since the density of successful transmissions is upper-bounded by λ, we know that there is an optimal value of P_{cs} which optimizes the density of successful transmissions. Studying a few examples, we have seen that the density of successful transmissions always has the same behavior, as shown in Figure 5.5.1. For small values of P_{cs}, when we increase P_{cs}, p increases faster than $p_c(r, P_{cs})$ decreases, and thus the density of successful transmissions is an increasing function of P_{cs}. This density reaches a maximum for a given value of P_{cs} and then becomes a decreasing function of P_{cs}. We assume that this is always the case although it seems difficult to show it mathematically. We use Maple to numerically compute this optimum of the density of successful transmissions.

In Figures 5.5.2 and 5.5.3, we present the carrier sense threshold versus the density of nodes when the density of successful transmissions is optimized.

5.5.2 Effect of the fading rate μ

We note that in the probability of transmission p found in Proposition 5.4.2, we can isolate μP_{cs}. It is the same for $p_c(r, P_{cs})$. This means that if we multiply μ by 10, exactly the same performance can be obtained with P_{cs} divided by 10. Thus, there is no influence of μ on the global performance of the system: the optimum density of successful transmissions, the probability of capture $p_c(r, P_{cs})$ and the probability of transmission p at the optimum value of P_{cs}. This remark regarding μ is valid for both 1D and 2D networks. In the following we use $\mu = 10$.

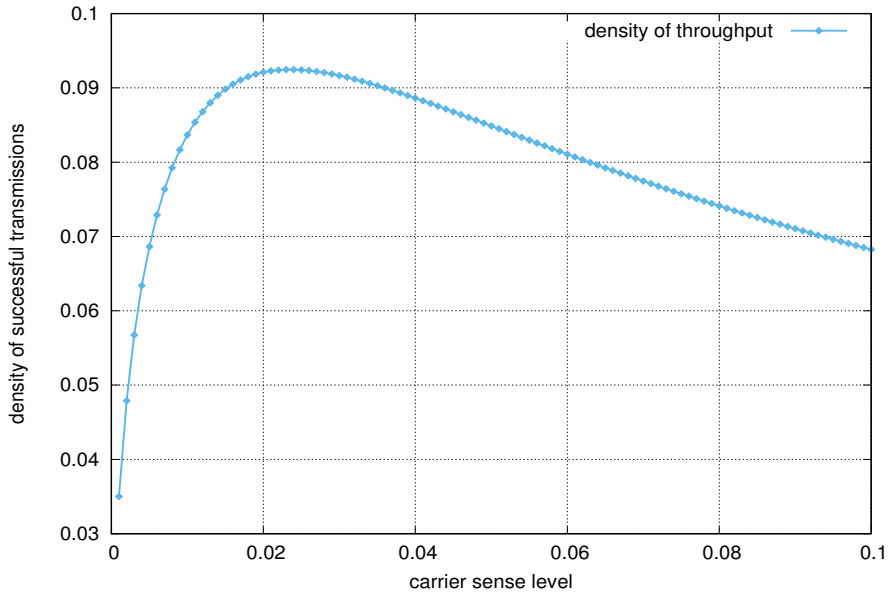

Figure 5.5.1: Density of successful transmissions versus carrier threshold (T=1, μ = 10, $\beta = 4$).

5.5.3 Effect of the density of nodes λ

We compute the optimum density of successful transmissions when P_{cs} is optimized versus λ the density of nodes in the network. We use the following parameters $T = 1$, $\mu = 10$ and $\beta = 4$. The results of these computations are shown in Figure 5.5.4 for 2D networks and in Figure 5.5.5 for 1D networks. Our numerical study shows that the density of successful transmissions is linear in λ. This means that the maximum of the product of $pp_c(r, P_{cs})$ does not depend on λ. This is an interesting result and one which is not easily apparent in the analytical formulas of $pp_c(r, P_{cs})$.

Figures 5.5.4 and 5.5.5 also show the density of successful transmissions when the carrier sense threshold is constant and taken as the optimal value for $\lambda = 1$. The loss is significant for small values of λ: 26% for $\lambda = 0.1$ and much more significant for large values of λ : 80% for $\lambda = 10$ in 2D networks and 85% for $\lambda = 10$ in 1D networks. This means for instance that in a VANET, the channel cannot be used efficiently if the carrier sense threshold is not properly optimized according to the density of vehicles. When $\lambda = 0.1$ and if we use the optimization for $\lambda = 1$ we do not have any restriction on the transmission rights and we actually have an excess of transmission rights. The problem comes from the probability of success for a given transmission.

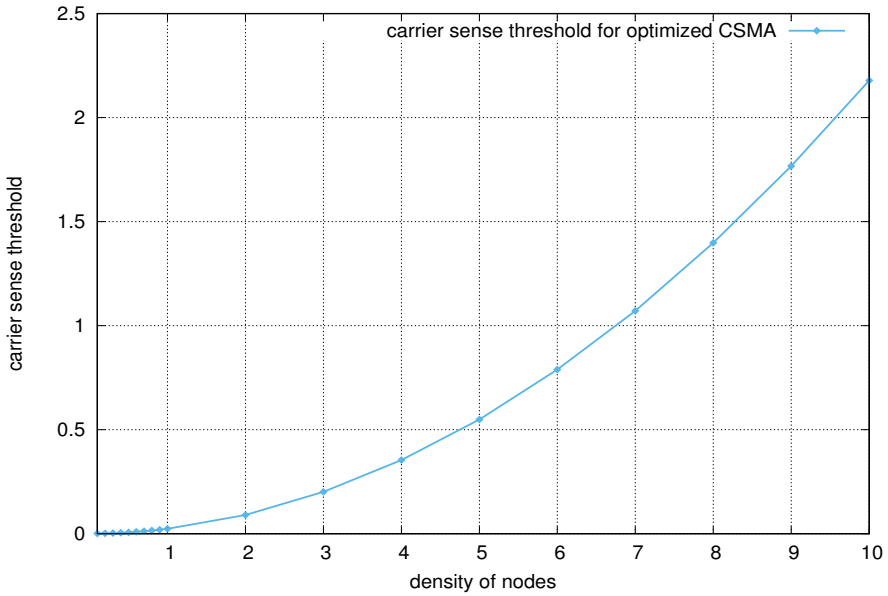

Figure 5.5.2: Optimized carrier threshold versus density, 2D network (T=1, $\mu = 10$, $\beta = 4$).

When $\lambda = 10$ and if we use the optimization for $\lambda = 1$ we have a stringent restriction[3] on the transmission rights, whereas a given transmission is very well protected by the CSMA scheme and thus every transmission is nearly always successful. The model shows that the problem concerning the access right is much more detrimental to the global throughput than collisions would have been if the density of nodes had been overestimated.

We have studied the probability of capture when the throughput is optimized. We observed that the optimum throughput is not obtained when most of the transmissions are successful but rather when the success rate is around 55% in 2D networks and around 70% in 1D networks. The numerical results we obtained show that, at the optimum, $p_c(r, P_{cs})$ does not depend on λ and we also deduce that p does not depend on λ. This is an interesting result which is not brought to light using the analytical formulas.

[3] the access right of CSMA (excess or stringent restriction) is determined by the equation given in Proposition 5.4.2.

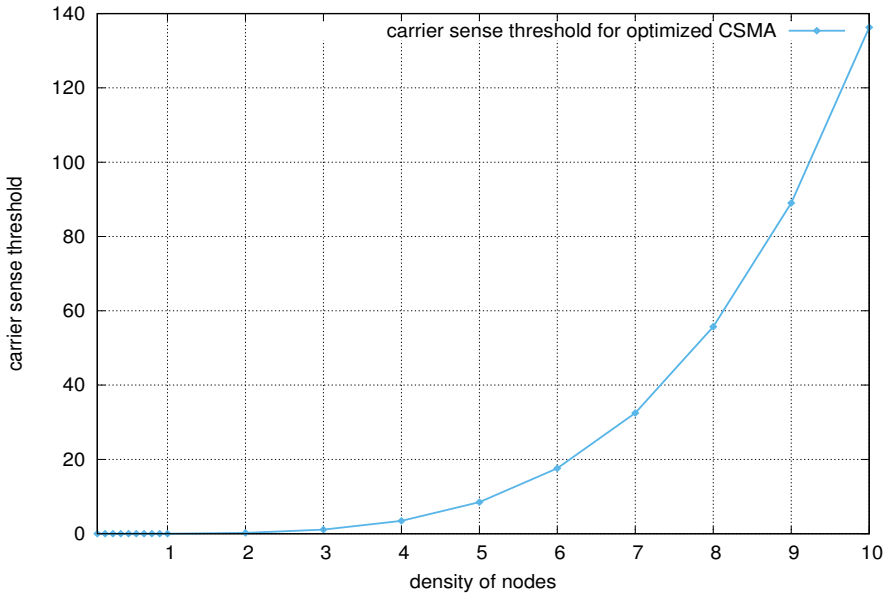

Figure 5.5.3: Optimized carrier threshold versus density, 2D network (T=1, $\mu = 10$, $\beta = 4$).

5.5.4 Evaluation of the exclusion area when the system is optimized

We computed the optimum value of P_{cs}: $P_{cs}(opt)$ in the previous section. CSMA is optimum when a transmission at a given point forbids a transmission where the signal power exceeds $P_{cs}(opt)$. This means that, on average, around a transmitter, any transmission at distance R_{cs} is forbidden such that $\frac{1}{\mu l(R_{cs})} = P_{cs}(opt)$. We study the ratio of R_{cs} by the distance between the transmitter and its receiver. We recall that this distance is $1/\sqrt{\lambda}$ in 2D networks and $1/\lambda$ in 1D networks. In Figure 5.5.6, we show the ratio of R_{cs} by the distance between the transmitter and its receiver for 2D networks versus the density of nodes λ . We see that the average exclusion area around a given transmitter ranges, on average, from 0.92 to 1.47 times the distance between the source and destination nodes for 2D networks T=1, $\mu = 10$ and $\beta = 4$. For 1D networks as there is only one degree of freedom, the nodes are more grouped and the average exclusion area around a given transmitter is larger; it ranges from 1.47 to 1.63 times the distance between the source and destination nodes depending on the density of the nodes.

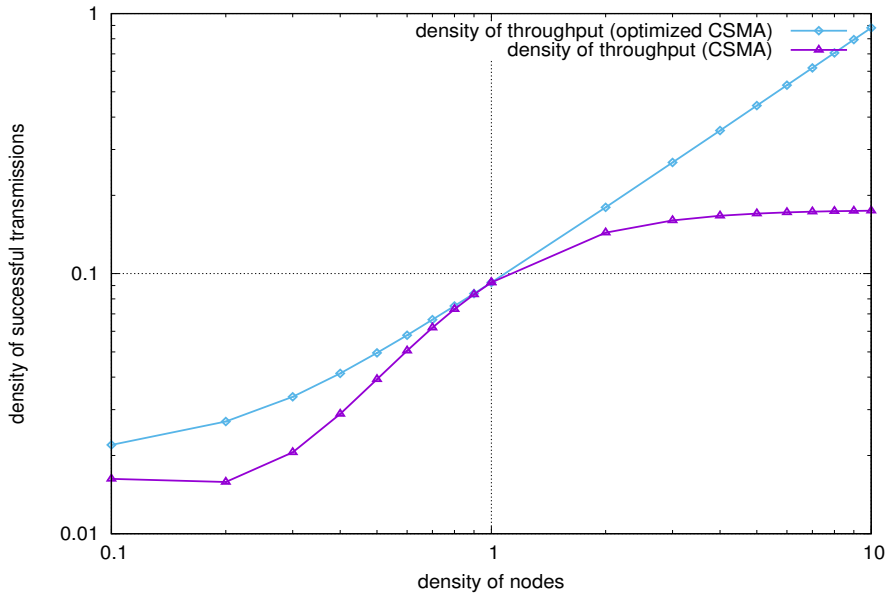

Figure 5.5.4: Density of successful transmissions versus density of nodes (T=1, μ = 10, $\beta = 4$). Spatial network (2 D)

5.5.5 Effect of the capture threshold T

We study the effect of the capture threshold on the maximum density of successful transmissions. In Figure 5.5.8 and Figure 5.5.9 we plot the maximum density of successful transmissions for T varying from 0.01 to 10 respectively for 2D and 1D networks. We observe that dividing the capture threshold by 100 leads to multiplying the density of successful transmissions by 5.6 and 1.9 for 2D and 1D networks. This means that a small capture threshold is much more beneficial in 2D networks. The study of the analytical model does not show any obvious scaling of the density of successful transmissions with the capture threshold T.

5.5.6 Effect of the transmission decay β

In Figures 5.5.10 and 5.5.11, we plot the maximum density of successful transmissions for β varying from 2 to 6 respectively for 2D and 1D networks. In 2D networks, we observe that the maximum density of successful transmissions is multiplied by 1.91 when β varies from 2.5 to 6. For linear networks (1D) the maximum density of successful transmissions is multiplied by 1.32 when β varies from 2.5 to 6. As for the capture threshold, the effect of a large transmission decay is less beneficial for 1D

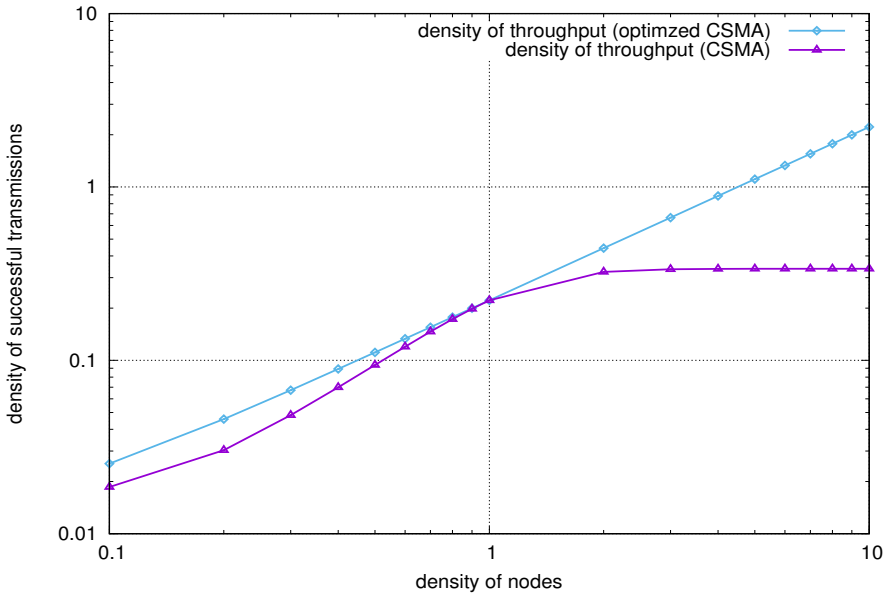

Figure 5.5.5: Density of successful transmissions versus density of nodes (T=1, μ = 10, $\beta = 4$). Linear network (1 D)

networks than for 2D networks. The study does not show any apparent scaling of the density of successful transmissions with the capture threshold β.

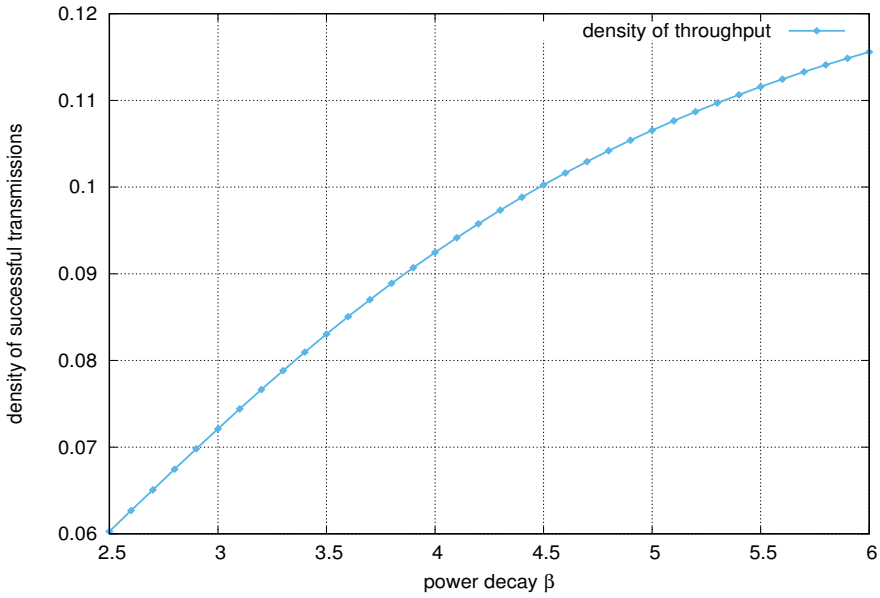

Figure 5.5.10: Density of successful transmissions versus the decay factor β for 2D networks (λ=1, $\mu = 10$, $T = 1$).

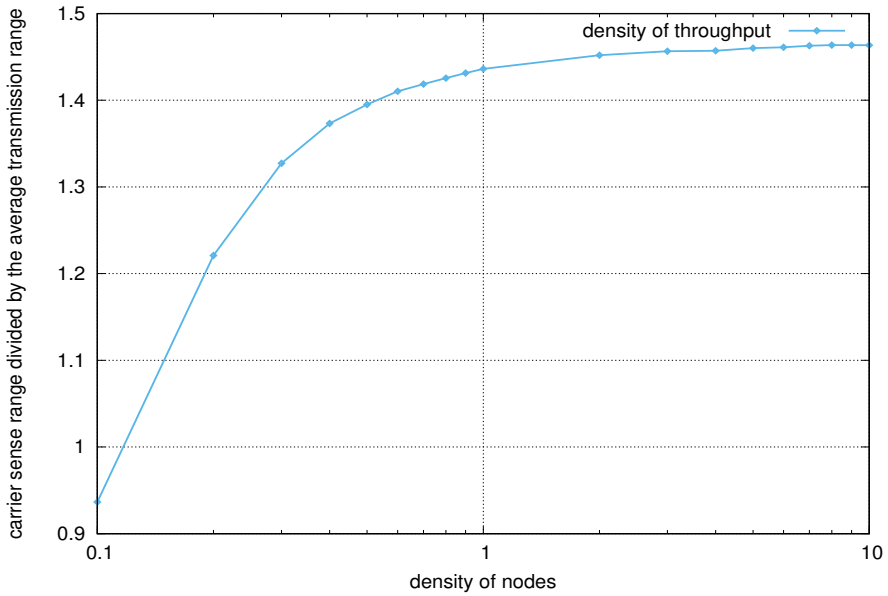

Figure 5.5.6: Ratio of carrier sense range and transmission range versus λ density of nodes for T=1, $\mu = 10$, $\beta = 4$ and a 2D network.

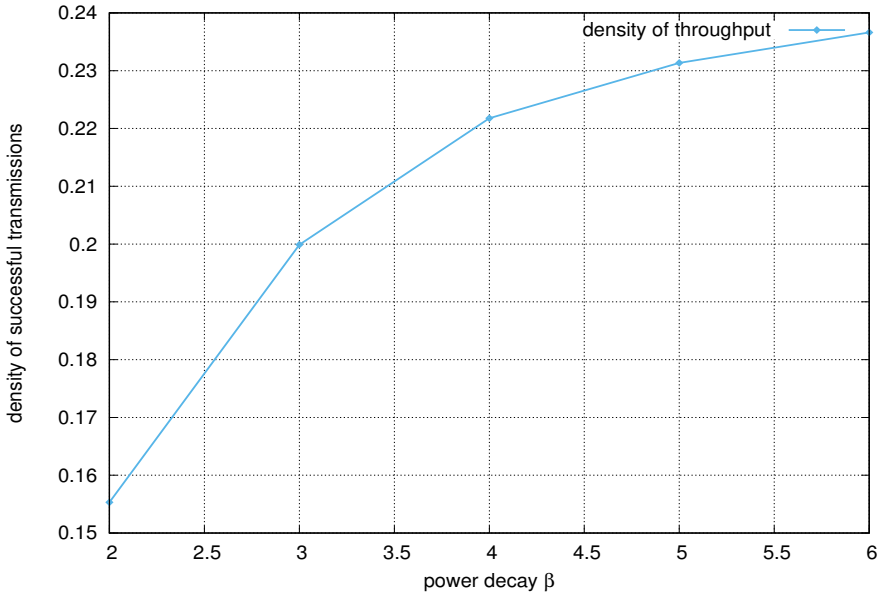

Figure 5.5.11: Density of successful transmissions versus the decay factor β (λ=1, $\mu = 10$, $T = 1$). Linear network (1 D)

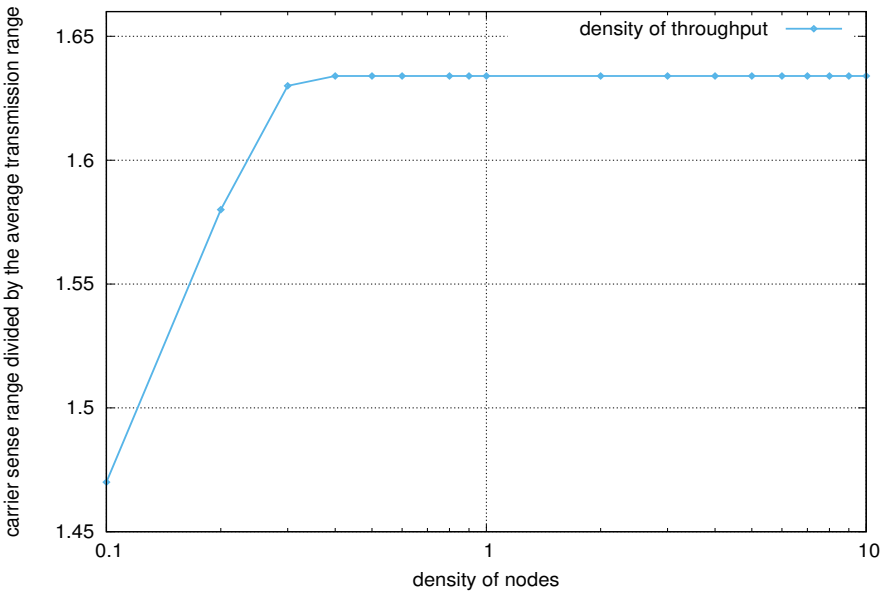

Figure 5.5.7: Ratio of carrier sense range and transmission range versus λ density of nodes for T=1, $\mu = 10$, $\beta = 4$ and a 1D network.

5.6 Comparison between the model an the simulations

In this section, we compare the results obtained by the mathematical model with those derived by simulations. We then use the model to analyze the network performance and the influence of the model's parameters. In the evaluations, the nodes (vehicles) are distributed following the Poisson Point Process in 1D and 2D geographical areas. Then, we study the transmissions for pairs of source-destination nodes at distances r which are $1/\lambda$ and $1/2\sqrt{\lambda}$ for 1D and 2D networks respectively. r can be seen as a typical distance in these networks since it is the average distance between a node and its closest neighbor. We also study the success transmission rate to the closest neighbor for each transmitter.

For the simulations we use two different tools. The first one is ns-3 simulator which implements a large number of networking modules including the IEEE 802.11p, which is the key module for the current study. module. The second simulation tool is a simulator that implements a simple IEEE 802.11 CSMA/CA protocol using the C programming language. Thanks to its simple architecture, in contrast to ns-3, the simulation run time is extremely short in our dedicated simulator. Since the

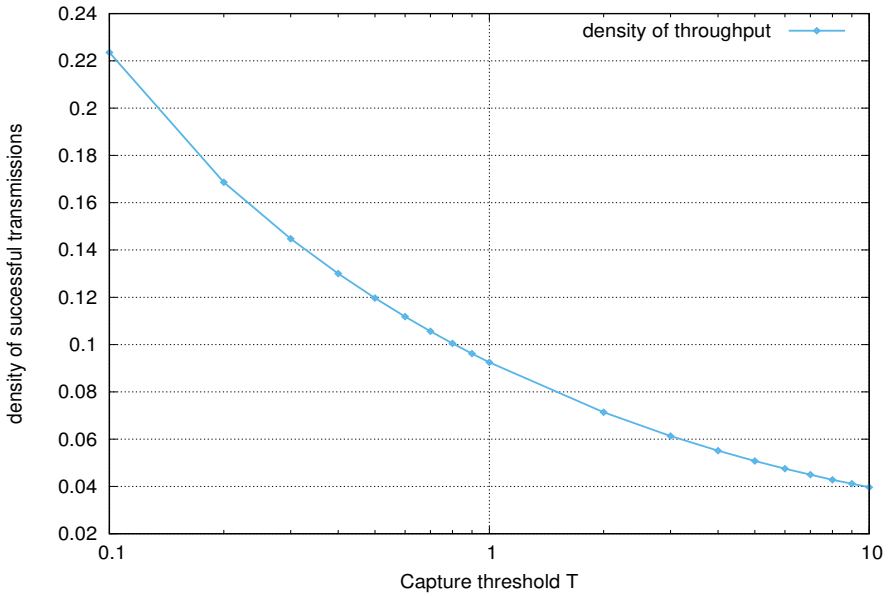

Figure 5.5.8: Density of successful transmissions versus capture threshold T for 2D networks (λ=1, $\mu = 10$, $\beta = 4$).

mathematical model is made for the saturated scenario, the packet generation interval in the simulations are set to very short values in such a way all nodes always have a packet to send. Moreover, the modulation rate is set to 6 Mbits/s, the packet size is set to 4000 bits, and the back-off window is 31 slots. To compare the results obtained by simulations to those established by the model, we define a metric, density of successful transmission, as follows:

$$D = \left(\frac{\frac{2}{3}10^{-3}Rx}{td}\right)$$

Here, Rx is the number of successfully received packets, $\frac{2}{3}10^{-3}$ is the duration of the packet, t is the simulation time, and d is the simulated distance. As regards the carrier sense threshold capability, we use the usual power measurement unity i.e. in decibels (dB). If for instance the current carrier sense threshold is $x\ dB$, the P_{cs} used in the analytical model will be $10^{-\frac{x}{10}}$. Moreover, we set the value of signal decay in both of the analytical model and the dedicated IEEE 802.11 CSMA/CA simulator to fit the default value of signal decay configured in ns-3, which is 2.

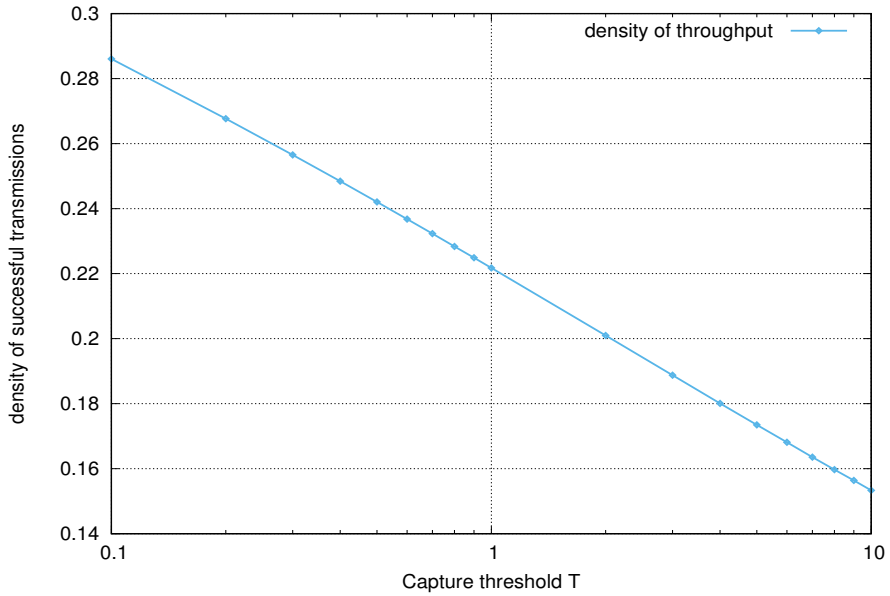

Figure 5.5.9: Density of successful transmission versus the capture threshold T (λ=1, $\mu = 10$, $T = 1$). Linear network (1 D)

5.6.1 Density of successful transmissions versus the carrier sense threshold P_{cs}

We start our work by studying the case of 1D networks. The simulation scenario consists in having a random distribution of nodes, whose density $\lambda = 0.05$, on a 1D network of 1000 meters of length. This means that the average inter-car (nodes) distance is equal to 20 meters, and thus, the positions of the nodes are x randomly selected between 0 and 1000 meters. To fit the simulation configuration to the conditions of the model, we have set two nodes at predefined positions: the sender at position (x = 490, y = 0) and the receiver at position (x = 510, y = 0), and randomly distributed the rest of the nodes (see Figure 5.6.1). The main purpose of this scenario is to study the successful transmission rate between two nodes positioned at a mean distance (which depends on nodes density) from each other. Figure 5.6.3 shows a comparison of the density of successful transmission obtained by both the analytical model and ns-3 simulator. The comparison shows a fairly good matching. In our study, we noticed that the condition of a successfully reception of a packet in ns-3 is implemented in a much complex way in comparison to a simple signal-over-interference-and-noise ratio model. The successful reception of a packet in ns-3 is rather conditioned by a random variable of the signal over the interference

ratio, see [151]. We observe that the successful reception conditions in ns-3 roughly correspond to the analytical model, with a capture threshold T between 5 and 10. Figure 5.6.4 shows a comparison of the density of successful transmission obtained by both the analytical model and our dedicated IEEE 802.11 CSMA/CA simulator. This time, we observe an overall better matching between the two approaches. This is probably due to the fact that the settings of our CSMA/CA simulator are closer to the analytical model than those of the ns-3 simulator.

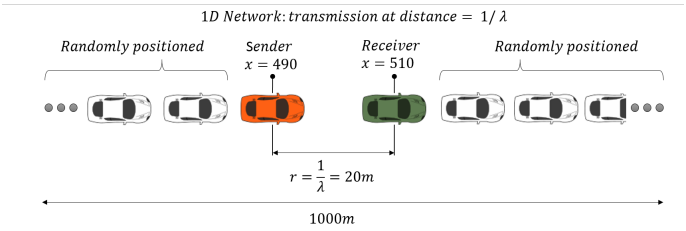

Figure 5.6.1: 1D Network: transmission at distance $1/\lambda$.

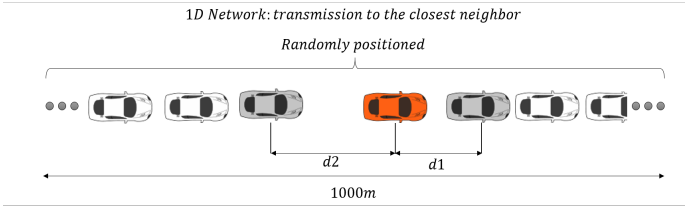

Figure 5.6.2: 1D Network, transmission to the closet neighbor.

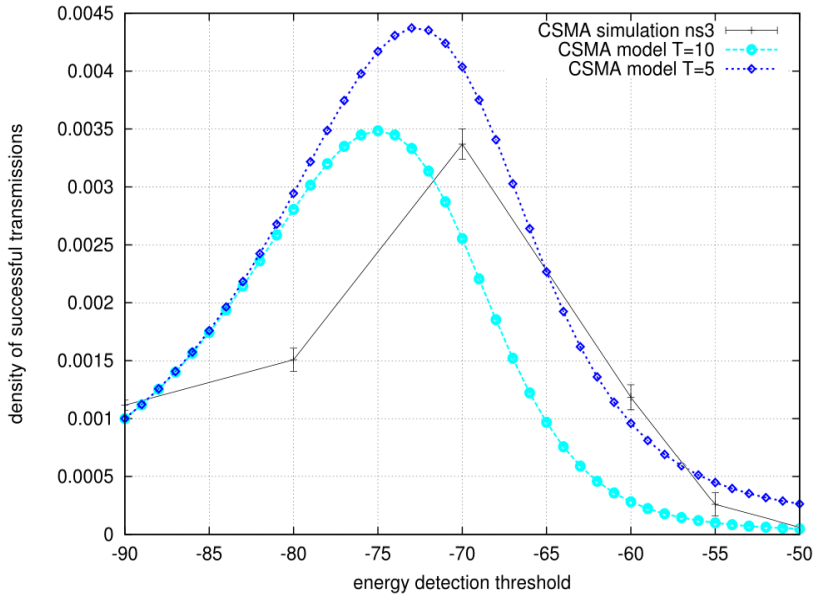

Figure 5.6.3: Density of successful transmissions versus carrier threshold ns3 simulation and analytical model for $T = 5$ and $T = 10$, $\beta = 2$ in a 1D network for a transmission at distance $1/\lambda = 20m$.

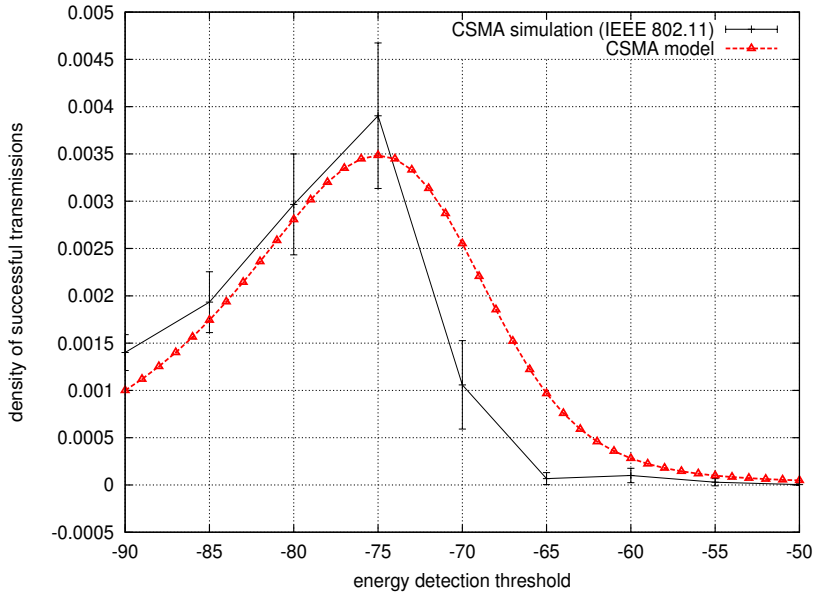

Figure 5.6.4: Density of successful transmissions versus carrier threshold for the IEEE 802.11 simulation and the analytical model $T = 10$, $\beta = 2$, 1D network for a transmission at distance $1/\lambda = 20m$.

We then study the transmission from each node to its closest neighbor as shown in

Figure 5.6.2. We count the successful transmissions from each node to its closest neighbor and compute the spatial density of these transmissions. Figure 5.6.5 illustrates the comparison between the analytical model and ns-3 simulation results. The matching is fair, we observe an increasing density of successful transmission with the increase of the carrier sense threshold as predicted by the analytical model. The range of these increases are visible and comparable. In Figure 5.6.6 the same comparison is made between the analytical model and the IEEE 802.11 CSMA/CA simulator. We observe a reasonable matching between both approaches but it appears better for larger values of the carrier threshold. This is probably due to the way on which carrier sense threshold is implemented in ns-3. It does not actually take into account the reception of packets below the energy detection threshold. This point will be further detailed below.

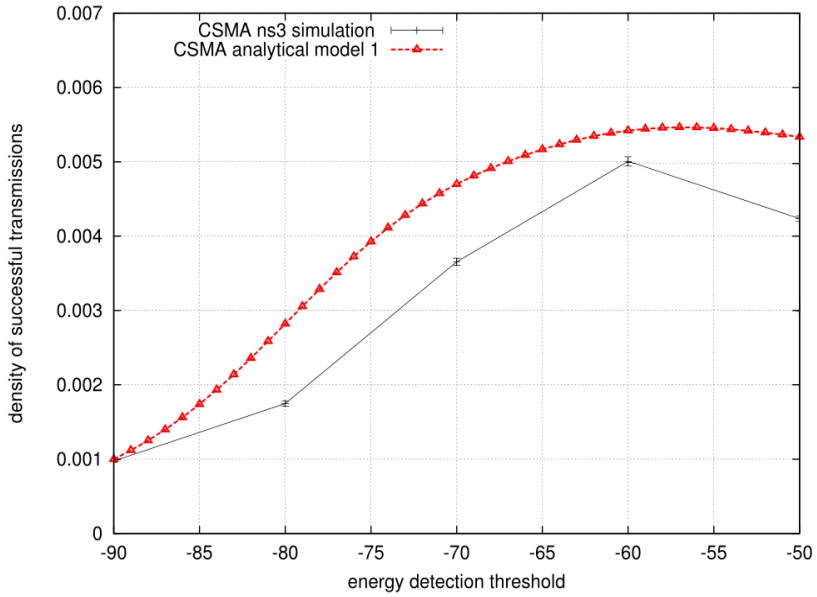

Figure 5.6.5: Density of successful transmissions versus carrier threshold for the IEEE 802.11 simulation and the analytical model $T = 10$, $\beta = 2$, 1D network for a transmission to the closest neighbor.

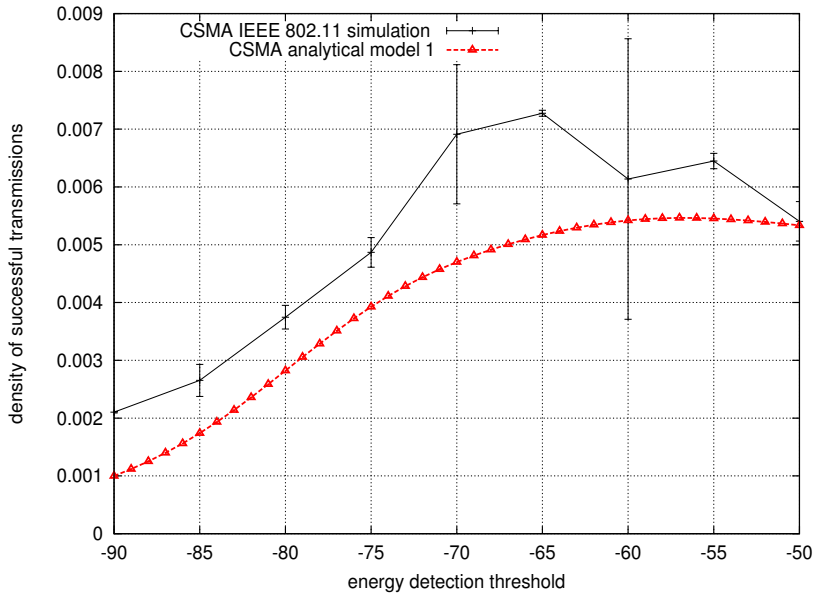

Figure 5.6.6: Density of successful transmissions versus carrier threshold for the IEEE 802.11 simulation and the analytical model $T = 10$, $\beta = 2$, 1D network for a transmission to the closest neighbor.

5.6.2 2D networks: simulations and modeling comparison

Here, compare the results obtained by the analytical model to those obtained by simulation for 2D networks. We set $\lambda = 0.0025$ and $\beta = 3$. The mean distance from one node to its closest neighbor is $1/2\sqrt{\lambda} = 10$ m. The scenarios of the simulations are presented in Figures 5.6.9 and 5.6.10. For this study, we only consider the results obtained by our IEEE 802.11 simulator. The results of the comparison are shown in Figures 5.6.7 and 5.6.8. The matching is fair, in particular the range of the increase of the density of successful transmissions is well estimated by the model, but the value of the carrier sense threshold for which the density of successful transmissions is maximized is not very well estimated.

5.6.3 Analysis of the results obtained

In this part we attempt to clarify the reasons behind the small discrepancy present in some of our comparison results. We believe that the reasons are:

- the model uses an imperfect modeling of the CSMA selection process (see sec-

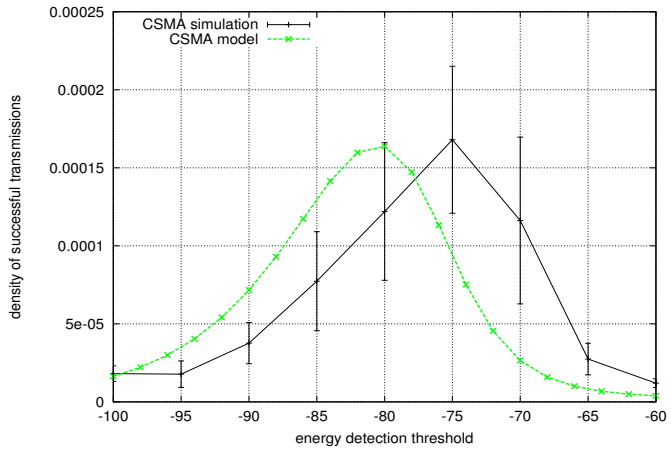

Figure 5.6.7: Density of successful transmissions versus carrier threshold for the IEEE 802.11 simulation and the analytical model $T = 10$, $\beta = 3$, 2D network for a transmission at distance $1/2\sqrt{\lambda} = 10$ m.

tion 6.3), and moreover the scheme used in the model is slotted whereas the real protocol is non-slotted,

- the model does not take into account the time spent by the protocol in the back-off state and thus the density of successful transmissions might well be overestimated,
- the model completely neglects the real collisions when different nodes start transmitting their packets at nearly the same time,
- ns-3 uses two thresholds : the energy detection threshold and the carrier-sense threshold. The energy detection threshold is the more important parameter which decide when to decrement the back-off in the access protocol, thus this parameter must be modified each time the density of nodes increases. However, the implementation of ns-3 is such that any signal below the energy detection threshold is systematically ignored by the node. When the energy detection threshold is high, transmissions from close vehicles may be rejected even they are successful transmitted with regards to the SIR rule.

5.7 Conclusion

In this chapter, we have presented a simple model of CSMA and we have shown the importance of optimizing it according to the density of nodes. We have shown that the

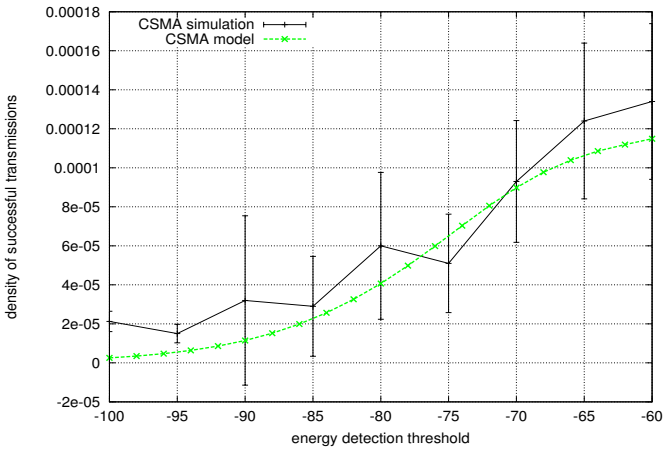

Figure 5.6.8: Density of successful transmissions versus carrier threshold for the IEEE 802.11 simulation and the analytical model $T = 10$, $\beta = 3$, 2D network for a transmission to the closest neighbor.

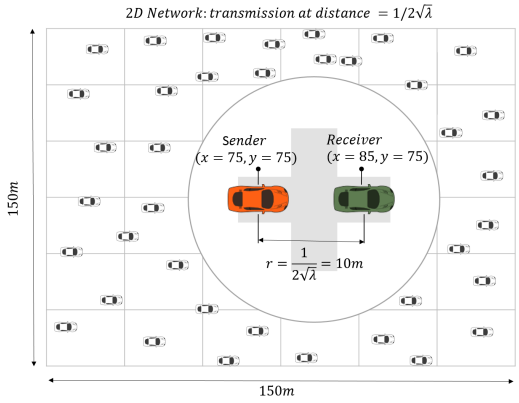

Figure 5.6.9: 2D Network, transmission at the distance $1/(2\sqrt{\lambda})$.

optimized density of successful transmissions scales linearly with the density of nodes. We have observed that using a constant carrier threshold leads to a very significant loss in the network's global throughput. This effect is much more penalizing when the density of nodes in the network is underestimated than when it is overestimated. The numerical computations we have carried out show that the best performance of the network is not reached when transmissions are nearly always successful but when there is a success rate of around 0.6. We have also studied the influence of the model's parameters : μ, T and β. The rate of fading does not influence the performance of the network if it is optimized. We show that T and β have a greater impact on 2D networks than on 1D networks. The results of this study have yet to be compared with

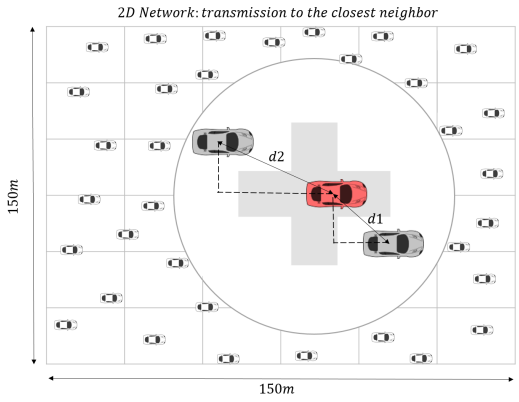

Figure 5.6.10: 2D Network, transmission to the closet neighbor.

simulation results, but preliminary tests show a good matching between the results of both approaches. This will form the subject of our future work. In addition the approximation of CSMA induced by the Matern selection process should be further investigated.

Part IV

Adaptive protocols: Dynamic CSMA protocols

Chapter 6

Adaptive CSMA protocols

Contents

6.1 Introduction

In the previous chapter and in [158], we have shown that the pertinent metric in large networks with a wide geographic extension is the density of successful transmis-

sions from the nodes to their neighbor nodes. This density of successful transmissions is greatly influenced by the carrier sense detection threshold. We have also shown that this optimal carrier sense detection threshold depends on the system's parameters, such as the fading, the power decay, and the capture threshold, but also depends on the spatial characteristic of the network: the density of nodes. Thus if the carrier sense range is tuned for a given density of nodes, this optimization will no longer be valid when the density of nodes changes. The aim of this chapter is to justify and analyze an algorithm which tunes the carrier sense threshold to a potentially varying density of nodes.

We use the Matern selection process with a random pattern of nodes distributed as a Poisson Point Process (PPP) to model the CSMA and we reuse the results of this model to justify our adaptive algorithm. The model allows us to compute the probability p that a random node in the PPP is retained by the CSMA selection process for transmission and the probability $P_c(P_{cs}, r)$ that a neighbor node at distance r from the transmitting node node receives the packet.

We consider neighbor communication thus transmission from one node to a random given node at a distance set as the average distance between a node and its closest neighbor. The crux of our adaptive algorithm is to remark that when the density of successful transmissions in CSMA is optimized with P_{cs}, the transmission probability p obtained with this optimal value of P_{cs} does not depend on λ. In other words, the optimal value of p is independent of λ.

The remainder of this chapter is organized as follows: Section 6.2 briefly reviews the state of the art in adaptive scheme for CSMA networks; Section 6.3 recalls the results of the model proposed to study CSMA based on the Matern selection process described in the previous chapter and justify the adaptive technique proposed using scaling arguments in Poisson Point Processes. In Section 6.4 we propose our carrier sense adaptive technique based on the average waiting time or the mean number of neighbor. We report the results of this adaptive technique where several scenarios are studied for 1D and 2D networks. We present several variants and their performance when the measurement of the network parameters are noisy. Section 6.5 presents simulation results of our adaptive algorithms. Finally, Section 6.6 concludes the chapter.

6.2 State of the art

[153] studies how to cope with the proliferation of IEEE 802.11 devices and the emergence of High-Density WLANs where hundreds or even thousands of client devices are serviced by dozens or hundreds of Access-Points in a multi-cell environment. [153] proposes to adapt CSMA/CA parameters in 802.11 MAC protocol to the changing network topology, traffic and interference. The authors in [153] design a combination of Receiving-Sensitivity adaptation to reduce stronger-last collisions and a Clear-Channel-Assessment adaptation to balance the hidden/exposed terminal problems. It is shown in [153] that up to 300% throughput increase can be observed with the adaptation algorithms proposed. This study uses the same techniques as those proposed in this chapter however there are important differences

- the transmission model is centralized with given access points whereas the model that we have introduced in the previous chapter and we will still use in this chapter is decentralized model on ad hoc networks. Moreover we target neighbor communications
- [153] does not provide any analytical tool to mathematically justify the adaptive schemes proposed and to evaluate the convergence of the scheme towards the optimum of the CSMA schemes.

Other studies such as [154] and [155] also pointed out the effect of the carrier sense threshold on the spatial reuse and the hidden node effect and the benefit of tunable carrier sense threshold but without providing any dynamic algorithm to adapt it and without proposing geometrical model to justify their remark.

6.3 System model

We reuse the model proposed in the previous Chapter 5. We briefly recall this model and the results that we will be useful in this chapter.

We consider a homogeneous Poisson-Point-Process (PPP) Φ extended over a 2D plan ($\mathcal{S} = \mathbb{R}^2$), or along a 1D infinite line $\mathcal{S} = \mathbb{R}$. As Vehicular Ad-hoc NETworks (VANETs) are generally linear networks, they are usually modeled by 1D networks whereas, Mobile Ad-hoc NETworks (MANETs) or Wireless Sensor Networks (WSNs) are modeled by 2D networks. As previously stated, we denote the intensity of the PPP by λ.

We assume that the transmission over a distance r is affected by a power-law decay $1/r^\beta$ where β varies between 3 and 6 depending on the propagation conditions and a random fading F. The power received at distance r from the source node is thus $P = \frac{P_0 F}{l(r)}$ and we set $P_0 = 1$ with $l(r) = r^\beta$. We adopt a Rayleigh fading i.e. exponentially distributed with parameter μ and thus a mean of $1/\mu$.

We also use the well-accepted SIR[1] (Signal-over-Interference-Ratio) with a capture threshold T. In other words, a successful transmission occurs when the ratio of the received signal divided by the interference (i.e., the other concurrent transmissions) will be greater than T.

We use a Matern selection process to mimic the CSMA selection process. The principle of the Matern selection process consists in attributing a random mark m_i to each node $X_i \in \Phi$ and selecting the node with the lowest mark in its neighborhood. We need to define the neighborhood of a node. We denote by $F_{i,j}$ the fading for a transmission between X_i and X_j and we also introduce the carrier sense threshold P_{cs}. We define the neighborhood of X_i as being $\mathcal{V}(X_i) = \{X_j \in X_i \ F_{i,j}/l(|X_i - X_j|) > P_{cs}\}$. A node, say X_i, will be selected by the Matern selection process if and only if $\forall X_j \in \mathcal{V}(X_i) \ m_i < m_j$, i.e., X_i, has the lowest mark m_i in its neighborhood. It is easy to verify that a selection process is well defined by this property. For the rest of the model the reader can refer to the previous chapter.

We recall the following proposals derived in the previous chapter.

Proposition 6.3.1 *The mean number of neighbors of a node is:*

$$\mathcal{N} = \lambda \int_{\mathcal{S}} P\{F \geqslant P_{cs} l(|x|)\} dx.$$

In a 1D network we have :

$$\mathcal{N} = \frac{2\lambda\Gamma(1/\beta)}{\beta(P_{cs}\mu)^{1/\beta}}.$$

In a 2D network we have :

$$\mathcal{N} = \frac{2\pi\lambda\Gamma(2/\beta)}{\beta(P_{cs}\mu)^{2/\beta}}.$$

An immediate computation yields the explicit value of $\mathcal{N}$ in the 1D and 2D cases.

[1]As pointed out in Chapter 5, we omit thermal noise, although it could easily be added. Also, a more realistic model, based on graded SIR model using Shannon's law is possible, but would to an increased computational cost.

Proposition 6.3.2 *The probability p that a given node X_0 transmits i.e. $e_0 = 1$ is:*

$$p = \mathbf{E}^0[e_0] = \frac{1 - e^{-\mathcal{N}}}{\mathcal{N}}.$$

If p is close to 1, then the carrier sense imposes no restriction of transmission. On the other hand, if p is close to 0, then the carrier imposes a severe restriction on transmission.

Proposition 6.3.3 *Given the transmission of a packet, we denote by $p_c(r, P_{cs})$ the probability of this packet being successfully received at distance r in a CSMA system (modeled by a Matern selection process with a carrier sense threshold P_{cs}) and with a capture threshold T. Let us define:*

$$h(r) = \frac{\frac{2}{b(r)-\mathcal{N}}\left(\frac{1-e^{-\mathcal{N}}}{\mathcal{N}} - \frac{1-e^{-b(r)}}{b(r)}\right)\left(1 - e^{-P_{cs}\mu l(r)}\right)}{\frac{1-e^{-\mathcal{N}}}{\mathcal{N}} - e^{-P_{cs}\mu l(r)}\left(\frac{1-e^{-\mathcal{N}}}{\mathcal{N}^2} - \frac{e^{-\mathcal{N}}}{\mathcal{N}}\right)}$$

In a 1D network, we have:

$$p_c(r, P_{cs}) \simeq \exp\Big(- \lambda \int_{-\infty}^{\infty} \frac{h(\tau)}{1 + \frac{l(|r-\tau|)}{Tl(r)}} d\tau \Big)$$

with

$$b(r) = 2\mathcal{N} - \lambda \int_{-\infty}^{\infty} e^{-P_{cs}\mu(l(\tau)+l(|r-\tau|))} d\tau$$

In a 2D network, we have:

$$p_c(r, P_{cs}) \simeq \exp\Big(- \lambda \int_0^{\infty} \int_0^{2\pi} \frac{\tau h(\tau)}{1 + \frac{l(\sqrt{\tau^2+r^2-2r\tau cos(\theta)})}{Tl(r)}} d\tau d\theta \Big)$$

with

$$b(r) = 2\mathcal{N} - \lambda \int_0^{\infty} \int_0^{2\pi} e^{-P_{cs}\mu(l(\tau)+l(\sqrt{\tau^2+r^2-2r\tau cos(\theta)}))} d\tau d\theta.$$

Proposition 6.3.4 *The spatial density of successful transmissions is thus:*

$$\lambda p p_c(r, P_{cs})$$

There are 1D and 2D versions of this spatial density and the value of p and $p_c(r, P_{cs})$ are chosen accordingly.

Proposition 6.3.5 *The mean waiting time for a packet (without taking into account the delay in the queue) is* $1/p - 1$ *where* p *is given by Proposition 6.3.2 and the transmission duration of a packet is one unit.*

Proof: The probability of transmitting after waiting for i slots is $(1-p)^i p$; the node defers i slot with probability $(1-p)^i$ and then transmit with probability p. Thus the mean waiting time is

$$\sum_{i=0}^{\infty} pi(1-p)^i = 1/p - 1.$$

■

6.4 The adaptive carrier sense threshold algorithm

Our adaptive protocol will operate in networks modeled by Poisson Point Processes in 1D and 2D geographical areas. We propose to optimize the transmissions for pairs of source-destination nodes at distance r which is the average distance between a node and its closest neighbor. Thus $r = 1/\lambda$ and $r = 1/2\sqrt{\lambda}$ for 1D and 2D networks respectively.

The aim of our adaptive algorithm will be to ensure that P_{cs} is tuned so that the spatial density of successful transmissions, as defined in Proposition 7.4.8, is optimized with respect to the spatial density of nodes λ in the Poisson Point Process.

6.4.1 The underlying idea and results of the algorithm in 1D networks

The idea of our algorithm is based on the fact that when the density of successful transmissions is optimized, the value of p is always the same when we vary the network density of nodes λ. For instance, we verify this conjecture with $\beta = 2$ and $T = 10$ and with λ varying between 0.001 and 0.1. In Figure 6.4.2 we show the optimal value of P_{cs} to optimize the density of successful transmissions. A simple calculation shows that if P_{cs} is not carefully selected, the density is far below its optimum value. In Figure 6.4.3 we show that the value of the CSMA transmission probability p for CSMA, as computed in Proposition **??**, is nearly constant when we vary λ if we have optimized the density of successful transmissions with regard to P_{cs}. We have verified this property with different values of the system parameters and we justify it by a

scaling argument. We present the argument for 2D networks, but we could adapt the argument to 1D networks.

In Figure 6.4.1 we present one realization of a PPP with a density λ_1 and the same realization of a PPP with a density λ_2 obtained with the suitable scaling of all the distances in the first PPP with rate $\sqrt{\frac{\lambda_2}{\lambda_1}}$. In the figure we have only represented a square of the first PPP and its corresponding transformation by scaling.

In the first PPP we compute the SIR ratio for a transmission from node A to its receiver R which is at distance $\frac{1}{\sqrt{2\lambda_1}}$ from A. We denote by r_i and F_i for $i = 1 \ldots$ the distance and the fading between the interferers and the receiver R. We can easily compute the Signal-over-Interference Ratio in the transmission from A to R.

$$SIR_1 = \frac{F_0}{2^{\beta/2}\lambda_1^{\beta/2}\sum_i \frac{F_i}{r_i^\beta}}$$

In the second PPP we compute the SIR ratio for a transmission from node A to its receiver R which is at distance $\frac{1}{\sqrt{2\lambda_2}}$ from A' to R', A' and R' correspond to the transformation of A and R in the first point process. We assume that we have the same fading F_i between the node in the second point process. The distance r_i' between the receiver R' and the interferers are

$$r_i' = \frac{r_i\sqrt{\lambda_2}}{\sqrt{\lambda_1}}$$

Thus the signal-over-interference ratio in the transmission from A' to R' is: thus

$$SIR_2 = \frac{F_0}{2^{\beta/2}\lambda_2^{\beta/2}\sum_i \frac{F_i}{r_i^\beta}\frac{\lambda_1^{\beta/2}}{\lambda_2^{\beta/2}}} = SIR_1$$

This shows that the signal-over-interference ratio is the same in the two PPPs. Moreover the neighborhood as defined by Propostion 6.3.1 is the same if we use P_{cs} as the carrier sense threshold in the first PPP and $P_{cs}\frac{\lambda_1^\beta}{\lambda_2^\beta}$ in the second PPP. This scaling of the optimization of P_{cs} is confirmed in Figure 6.4.2.

Thus the optimization of the density of the successful transmission is the same in the two PPPs leading to the same value of $\mathcal{N}$ and p.

The argument in 1D networks is the same except that the scaling of the distance between the two point processes is $\frac{\lambda_1}{\lambda_2}$. The mean distance from one node to this closest neighbor is $\frac{1}{\lambda_1}$ and $\frac{1}{\lambda_2}$ in the first and second point processes respectively.

Thus the main result that we have obtained is that the maximum density of successful transmissions is obtained when the mean number of neighbors $\mathcal{N}$ is equal to a given

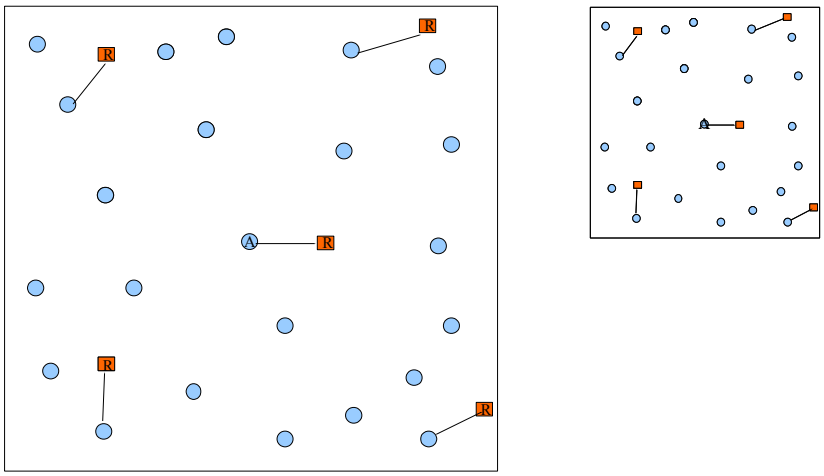

Figure 6.4.1: Scaling between two random networks of transmitters. On the left PPP of rate λ_1, on the right PPP of rate λ_1

fixed $\mathcal{N}_{target}$ and when p is equal to a given fixed p_{target}. These two numbers are functions of the system parameters β and T.

The adaptive algorithm must therefore lead to the convergence of p and $\mathcal{N}$ towards $\mathcal{N}_{target}$ and p_{target}. Therefore we must find a network parameter that is linked to p or $\mathcal{N}$. This parameter can be in Proposition 6.3.5 which shows that the access delay is: $D = 1/p - 1$. In other words, the network operates optimally when the mean CSMA access delay is a fixed given value: $D_{target} = 1 - 1/p_{target}$.

Thus we propose the following algorithm

---

while "Stabilization on" **do**
  Estimate the current average access delay D
  Periodically process the following tests :
  if $D > D_{target}$ **then**
    $P_{cs} = P_{cs} * 2$.
  end if
  if $D < D_{target}$ **then**
    $P_{cs} = P_{cs}/1.1$.
  end if
end while

The stabilization algorithm continuously updates the value of the average access delay D. This delay can be simply obtained using a sliding window. Periodically, the algorithm compares the current access delay D with the targeted access delay D_{target} and updates P_{cs} accordingly.

If the delay D is greater than the targeted access delay D_{target}, the carrier sense threshold P_{cs} is multiplied by 2 and if D is smaller than the targeted access delay D_{target} then P_{cs} is divided by 1.1.

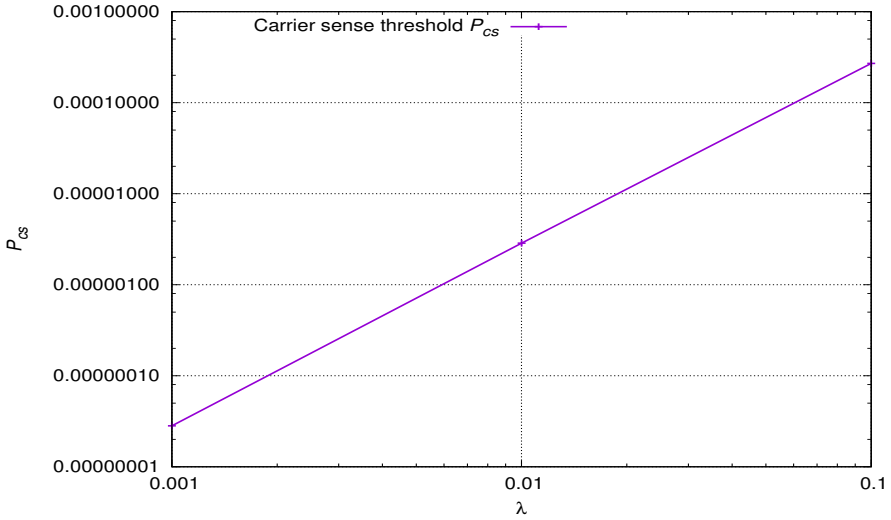

Figure 6.4.2: Optimal carrier sense power P_{cs} versus λ with $T = 10$, $\beta = 2$.

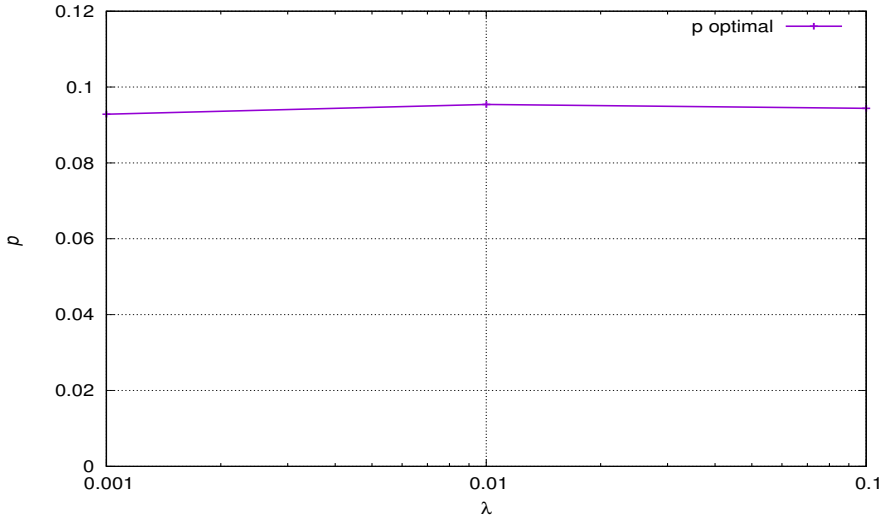

Figure 6.4.3: Optimal CSMA transmission p versus λ with $T = 10$, $\beta = 2$.

We test our adaptive algorithm with two examples. In the first example we adopt the following values $\mu = 1$, $T = 10$ and $\beta = 2$. We also use a random value for $P_{cs} = 2.8\,10^{-6}$ and we study how the algorithm adapts to the actual density $\lambda = 0.1$. We assume that every second the adaptive algorithm evaluates D and updates P_{cs} accordingly. In Figure 6.4.4 we show the evolution of the density of successful transmissions compared with the optimal density when the carrier threshold is optimized. We observe that in 8 seconds the adaptive algorithm converges in the neighborhood of the optimal value. When the optimal value is reached, the algorithm remains close to this optimal. We present the results with a Gaussian error on the measurement of the delay. We assume that the variance of the noise is such that with a probability of 0.95, the error in the measure is less than 40%. We observe that this algorithm is very robust to errors in the access delay estimation.

In Figure 6.4.5 we continue to study the adaptive algorithm. From time $t = 1$s to $t = 15$s the density of the network is $\lambda = 0.1$ and then from $t = 16$s to $t = 30$s, the network becomes sparser, $\lambda = 0.01$ for instance resulting from the end of a traffic jam. At the beginning of the network, the carrier threshold is not optimized. We observe the quick adaptation of the algorithm to the actual density of the network. The noise in the measurement of the delay is also well tolerated by the adaptive algorithm.

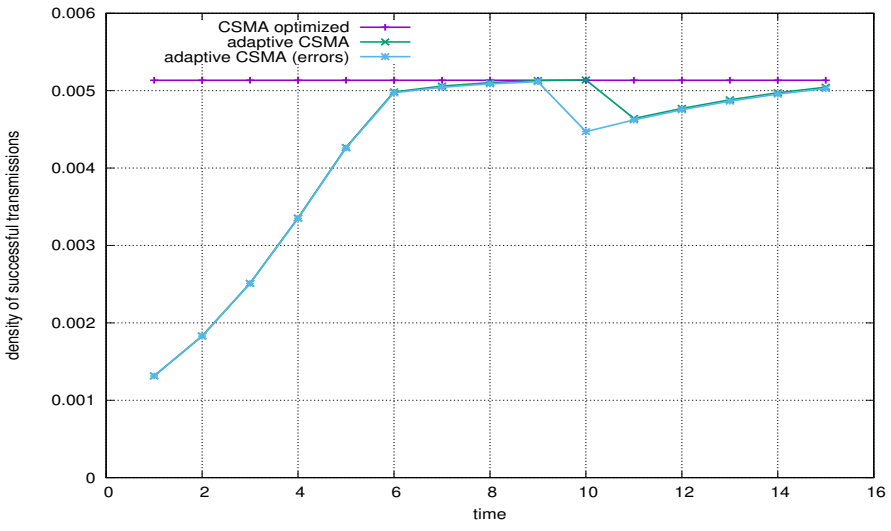

Figure 6.4.4: Adptation of the carrier sense detection threshold to optimize the density of successful transmissions. The initial value of P_{cs} is for $\lambda = 0.01$ but the actual value of λ is 0.1. ($\mu = 1$ and $T = 10$, $\beta = 2$, 1D network).

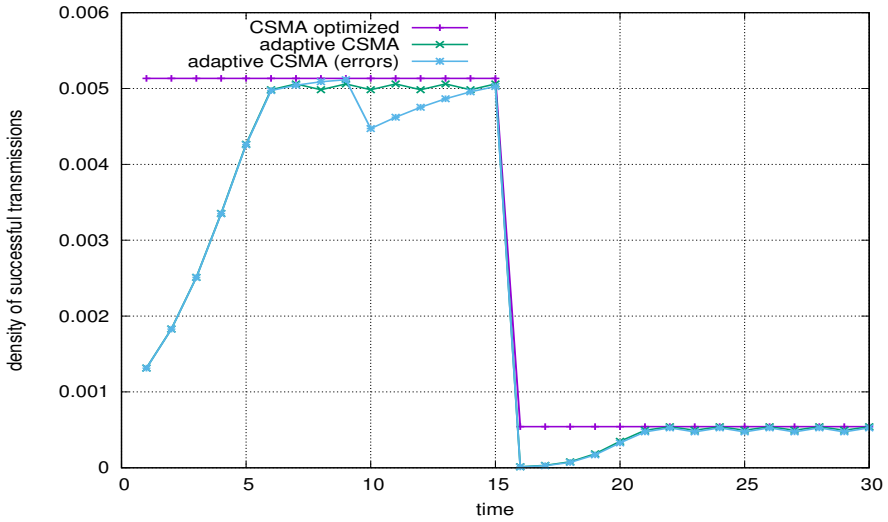

Figure 6.4.5: Adaptation of the carrier sense detection threshold to optimize the density of successful transmissions. At the beginning of the experiment $\lambda = 0.1$ and then at time $\geqslant 16$, λ becomes 0.01 ($\mu = 1$ and $T = 10$, $\beta = 2$, 1D network).

6.4.2 Results in 2D networks

We conduct the same analysis for 2D networks. In this case, we assume that $\beta = 4$ and we still set $\mu = 1$ and $T = 10$. We also vary λ from 0.001 to 0.1. The density of successful transmissions is evaluated at the average distance between a node and its nearest neighbor (i.e., $r = 1/2\sqrt{\lambda}$) thus $r \simeq 1.581$ m for $\lambda = 0.1$, $r = 5$ m for $\lambda = 0.01$ and $r \simeq 15.81$ m for $\lambda = 0.001$. Figure 6.4.6 displays the optimal values of the CSMA transmission probability when we vary λ from 0.001 to 0.1. We observe that this value is around 0.24, irrespectively of the value of λ.

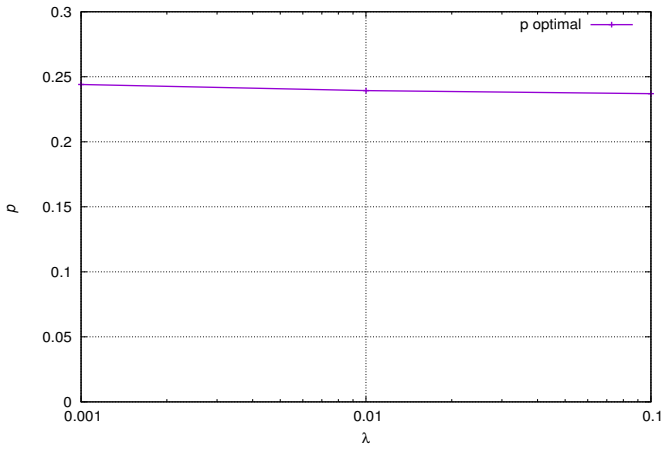

Figure 6.4.6: Optimal CSMA transmission p versus λ with $T = 10$, $\beta = 4$, 2D network

.

Hence the algorithm described above can be used satisfactorily, as can be seen in Figure 6.4.7. This figure represents the worst case where the carrier sense threshold is set for a small density $\lambda = 0.001$ whereas the actual density is $\lambda = 0.1$. We observe a fast convergence close to the optimal value of the density of successful transmissions and then the algorithm maintains the throughput close to this value. In this case we do not observe any influence of measurement error on the behavior of the adaptive algorithm.

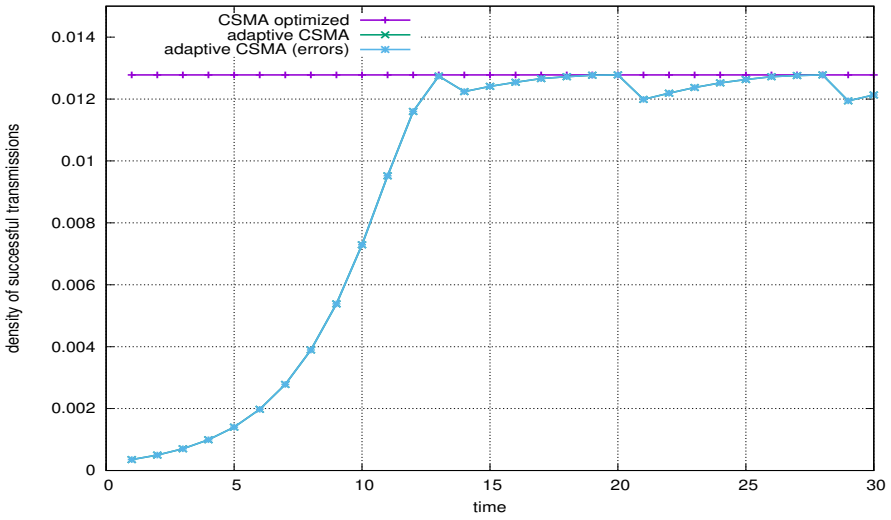

Figure 6.4.7: Adptation of the carrier sense detection threshold to optimize the density of successful transmissions in a 2D network. The initial value of P_{cs} is set to the optimal value for $\lambda = 0.001$ but the actual value of the network density is λ is 0.1. ($\mu = 1$ and $T = 10$, $\beta = 4$, 2D network).

6.4.3 Variant of the adaptive algorithm

We observe that according to Proposition 6.3.2, the CSMA transmission probability p is directly linked to $\mathcal{N}$ and thus we can control p using $\mathcal{N}$. This can be implemented by monitoring the Cooperative Awareness Messages (CAMs). The adaptive algorithm has to evaluate the mean number of neighbors; CAM packets received below the carrier sense detection threshold are discarded even if they are correctly decoded. Thus a node can determine the number of its neighbors.

1: **while** "Stabilization on" **do**
2: Estimate the current average number of neighbors (i.e., nodes from which CAMs are received above the carrier sense threshold)
3: Periodically process the following tests :
4: **if** $\mathcal{N} < \mathcal{N}_{target}$ **then**
5: $P_{cs} = P_{cs} * 2$.
6: **end if**
7: **if** $\mathcal{N} > \mathcal{N}_{target}$ **then**
8: $P_{cs} = P_{cs}/1.1$.
9: **end if**
10: **end while**

We come back to the situation where we measure the access delay D. The idea is to compute the new value of P_{cs} using the delay measured and the targeted delay. We have the following formulas.

$$p_{target} = \frac{1}{D_{target} - 1} \text{ and } p = \frac{1}{D - 1}$$

$$\mathcal{N}_{target} = \frac{1}{p_{target}} = D_{target} - 1 \text{ and } \mathcal{N} = \frac{1}{p} = D - 1$$

$$\mathcal{N}_{target} = \frac{2\pi\lambda\Gamma(2/\beta)}{\beta(P_{cs}(opt)\mu)^{2/\beta}} \text{ and } \mathcal{N} = \frac{2\pi\lambda\Gamma(2/\beta)}{\beta(P_{cs}\mu)^{2/\beta}} \text{ for 2D networks}$$

$$\mathcal{N}_{target} = \frac{2\lambda\Gamma(1/\beta)}{\beta(P_{cs}(opt)\mu)^{1/\beta}} \text{ and } \mathcal{N} = \frac{2\lambda\Gamma(1/\beta)}{\beta(P_{cs}\mu)^{1/\beta}} \text{ for 1D networks}$$

and we obtain:

$$P_{cs}(opt) = \left(\frac{D-1}{D_{target}-1}\right)^{\beta/2} P_{cs} \text{ for 2D networks}$$

$$P_{cs}(opt) = \left(\frac{D-1}{D_{target}-1}\right)^{\beta} P_{cs} \text{ for 1D networks}$$

Thus we propose the following algorithm.

while "Stabilization on" **do**
  Estimate the current average access delay D
  Update P_{cs} using the formula below
  if The network is 1D **then**
    $P_{cs} = \left(\frac{D-1}{D_{target}-1}\right)^{\beta} P_{cs}$
  end if
  if The network is 2D **then**
    $P_{cs} = \left(\frac{D-1}{D_{target}-1}\right)^{\beta} P_{cs}$
  end if
end while

We test this algorithm on a 1 D network. We adopt the following values $\mu = 1$, $T = 10$ and $\beta = 2$. We also use a random value for $P_{cs} = 2.8\,10^{-6}$ and we study how the algorithm adapts to the actual density $\lambda = 0.1$. We assume that every second, the adaptive algorithm evaluates D and updates P_{cs} accordingly. In Figure 6.4.8 we show the evolution of the density of successful transmission compared with the optimal density. The optimized adaptive algorithm reacts more rapidly than the multiplicative algorithm. The tolerance to measurement error is also better.

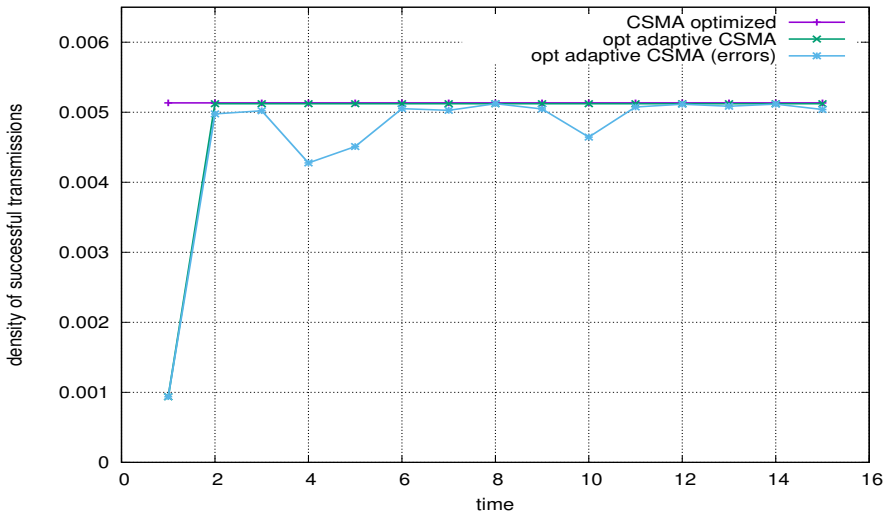

Figure 6.4.8: Adptation of the carrier sense detection threshold to optimize the density of successful transmissions. The initial value of P_{cs} is for $\lambda = 0.01$ but the actual value of λ is 0.1. ($\mu = 1$ and $T = 10$, $\beta = 2$, 1D network).

In Figure 6.4.9 we continue to study the adaptive algorithm. From time $t = 1$ s to $t = 15$ s the density of the network is $\lambda = 0.1$ and then from $t = 16$ s to $t = 30$ s, the network becomes sparser, $\lambda = 0.01$ for instance resulting from the end of a traffic jam. At the beginning of the network the carrier threshold is not optimized. We observe the very quick adaptation of the optimized adaptive algorithm to the actual density of the network and the tracking of the actual density of nodes is excellent. The tolerance to measurement error is excellent.

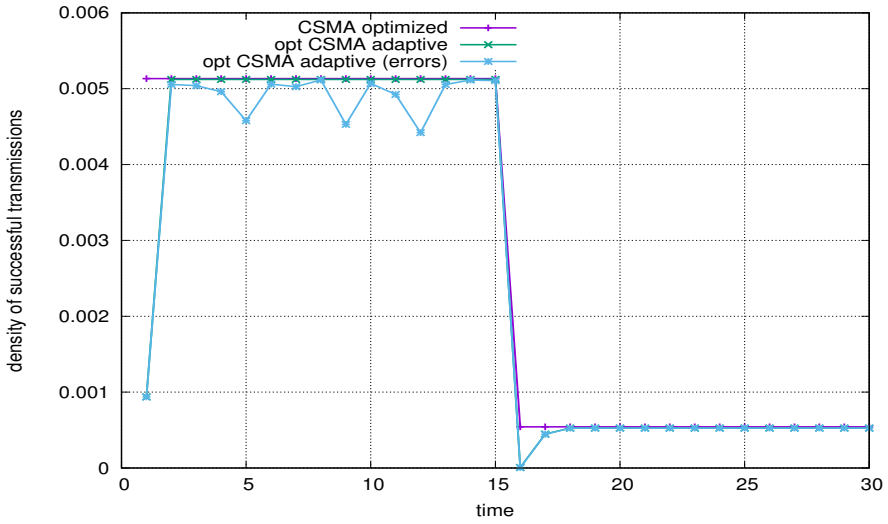

Figure 6.4.9: Adaptation of the carrier sense detection threshold to optimize the density of successful transmissions. At the beginning of the experiment $\lambda = 0.1$ and then at time $\geqslant 16$, λ becomes 0.01 ($\mu = 1$ and $T = 10$, $\beta = 2$, 1D network).

6.4.4 Effect of the parameters

We observe that p and $p_c(r, P_{cs})$ only depend on the product μP_{cs}. The optimization in P_{cs} of the density of successful transmissions $\lambda p p_c(P_{cs}, r)$ does not depend on μ. Thus the stabilization algorithm can ignore the parameter μ to compute the targeted value of p and then the value of D_{target}.

In Figure 6.4.10 we study the optimal value of p with respect to the capture threshold T. We observe a clear dependence of p which requires knowing the value of T to use the adaptive algorithm. This should not really be a problem since this parameter should be known by the designer of the radio transmission system.

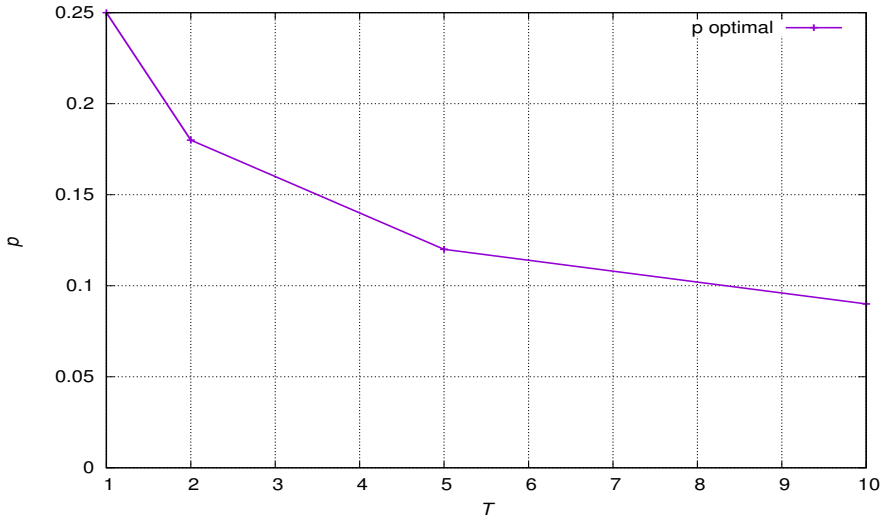

Figure 6.4.10: Optimal CSMA transmission p versus T with $\mu = 1$, $\beta = 2$.

We adopt the following values $\mu = 1$, $T = 10$ and $\beta = 2$ and we also use a random value for $P_{cs} = 2.8\ 10^{-6}$. We study how the algorithm adapts to the actual density $\lambda = 0.1$, but we assume that we have made a mistake in the evaluation of T, considering that $T = 5$ and $T = 2$ as the real value of T is 10. In Figure 6.4.11 we show the evolution of the density of successful transmissions compared with the optimal density when the carrier threshold is optimized. We observe that the adaptive algorithm very significantly improves the density of throughput but fails to converge towards the actual optimum. The system is still viable when T is assumed to be 5, but it is more problematic when T is assumed to be 2.

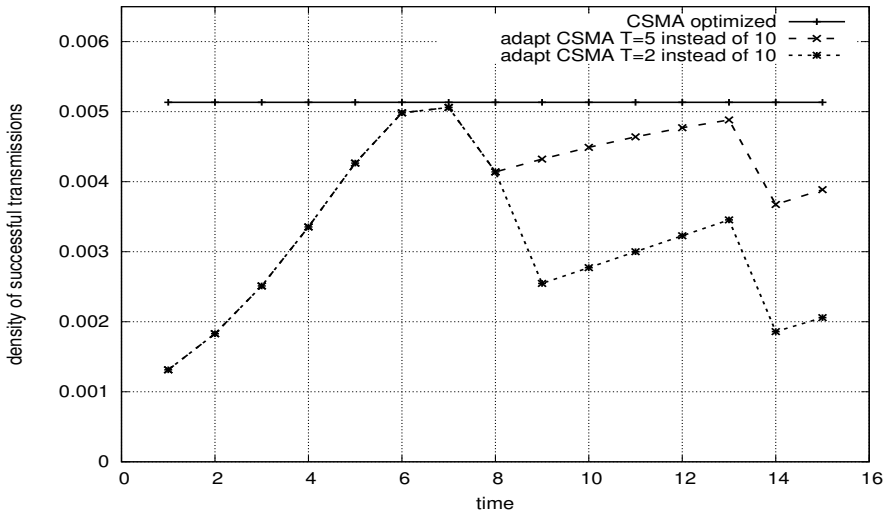

Figure 6.4.11: Adaptation of the carrier sense detection threshold to optimize the density of successful transmissions when $T = 10$ is not well estimated. ($\mu = 1$ and $T = 10$, $\beta = 2$, 1D network).

In Figure 6.4.12 we compute the optimal value of p with respect to the capture threshold β. We observe a clear dependence of p on β but we note that for $\beta \geqslant 3.5$ the dependence of p on β tends to be small. Thus an inaccurate evaluation of β will not produce a large error in the evaluation of D_{target} or $\mathcal{N}_{target}$. and consequently the adaptive algorithm will continue to provide densities of successful transmissions close to the optimal.

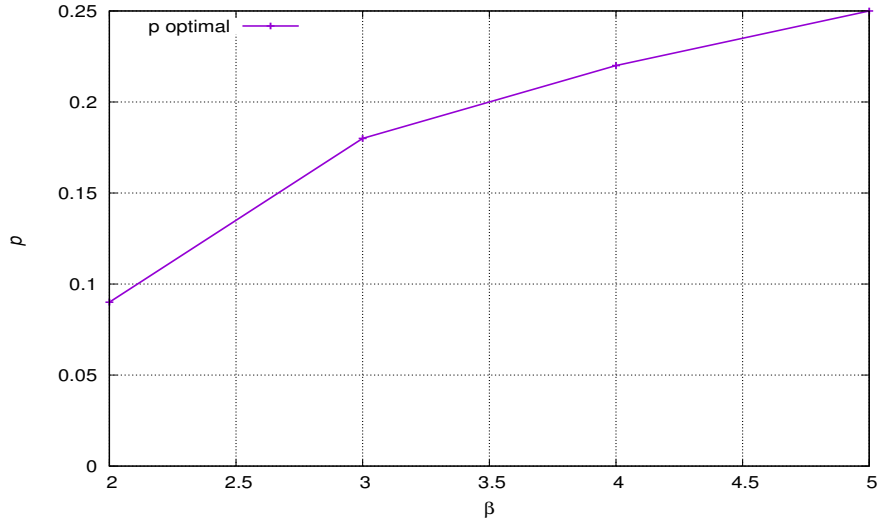

Figure 6.4.12: Optimal CSMA transmission p versus β with $\mu = 1$, $T = 10$.

6.5 Performance Evaluation

In this section we evaluate the performances of carrier-sense adaptive algorithms with simulations on real scenarios. We will consider two algorithms. The first one has already been introduced: it is delay-based algorithm (Delay-based protocol) . The second one is the new algorithm; it is based on the measurement busyness ratio of the channel (CBR-based protocol)

6.5.1 CBR-based algorithm

The second algorithm works in the same way as the first one, except that it uses another metric : the Channel Busy Ratio (CBR), which is the ratio of the time the channel is perceived as busy, over the monitoring interval:

$$CBR = T_{busy}/T_{monitor}$$

The CBR-based algorithm periodically monitors the channel load status and updates P_{cs} accordingly. Since the wireless channel is shared by all the nodes that are in the vicinity of each other, CBR monitored at each node takes similar values.

The stabilization algorithm continuously updates the value of CBR. Periodically, the algorithm compares the current CBR value to CBR_{target} and updates the carrier sense threshold P_{cs} accordingly.

If CBR is greater than CBR_{target}, the carrier sense threshold P_{cs} is multiplied by 2, however, if CBR is smaller than CBR_{target}, then P_{cs} is divided by 1.1.

Algorithm 1 CBR-based Algorithm

```
1: while "Stabilization ON" do
2:    Calculate the current average CBR
3:    Periodically process the following tests :
4:    if CBR > CBR_target then
5:       P_cs = P_cs * 2
6:    end if
7:    if CBR < CBR_target then
8:       P_cs = P_cs/1.1
9:    end if
10: end while
```

CBR_{target} is a fixed interval that was chosen after a number of experiments and observations of the mean channel load while considering different node densities. If $CBR > CBR_{target}$, this means that the channel is congested and the value of the carrier sense threshold needs to be increased. And if $CBR < CBR_{target}$, this means that the channel is not congested and we can slowly decrease the value of the carrier sense threshold to extend the transmission range.

In the next sub-section we briefly recall the delay-based algorithm.

6.5.2 *delay*-based algorithm

This algorithm periodically monitors the channel access delay (*delay*) and updates the carrier sense threshold P_{cs} accordingly. The *delay* is the mean waiting time for a packet to be transmitted after leaving the MAC queue. It is directly affected by channel congestion. As there is an optimal value of *delay* for which the CSMA system operates optimally, we use the measurement of the access delay to adapt the carrier sense threshold accordingly.

If *delay* is greater than $delay_{target}$, the carrier sense threshold P_{cs} is multiplied by 2, however, if *delay* is smaller than $delay_{target}$, the P_{cs} is then divided by 1.1.

Algorithm 2 *delay*-based Algorithm

```
1: while "Stabilization ON" do
2:    Calculate the current average delay
3:    Periodically process the following tests :
4:    if delay > delay_target then
5:       P_cs = P_cs * 2
6:    end if
7:    if delay < delay_target then
8:       P_cs = P_cs/1.1
9:    end if
10: end while
```

$delay_{target}$ is a fixed value that was chosen after several experiments and observations of the mean waiting time for a packet to be transmitted after leaving the MAC queue while considering different node densities. If $delay > delay_{target}$, this means that the channel is congested and the value of the carrier sense threshold needs to be increased.

6.5.3 Simulation results

This section is devoted to simulation results concerning the two above-described adaptive CSMA algorithms. The simulation tool is the ns-3 Network Simulator and the simulation setup follows the ETSI recommendations for congestion control evaluation [75]. The scenario consists of vehicles distributed on a section of a highway 1000 meters long and 18 meters wide. The highway contains three lanes, each 3 meters wide, with traffic moving in both directions.

Communication parameters are listed in Table 6.1.

Table 6.1: non-controlled CSMA System : communication parameters

Parameters	Value
Channel Bandwidth	10 Mhz
Transmission Power	23 dBm
Energy Detection Threshold	-95 dBm
Carrier Sense Threshold	-85 dBm
Propagation Model	Log-distance
CAM generation rate	10 Hz
CAM size	437 Bytes

Simulation time is equal to 50 seconds, and the computation duration varies between 1 and 40 minutes according to the scenario simulated. Node density varies between 66 and 606 nodes according to four scenarios : Sparse, Medium, Dense, and Extreme. The inter-vehicle distance is 100, 45, 20, and 10 meters respectively. See Table 6.2.

Table 6.2: Scenarios density

Scenario	Inter-vehicle distance (m)	Node density (Nodes/Km)
Sparse	100	66
Medium	45	138
Dense	20	303
Extreme	10	606

We consider the inter-vehicle distance as the average distance between each node and its closest neighbor [156]. For instance, for the Sparse scenario, the closest neighbor

for a given node is at a typical distance of 100 meters. For the Medium scenario, the closest neighbor for a given node is at a typical distance of 45 meters, and so on.

We start the evaluation of the non-controlled CSMA system by defining a performance metric, the Packet Delivery Ratio (PDR). PDR refers to the ratio of the number of packets received over the number of packets generated. PDR is measured at individual nodes targeting CAMs transmitted by each neighbor node.

We evaluate the performances of both CBR-based and *delay*-based algorithms a nd compare them to those obtained by the non-controlled CSMA system. We first evaluate the Packet Delivery Ratio (PDR). We highlight that we are focusing on optimizing the PDR between each node and its closest neighbor. We then evaluate the capacity of the algorithms to optimize the PDR even if the initial P_{cs} value has been deliberately configured to be unsuitable for the actual density. We finally compare the performances of the algorithms to each other to determine which of them is the most efficient.

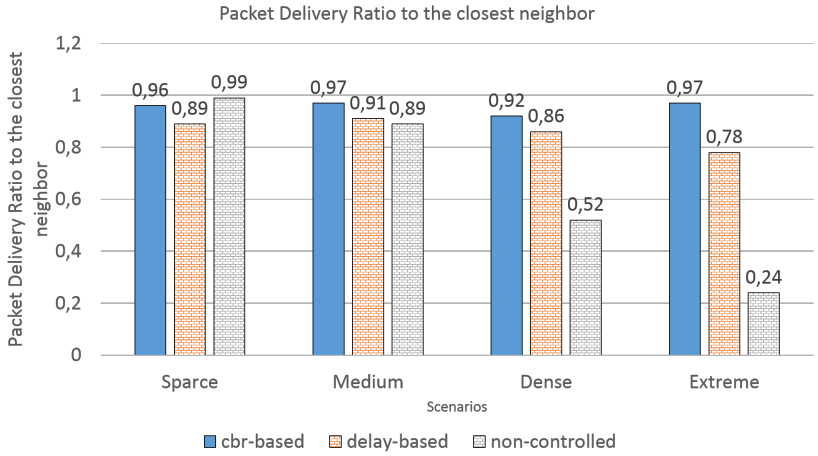

Figure 6.5.1: Packet Delivery Ration, transmission to the closest neighbor.

Figure 6.5.1 plots the average packet delivery ratio (PDR) of both the CBR-based and the *delay*-based algorithms while transmitting to the closest neighbor in different node densities. The comparison also considers the non-controlled CSMA system.

The CBR-based algorithm shows interesting results. For the Sparse scenario, the inter-vehicle distance =100 meters and the PDR = 96% vs. 99% for the non-controlled system. For the Medium scenario, the inter-vehicle distance = 45 meters and the PDR = 97%, vs. 89% for the non-controlled system. For the Dense scenario, the inter-vehicle distance = 20 meters and the PDR = 92%, vs. 52% for the

non-controlled system. And for the Extreme scenario, the inter-vehicle distance = 10 meters and the $PDR = 97\%$, vs. 24% for the non-controlled system.

Like the CRB-based algorithm, the *delay*-based algorithm shows interesting performances if we consider transmission to the closest neighbor. For the Sparse scenario, the $PDR = 89\%$, vs. 99% for the non-controlled system. For the Medium scenario, the $PDR = 91\%$, vs. 89% for the non-controlled system. For the Dense scenario, the $PDR = 86\%$, vs. 52% for the non-controlled system. And for the Extreme scenario, the $PDR = 78\%$, vs. 24% for the non-controlled system.

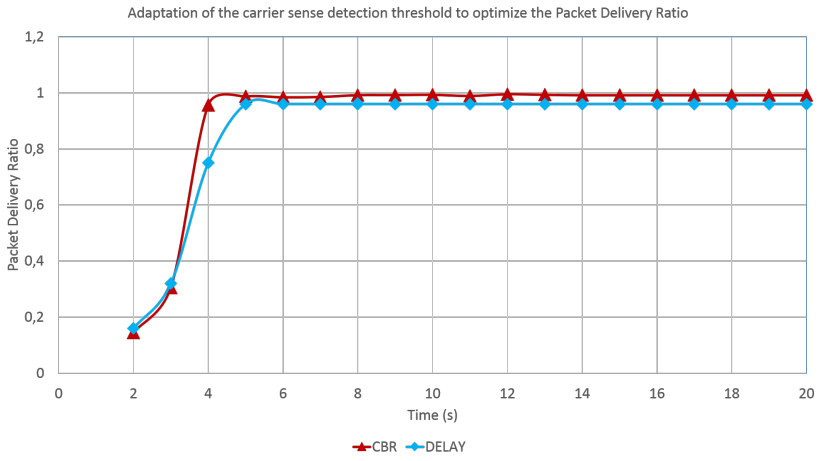

Figure 6.5.2: Adaptation of the carrier sense threshold to optimize the packet delivery ratio : convergence time.

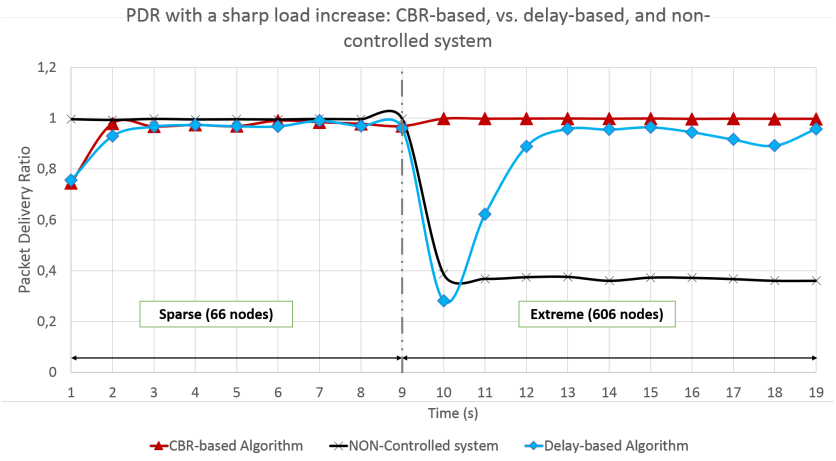

Figure 6.5.3: Adaptation of the carrier sense threshold to optimize the packet delivery ratio. At the beginning of the simulation, node density = 66, then at time $\geqslant$ 10s, node density becomes = 606.

Figure 6.5.2 shows the capacity of the algorithms to adapt their P_{cs} values to the actual density. We deliberately set P_{cs} to a non-optimized value and then observe how both algorithms continually tune their P_{cs} values until reaching an optimal packet delivery ratio. We note that each algorithm updates the P_{cs} every 100ms. We observe that in less than 5 seconds, both algorithms converge in the neighborhood of the optimal PDR value. Once this optimal value has been reached, the PDR remains close to this value for the rest of the simulation.

Figure 6.5.3 shows the ability of the algorithms to handle a sudden increase in load. From time t = 1s to t = 9s, the node density is equivalent to the Sparse scenario. Then, from t = 10s to t = 20s, the node density becomes equivalent to the Extreme scenario.

At the beginning of the simulation (t = 1s), the carrier sense threshold is deliberately set to a non-optimal value. We observe the quick convergence phase from t = 1s to t = 3s, then a stabilization phase from t = 4s to t = 9s. At t = 10s, the node density suddenly increases from 66 to 606 nodes. The impact of this increase is clearly noticeable on the non-controlled system where the PDR drops from almost 99% to less than 40%. The delay-based algorithm is also impacted at t = 10s, but we observe the quick adaptation of the algorithm to the actual density of the network. Surprisingly, the CBR-based algorithm is not at all affected by the load increase event. This is may be due to the fact that the CBR-based algorithm uses a collaborative measurement reference - the channel, while the delay-based algorithm uses a local measurement reference - the local waiting time. Thus, for this evaluation setup, we can conclude that the CBR metric is clearly more accurate than the delay metric.

6.5.4 Feasibility tests

This section is devoted to real experimentation results concerning the CBR-based algorithm. The experiment took place on the Satory test track (Versailles, France). See Figure 6.5.10. We set up two different experimentation scenarios: a line of sight (LOS) experiment with two moving vehicles and stationary ITS-G5 communication modules, and a non-LOS experiment with stationary ITS-G5 communication modules.

6.5.4.1 The line of sight (LOS) experiment : moving through a congested area

The first experiment took place on the Satory speed track, which is separated from regular traffic and used for testing vehicles. The speed track includes a 1-km stretch of direct LOS (see Figure 6.5.10). Two vehicles, each equipped with ITS-G5 communication modules (see Figure 6.5.4), were used for the experiments. 22 additional ITS-G5 communication modules were placed on supports at the end of the track, at a roundabout, to simulate a congested area (see Figure 6.5.8). The vehicles are exchanging CAM messages and moving within direct line of sight (LOS) of each other. We consider the front vehicle as a sender and the rear vehicle as a receiver. The distance between the vehicles is around 80 meters. The speed of the vehicles is around 40 Km/h, which decreases until reaching 15 Km/h when the vehicles get closer to the roundabout. On reaching the congested area, the roundabout, the vehicles turn around and come back to the starting point. The objective of this experiment is to analyze the ability of the *CBR*-based algorithm to optimize the PDR between the sender (the front vehicle) and the receiver (the rear vehicle) while moving through the congested area (see Figure 6.5.9).

Figure 6.5.4: The sender and the receiver vehicles, each equipped with an ITS-G5 communication module.

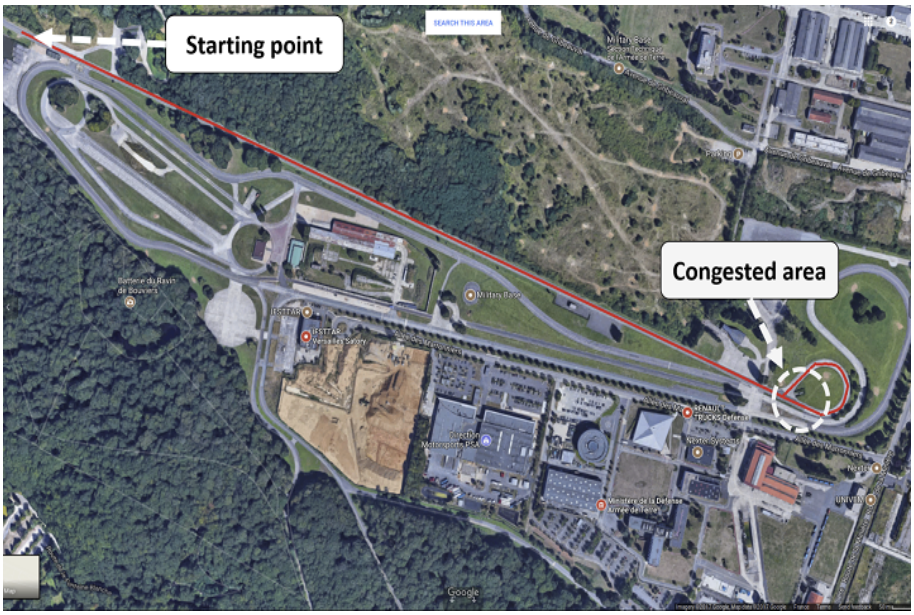

Figure 6.5.5: The line of sight (LOS) experiment. Satory site (Versailles, France)

The ITS-G5 communication modules integrate IEEE 802.11p chipset modules and are manufactured by Autotalks. They also implement the ETSI stack protocol and generate CAM and DENM messages. The ITS-G5 communication modules are remotely managed through a V2X Supervision and Control Interface made by the VEDECOM Institute (see Figures 6.5.6 and 6.5.7). This interface makes it possible to remotely control the CAM size, the transmission power, the carrier sensing, the transmission rate, and the data rate. It also allows the CBR perceived by each node to be displayed in real time.

The communication parameters are listed in Table 6.3.

6.5.4.2 The non-line of sight (non-LOS) experiment : optimizing transmission to the closest neighbor

The second experiment took place on two small tracks of the Satory site; the tracks intersect perpendicularly and have obstacles that prevent LOS communications (see Figure 6.5.10). The communication modules are linearly distributed on supports on the two tracks. The distances between the communication modules are unequal. The objective is to analyze the ability of the CBR-based algorithm to optimize the PDR between each node and its closest neighbor (see Figure 6.5.11).

Figure 6.5.6: Autotalks ITS-G5 communication module.

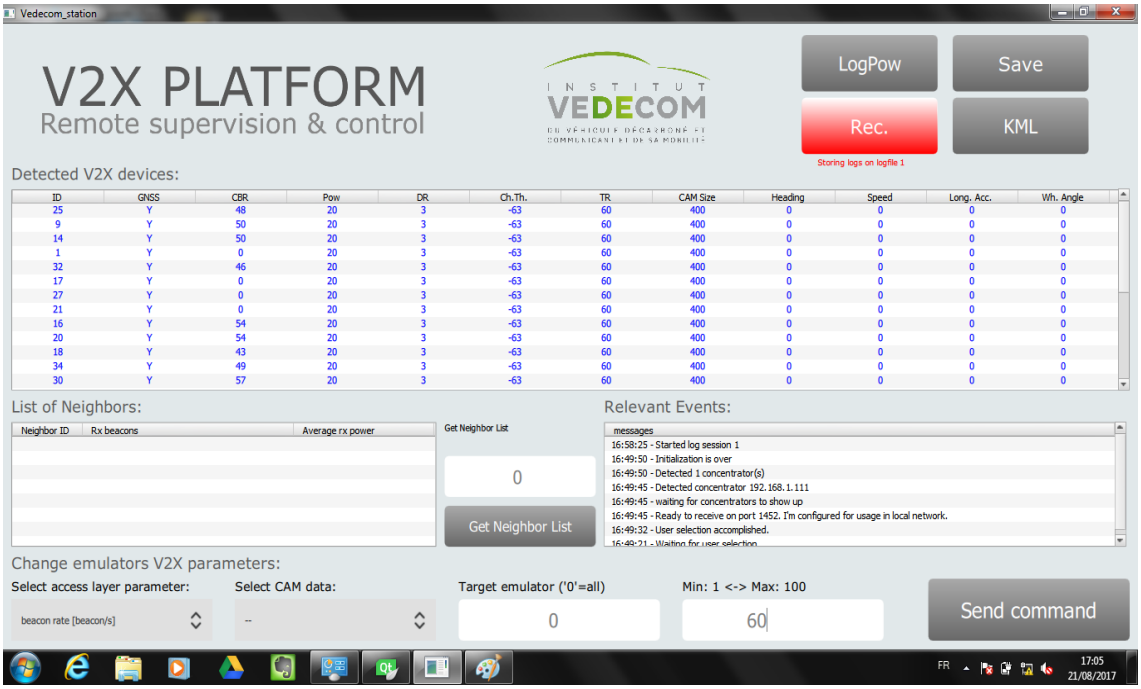

Figure 6.5.7: VEDECOM's V2X Remote Supervision and Control Interface.

Figure 6.5.8: Experiment 1: Line of sight communication, traveling through a congested area. The congested area.

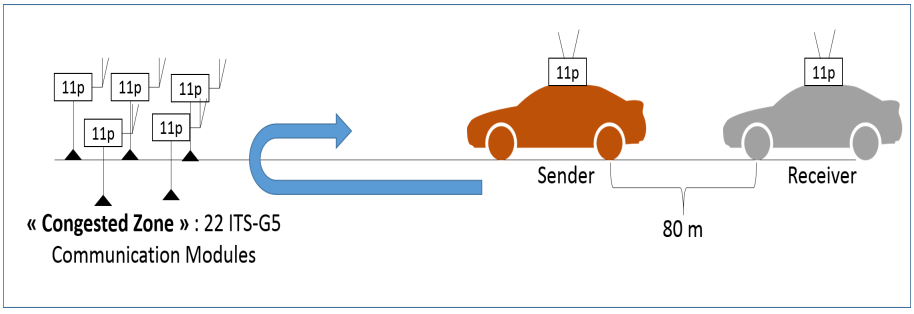

Figure 6.5.9: Experiment 1: traveling through a congested area.

Figure 6.5.10: The non-line of sight (non-LOS) experiment. Satory site (Versailles, France)

Figure 6.5.11: Experiment 2: non-Line of sight communication, optimizing transmission to the closest neighbor.

Table 6.3: Autotalks communication parameters

Parameters	Value
Channel Bandwidth	10 Mhz
Transmission Power	23 dBm
non-controlled system's Carrier Threshold	-95 dBm
Controlled system's Carrier Threshold	-45 to -95 dBm
Propagation Model	Log-distance
CAM generation rate	10 Hz (up tp 50 Hz for the controlled system)
CAM size	400 Bytes

6.5.4.3 Experimental results

Figure 6.5.12 shows the packet delivery ratio (PDR) between the front vehicle (the sender) and the rear vehicle (the receiver). The blue curve refers to the CBR-based algorithm, and the orange curve refers to the non-controlled CSMA/CA system. The point zero of the X axis refers to the congested zone: the roundabout. At the beginning of the experiment, both controlled and non-controlled systems show good performances: almost 100% of the transmitted packets are successfully received by the receiver. The performance of the non-controlled system begins to degrade from the distance -400m. This is due to transmission interferences with the congested area. The closer the vehicles get to the congested area, the more the performances of the non-controlled system continue to degrade until reaching a minimum of 51% of PDR at X = 0. The controlled system, however, gradually adapts the carrier sense threshold according to the channel load. The PDR is therefore slightly degraded at a distance X $\in [-400m, -200m]$, then it reaches a minimum of 90% at distance X = 0. The same behavior is repeated, but in the opposite way, when both vehicles leave the congested area.

Figure 6.5.13 shows the PDR between each node and it closest neighbor. Every 30 seconds we double the number of transmitted CAM messages. During the first 30 seconds, each node transmits 10 CAMs per second. Then, between t=30s and t=59s, the number CAMs increases from 10 to 20. At t=89s, the number of CAMSs becomes 30, and so on until reaching 50 CAMs/s at t=120s. We observe that during the first 30 seconds both systems have the same performance. At t=30s, the number of CAM messages doubles and the performances of the non-controlled system degrade.

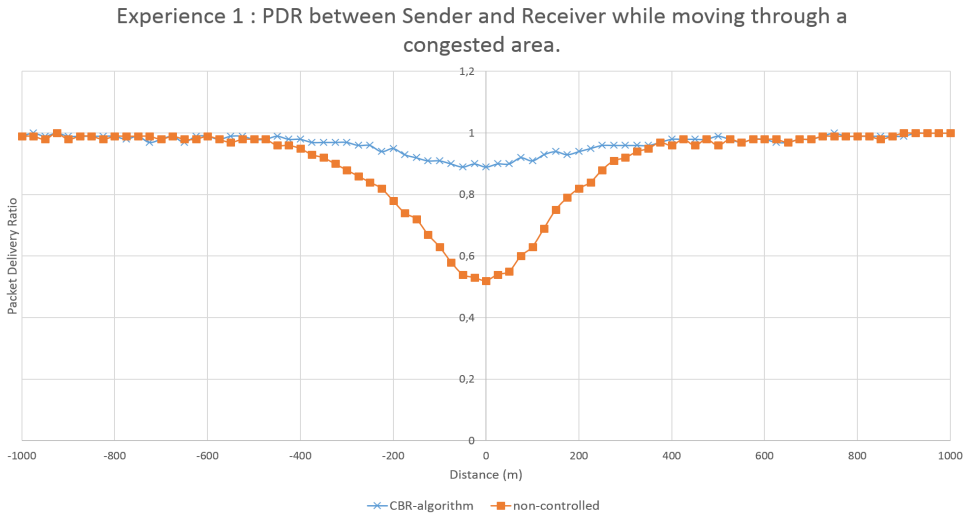

Figure 6.5.12: Results of experiment 1: PDR while moving through a congested area.

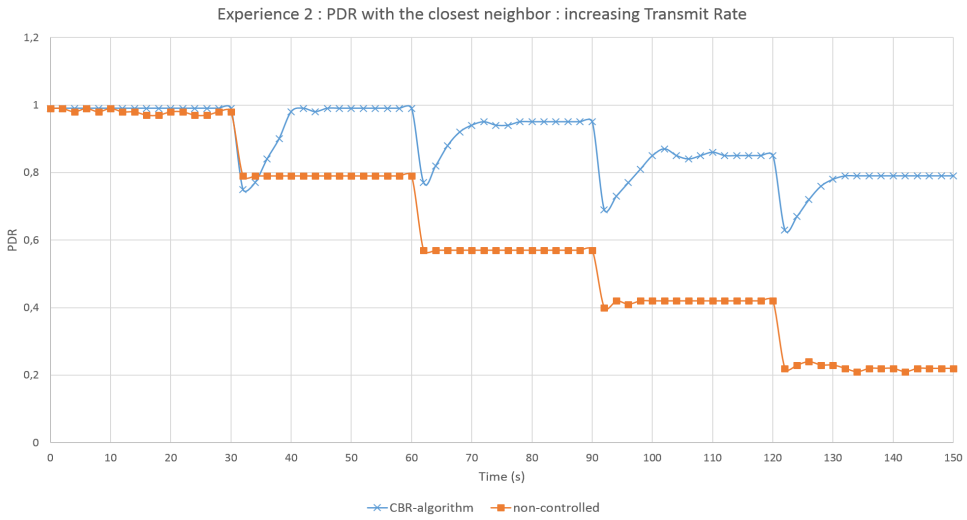

Figure 6.5.13: Results of experiment 2: PDR with transmission to the closest neighbor and load increase every 30 seconds.

The controlled system, however, goes through an adaptation phase and adapts the carrier sense threshold until reaching an optimized PDR close to 100%. The same behavior is repeated each time the number of CAM messages doubles, but with greater degradation each time. However, the performance of the controlled system remains largely superior to the performances of the non-controlled system.

6.6 Conclusion

In this chapter, we present a simple stochastic model for spatial CSMA in homogeneous Poisson Point Processes. We focus on transmissions from nodes to their closest neighbors and we observe that the density of successful transmissions strongly depends on the carrier sense threshold P_{cs} which governs the transmissions in CSMA. The optimal value of P_{cs} is a function of the density of nodes in the network.

We observe that when the network is optimized (for the density of successful transmissions) the value of the optimal value of the transmission probability (denoted by p in our model) does not depend on λ. Moreover p is directly linked to the average access delay D of CSMA. Thus, we can design an adaptive transmission algorithm which updates P_{cs} to reach the optimal value of D: D_{target}. We have verified that this stabilization scheme actually adapts P_{cs} quickly and accurately. We have tested our adaptive algorithm with our analytical model both for 1D and 2D networks. We have successfully studied the influence of the network model parameters and found that a roughly estimating these parameters is enough to obtain a adaptive protocol.

We have also verified that the stabilization proposed scheme adapts P_{cs} quickly and accurately to variations in node density, with more accurate results for the CBR-based algorithm. This is may be due to the fact that the CBR-based algorithm uses a collaborative measurement reference: the channel, whereas the delay-based algorithm uses a local measurement reference: the local mean waiting time for a packet to be transmitted without taking into account the delay in the queue.

The results obtained are very encouraging and prove that the P_{cs} governs the transmissions in CSMA in VANETs. It also proves that dynamically adapting the P_{cs} according to the CBR or the delay, allows us to obtain a high packet delivery ratio when transmitting to the nodes that are most concerned by signaling messages - the closest neighbors.

Finally we have implemented and tested the CBR-based algorithm under real conditions. Two test scenarios were proposed. The results obtained are very encouraging

and prove that the dynamic adaptation of carrier sense threshold allows to optimize the PDR.

Chapter 7

Evaluating the Gain of Directional Antennas in Linear VANETs using Stochastic Geometry

Contents

7.1 Executive summary

In Vehicular Ad Hoc NETworks (VANETs), a very significant part of communication is between one node and its neighbors and simultaneous transmissions or, in

other words spatial reuse, is required to insure good performance. When we consider communication from one node to its neighbors,a key metric is the density of successful simultaneous transmissions. Several studies, such as [152, 157], have shown how this density of transmissions can be improved in Aloha or in CSMA networks. The aim of this chapter is to show that the use of directional antennas can greatly improve the performance of the network in our neighbor-to-neighbor communication model because interference is greatly reduced. The model we build here allows a quantitative study of the performance and the improvement obtained with directional antennas to be achieved. The study of Aloha (slotted and non-slotted) is very easy to accomplish and leads to closed formulas for the density of successful transmissions. The study of CSMA is more complex. We use a Matern selection process to mimic the behavior of CSMA in a random pattern of nodes distributed as a Poisson Point Process (PPP): each node receives a random mark and the nodes that have the smallest mark in their neighborhood are elected for transmission. Previous studies, such as [152], show that in CSMA networks, the density of successful transmissions is greatly influenced by the carrier sense detection threshold, which is one of the main parameters of CSMA. In this study we will assume that the carrier sense detection threshold is optimized to obtain the best performance of the CSMA network and our evaluations are performed under this condition. Our analytical models and our computation show that using directional antennas can lead to an improvement of up to more than 100% in the density of throughput compared to the normal use of unidirectional antennas.

7.2 Introduction

Tools from stochastic geometry, such as Poisson Point Processes (PPPs) are very suitable to capture the spatial effect of new networks in the IoT such as VANETs and WSNs and to provide efficient tools to evaluate the spatial density of given events in the network (e.g successful transmissions). Moreover, they can also model random networks. As shown below, it is easy in PPPs to model the typical neighbors of a given node. Here, we adopt PPPs to model node locations and we denote the node density of our network by λ. We use the density of successful transmissions as the performance metric.

In this chapter we will study two different access techniques : Aloha and CSMA. We also assume random fading which simplifies the computation. Similar evaluations to those presented below are possible with other fading laws but would involve more nu-

merical computations. Spatial Aloha networks are quite easy to model and accurately analyze in PPPs [157] mostly because the pattern of simultaneous transmissions remains a random PPP of intensity λp where p is the transmission rate of Aloha. Thus we easily obtain closed formulas for the density of successful transmissions. The case of non-slotted Aloha is slightly more complex, but if we use the results of [159] we can also obtain closed formulas with slightly different PPPs. Modeling CSMA networks is much more complex. In this paper we use the Matern process to mimic the CSMA selection process in a random PPP. As far as we know, there is no other technique available to directly model CSMA[1]. We combine a classical Signal over Interference and Noise Ratio (SINR) and the selection obtained by the Matern process to analytically compute the density of successful transmissions.

The remainder of this chapter is organized as follows. Section 7.3 briefly reviews related work. Section 7.4 describes the model proposed to study Aloha and CSMA. We optimize the density of successful transmissions versus the transmission probability for Aloha and versus the carrier sense threshold for CSMA. We deal with the case of omni-directional and directional antennas in order to perform the comparison. In Section 7.5 we report the results of our analytical study and compare the results obtained with omni-directional and directional antennas. Finally, Section 7.6 concludes the chapter.

7.3 Related work

In 2000, the pioneering article [160] was the first to provide an in-depth study of the performance of ad hoc networks in terms of total bandwidth, taking into account the inherent spatial effect of these networks. The assumptions were a random network and a simplified model to handle interference. The traffic model was point-point with random source and destination nodes.

In the footsteps of the seminal work by Gupta and Kumar, [161] studies the gain in an ad hoc network when directional antennas are used. The work focuses on 2D networks and shows that the bandwidth gain is $\frac{2\pi}{\alpha}$ with a directional antenna at the transmitter (with an emitting angle α) and $\frac{4\pi^2}{\alpha\beta}$ when we use directional antennas simultaneously in both the receiver and the transmitter with an emitting angle α and a receiving angle β.

[1] Other techniques are based on simulations.

In the domain of VANETs there are apparently no theoretical studies like [160, 161] and our study appears to be one of the first (if not the first) contribution. However, there are numerous papers which study the impact of antenna patterns in VANETs. In 1985, [162] carried out extensive measurements and showed that not only the antenna itself, but more so its position on the car and the existence of sirens and lights on the roof can significantly modify the radiation pattern of the antenna. Using ray tracing simulation, [163] studied the effects of antenna placement on car-to-car communication. The authors found that the received signal power greatly depends on the antenna position and causes huge differences in the received power (up to 30 dB). Using measurements in the 5.9 GHz frequency band, as used by the IEEE 802.11p standard, [164] investigated the effect of panoramic glass roofs on the antenna radiation pattern. The authors noted a significant negative impact due to reflections inside the glass. This causes a considerably reduced forward transmission range.

7.4 System model

We consider a homogeneous Poisson-Point-Process (PPP) Φ extended over a 1D infinite line $\mathcal{S} = \mathbb{R}$. As Vehicular Ad-hoc NETworks (VANETs) are generally linear networks, they are usually modeled by 1D networks. As previously stated, we denote the intensity of the PPP by λ.

We assume that the power of a transmission over a distance r is affected by a power-law decay $1/r^\beta$ where β varies between 2 and 6 depending on the propagation conditions and a random fading F. The power received at distance r from the source node is thus $P = \frac{P_0 F}{l(r)}$ and we set $P_0 = 1$ with $l(r) = r^\beta$. We also adopt a Rayleigh fading i.e., exponentially distributed with parameter μ and thus a mean of $1/\mu$.

We use the well-accepted SIR[2] (Signal-to-Interference-Ratio) with a capture threshold T. In other words, a successful transmission occurs when the ratio of the received signal divided by the interference (i.e., the other concurrent transmissions) will be greater than T.

[2]We omit thermal noise but it could be easily added, as explained below. An even more realistic model than the SIR based on a graded SIR model using Shannon's law is possible in our framework though with an increased computational cost.

7.4.1 Model for directional transmission

As we are dealing with vehicles moving along roads, the vehicular network consists in 1D lines which can be modeled by $\mathbb{R}$. We assume that the vehicles send their packets such as CAMs (Car Awareness Messages) or DENMs (Decentralized Emergency Notification Messages) only in one direction. For instance, on motorways we can assume that the messages are only sent downstream. If we assume that the vehicles follow a one-dimensional Poisson Point Process of rate λ, the consequence of using a directional antenna is that another vehicle will interfere with the current transmission with probability 0.5 and with the same probability the vehicle will not interfere. This is true if we assume here that half of the vehicles are moving in one direction while the other half are moving in the opposite direction. Thus with omni-directional antenna the population of interfering vehicles must be selected by the access scheme in a PPP of rate λ whereas with directional antennas the population of interfering vehicles must be selected in a PPP of rate $\lambda/2$. In these two populations the Aloha protocol uses a random selection to select the transmitters whereas in CSMA the selection relies on the carrier sense threshold and the backoff timers. This will be explained in the following sections.

7.4.2 Slotted and non-slotted Aloha

In Aloha, the MAC scheme consists in a random selection of the transmitting nodes. Each node will transmit its packets with given transmission probability p. The protocol can be slotted if we have given time-slots or non-slotted when we use asynchronous transmissions. We use the results of [157] for slotted Aloha and [159] for non-slotted Aloha.

Proposition 7.4.1 *For slotted Aloha, the density of successful transmissions for omni-directional antennas is:*

$$\lambda p e^{-\frac{2\pi r \lambda p T^{\frac{1}{\beta}}}{\beta \sin\left(\frac{\pi}{\beta}\right)}}$$

and the maximum value of this density is:

$$\frac{\beta \sin(\pi/\beta) e^{-1}}{2\pi r T^{\frac{1}{\beta}}}$$

For directional antennas, the density of successful transmissions is:

$$\lambda p e^{-\frac{\pi r \lambda p T^{\frac{1}{\beta}}}{\beta \sin\left(\frac{\pi}{\beta}\right)}}$$

and the maximum value of this density is:

$$\frac{2\beta \sin(\pi/\beta)e^{-1}}{\pi r T^{\frac{1}{\beta}}}$$

The proof of Proposition 7.4.1 can be found in [157] with the only change being that the computation of the shot-noise is done in $\mathbb{R}$ instead of $\mathbb{R}^2$.

Proposition 7.4.2 *Here to obtain closed formulas, we use a slightly different model, the Poisson Rain model see [159]. This means that at each transmission the positions of the vehicles are re-sampled* [3]*. For non-slotted Aloha, the density of successful transmissions for omni-directional antennas is:*

$$\lambda p e^{-\frac{4\pi r \lambda p T^{\frac{1}{\beta}}}{(\beta+1)\sin\left(\frac{\pi}{\beta}\right)}}$$

and the maximum value of this density is:

$$\frac{(\beta+1)\sin(\pi/\beta)e^{-1}}{4\pi r T^{\frac{1}{\beta}}}$$

For directional antennas, the density of successful transmissions is:

$$\lambda p e^{-\frac{2\pi r \lambda p T^{\frac{1}{\beta}}}{(\beta+1)\sin\left(\frac{\pi}{\beta}\right)}}$$

and the maximum value of this density is:

$$\frac{(\beta+1)\sin(\pi/\beta)e^{-1}}{2\pi r T^{\frac{1}{\beta}}}$$

The proof of Proposition 7.4.1 can be found in [159], again with the only change being that the shot-noise is computed in $\mathbb{R}$ instead of $\mathbb{R}^2$. Moreover to obtain this simple formula for non-slotted Aloha, we have to assume a model of Poisson rain nodes but this model also seems to be accurate in traditional Poisson Point Processes, see [159].

7.4.3 CSMA

We re-use the model introduced in Chapter 5. To mimic the CSMA selection process, we use a Matern selection process. In this scheme each node $X_i \in \Phi$ receives

[3] This model provides very good results even if we assume that the vehicles' positions are not re-affected after each transmission. The advantage of the Poisson Rain model is that it gives closed and compact formulas

a random mark m_i and the process selects the node with the lowest mark in its neighborhood. This neighborhood is defined as follows. We denote by $F_{i,j}$ the fading for a transmission between X_i and X_j and we also introduce the carrier sense threshold P_{cs} of our CSMA protocol. In our definition, the neighborhood of X_i is $\mathcal{V}(X_i) = \{X_j \in X_i \ F_{i,j}/l(|X_i - X_j|) > P_{cs}\}$. A node, say X_i will be selected by the Matern selection process if and only if $\forall X_j \in \mathcal{V}(X_i) \ m_i < m_j$, i.e X_i has the lowest mark m_i in its neighborhood. It is easy to verify that a selection process is well defined by this property.

In CSMA networks, the selection process is actually performed according to the back-off value; this back-off is decremented by the node during idle periods until the transmission of the packet. Thus the node with the lowest back-off time in its neighborhood will be chosen to transmit. The random marks of the Matern selection process, can be interpreted as the back-off times of the waiting nodes. However, in a real CSMA network when a node transmits its packet, the other nodes in its neighborhood have already been eliminated and will no longer be able to eliminate other nodes. This is not the case in the Matern selection process which produces an over-elimination and thus underestimates the density of transmissions. This is illustrated in Figure 7.4.1. Following the Matern selection process, node i has correctly eliminated node k; even so, node k is still able to eliminate node l. In contrast, in a real CSMA system, once node i has eliminated node k, node k will no longer be able to eliminate any other neighbor. We note that in Figure 7.4.1 we have used omni-directional antennas.

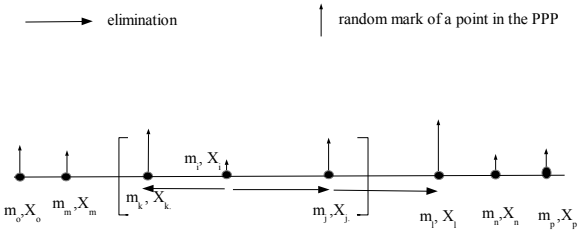

Figure 7.4.1: Matern CSMA selection process and an example of over-elimination.

We note the medium access indicator of node X_i $e_i = \mathbb{1}_{\{(\forall X_j \in \mathcal{V}(X_i) \ \ m_i < m_j\}})$

Proposition 7.4.3 *The mean number of neighbors of a node is:*

$$\mathcal{N} = \lambda \int_{\mathcal{S}} P\{F \geqslant P_{Cs} l(|x|)\} dx.$$

With omni-directional antennas we have :

$$\mathcal{N}_o = \frac{2\lambda\Gamma(1/\beta)}{\beta(P_{cs}\mu)^{1/\beta}}.$$

With directional antennas we have :

$$\mathcal{N}_d = \frac{\lambda\Gamma(1/\beta)}{\beta(P_{cs}\mu)^{1/\beta}}.$$

This result is straightforward. Let F_j^0 be the fading between the transmitting node at the origin X_i and the receiving node X_j. This is just the application of Slivnyak's theorem and Campbell's formula, see [170, 172]

$$\begin{aligned} \mathcal{N}_{\{o,d\}} = & \quad E^0\Big[\sum_{X_j \in \phi} \mathbb{1}_{\{()} F_j^0 l(|X_j - X_i|) \geqslant P_{cs}\Big] \\ = & \quad \lambda_{\{o,d\}} \int_{\mathcal{S}} P\{F \geqslant P_{cs} l(|x|)\} dx \end{aligned}$$

with $\lambda_o = \lambda$ for omni-directional antennas and $\lambda_d = \lambda/2$ for directional antennas. An immediate computation yields the explicit value of $\mathcal{N}_{\{o,d\}}$.

Proposition 7.4.4 *The probability $p_{\{o,d\}}$ that a given node X_0 transmits i.e. $e_0 = 1$ is:*

$$p_{\{o,d\}} = \mathbf{E}^0[e_0] = \frac{1 - e^{-\mathcal{N}_{\{o,d\}}}}{\mathcal{N}_{\{o,d\}}}.$$

Proof: We compute the probability of a given node at the origin with the mark $m = t$ being allowed to transmit. Deconditioning on t provides the result, see [170] for details. $\mathcal{N}$ is either $\mathcal{N}_o$ or $\mathcal{N}_d$ depending on whether we use directional antenna. ■

If p is close to 1, then the carrier sense imposes no restriction on transmission. On the other hand, if p is close to 0, then the carrier imposes a severe restriction on transmission.

Proposition 7.4.5 *The probability that X_0 transmits given that there is another node $X_j \in \Phi$ at distance r is $p_r^{\{o,d\}}$ with*

$$p_r^{\{o,d\}} = p_{\{o,d\}} - e^{-P_{cs}\mu l(r)} \Big(\frac{1 - e^{-\mathcal{N}_{\{o,d\}}}}{{\mathcal{N}_{\{o,d\}}}^2} - \frac{e^{-\mathcal{N}_{\{o,d\}}}}{\mathcal{N}_{\{o,d\}}} \Big)$$

Proof: The proof is the same as that of Proposition 7.4.4. ■

Proposition 7.4.6 *Let us suppose that X_1 and X_2 are two points in Φ such that $|X_1 - X_2| = r$. We suppose that node X_2 is retained by the selection process. The probability of X_1 being of also retained is:*

$$h_{\{o,d\}}(r) = \frac{\frac{2}{b_{\{o,d\}}(r)-\mathcal{N}_{\{o,d\}}}\left(\frac{1-e^{-\mathcal{N}_{\{o,d\}}}}{\mathcal{N}_{\{o,d\}}} - \frac{1-e^{-b_{\{o,d\}}(r)}}{b_{\{o,d\}}(r)}\right)(1-e^{-P_{cs}\mu l(r)})}{\frac{1-e^{-\mathcal{N}_{\{o,d\}}}}{\mathcal{N}_{\{o,d\}}} - e^{-P_{cs}\mu l(r)}\left(\frac{1-e^{-\mathcal{N}_{\{o,d\}}}}{\mathcal{N}^2_{\{o,d\}}} - \frac{e^{-\mathcal{N}_{\{o,d\}}}}{\mathcal{N}_{\{o,d\}}}\right)}$$

with for omni-directional antennas

$$b_o(r) = 2\mathcal{N}_o - \lambda \int_{-\infty}^{\infty} e^{-P_{cs}\mu(l(|x|)+l(|r-x|)}dx.$$

and for directional antennas

$$b_d(r) = 2\mathcal{N}_d - \frac{\lambda}{2} \int_{-\infty}^{\infty} e^{-P_{cs}\mu(l(\tau)+l(|r-\tau|))}d\tau$$

Proof: The proof can be found in [170]. The formula is a simple adaptation of the 2D case to the 1D case and is left to the reader. Careful attention must be paid to distinguish the directional antenna and omni-directional antenna cases. ■

Proposition 7.4.7 *Given the transmission of a packet, we denote by $p_c(r, P_{cs})$ the probability of this packet being successfully received at distance r in a CSMA system (modeled by a Matern selection process with a carrier sense threshold P_{cs}) and with a capture threshold T. We have:*

$$p_c^{\{o,d\}}(r, P_{cs}) \simeq \exp\Big(- \lambda_{\{o,d\}} \int_{-\infty}^{\infty} \frac{h_{\{o,d\}}(\tau)}{1 + \frac{l(|r-\tau|)}{Tl(r)}}d\tau\Big)$$

Proof: Assuming a packet is transmitted, $p_c(r, P_{cs})$ denotes the probability of this packet being successfully received at distance r in a CSMA system using a Matern selection process with a carrier sense threshold P_{cs} and with a capture threshold T. The idea is to consider a transmitter at the origin and to evaluate the probability of successful reception by a receiver located at distance r. We condition the reception of a packet by the presence of another transmitting node at distance τ. According to proposition 7.4.6, the density of such nodes is $\lambda_{\{o,d\}}h_{\{o,d\}}(\tau)$. We obtain the result by integrating on τ. The details of the proof can be found in [170] for 2D networks. The 1D network case is a simple adaptation of the 2D case. ■

It is easy to add thermal noise W to the model. The expression of $p_c(r, P_{cs})$ must then be multiplied by $\mathcal{L}_W(\mu Tl(r))$ where $\mathcal{L}_W(.)$ is the Laplace Transform of the noise.

Proposition 7.4.8 *The spatial density of successful transmissions is thus:*

$$\lambda p^{\{o,d\}} p_c^{\{o,d\}}(r, P_{cs})$$

using o for omni-directional antennas and d for directional antennas.

Proof: Proposition 7.4.8 is just the exploitation of Propositions 7.4.4 and 7.4.7. ■

7.5 Results of the modem and comparison directional / omni-directional antennas

We study the transmissions for pairs of source-neighbor nodes We know that the average distance between one node and its neighbor node is $r = 1/\lambda$, thus we adopt the value of r in the following.

The aim of our adaptive algorithm will be to ensure that P_{cs} is tuned so that the spatial density of successful transmissions as defined in Proposition 7.4.8 is optimized with respect to the spatial density of nodes λ in the Poisson Point Process.

7.5.1 Results with Aloha

In Figure 7.5.1, we present the density of successful transmissions for slotted Aloha with omni directional and directional antennas for different values of p. We use the following parameters $\lambda = 0.1$, $r = 10$ and $\beta = 2$. The gain when we use a directional antenna (rather than an omni-directional antenna) is 2.7 for $p = 0.2$, 7.5 for $p = 0.4$ and up 30 to when $p = 0.6$.

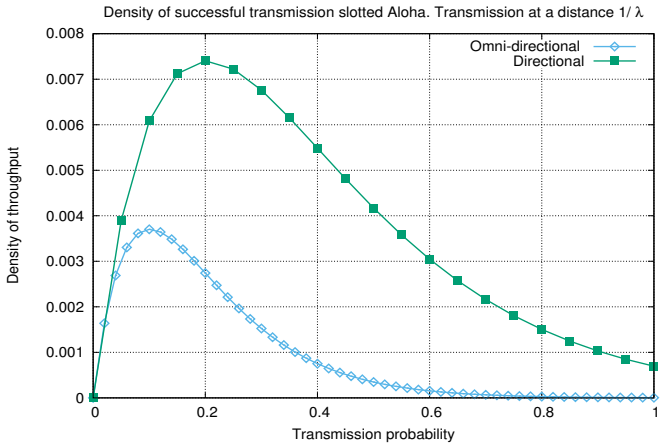

Figure 7.5.1: Density of successful transmissions versus p with $T = 10$, $\beta = 2$ (Slotted Aloha).

In Figure 7.5.2 we present the density of successful transmissions for non-slotted Aloha with omni directional and directional antennas for different values of p and $\lambda = 0.1$, $r = 10$ and $\beta = 2$. We note again a significant gain if directional antennas are used. A comparison of Figure 7.5.1 and Figure 7.5.2 allows us to compare the performances of non-slotted and slotted Aloha. If p is optimized for each scheme, the gain of slotted Aloha over non-slotted Aloha is around 1.35 for directional antennas and omni-directional antennas.

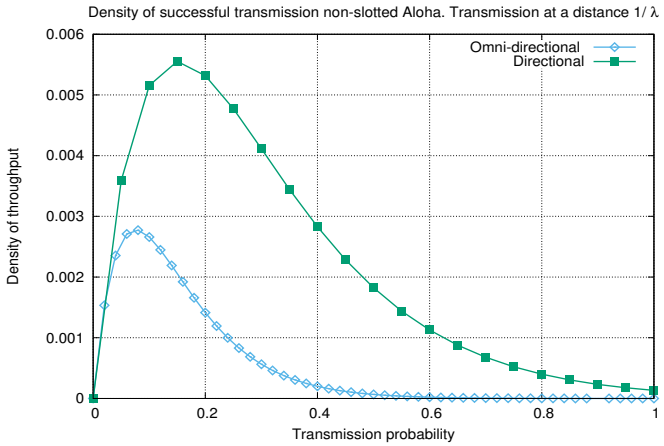

Figure 7.5.2: Density of successful transmission versus p with $T = 10$, $\beta = 2$ (Non-slotted Aloha).

In order to make the best use of our MAC protocols, we optimize Aloha in p with

directional and omni-directional antennas and we present the value of the density of successful transmissions with this optimization. The results of these computations are given in Figure 7.5.3, where we vary the transmission decay β. The gain of the directional antenna over the omni-directional antenna is uniformly equal to 2.

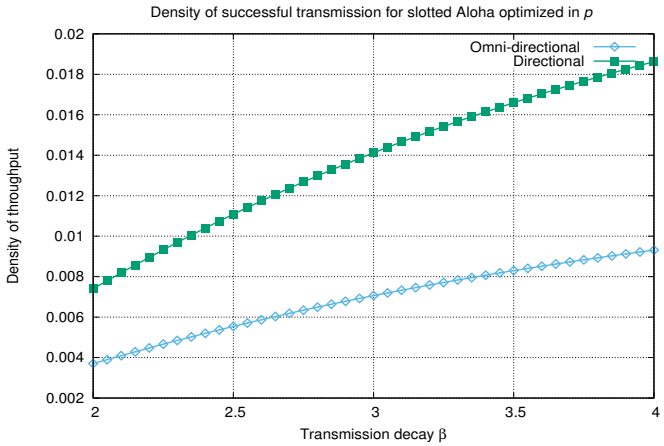

Figure 7.5.3: Density of successful transmissions optimized in p with $T = 10$, $\beta = 2$.

Figure 7.5.4 gives the density of successful transmissions for non-slotted Aloha when we vary the transmission decay β. The gain of the directional antenna over the omni-directional antenna is again uniformly equal to 2.

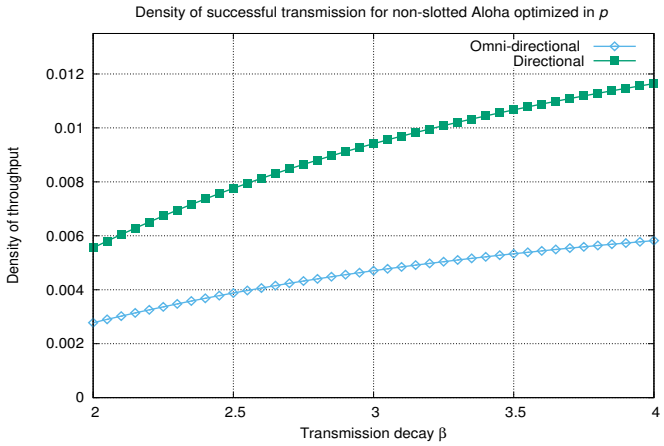

Figure 7.5.4: Density of successful transmissions versus p with $T = 10$, $\beta = 2$ (Non-slotted Aloha).

7.5.2 Results with CSMA

We still use the following parameters $\lambda = 0.1$, $r = 10$ and $\beta = 2$ if not otherwise specified. In Figure 7.5.5 we study the density of successful transmission for CSMA when we use omni-directional and directional antennas. Using directional antennas provides better performance than using omni-directional antennas. For $P_{cs} = 0.002$, the gain obtained when we use directional rather than of omni-directional antennas is 2. For $P_{cs} = 0.0045$ the gain of directional antennas is 1.8.

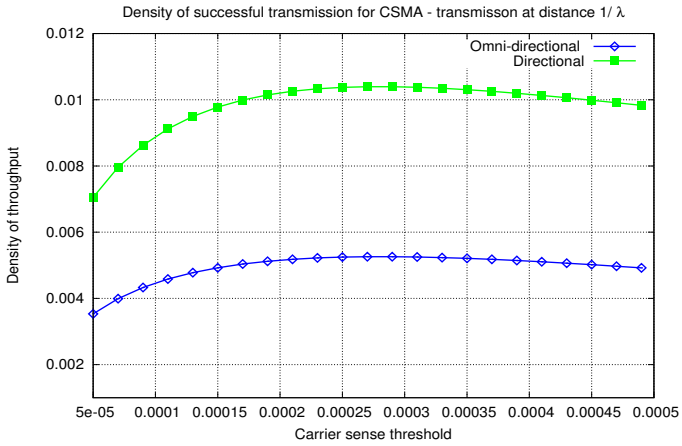

Figure 7.5.5: Density of successful transmissions for different values of P_{cs} for CSMA with omni-directional and directional antennas ($\lambda = 0.1$, $r = 10$, $T = 10$ and $\beta = 2$).

To obtain the best performance we study the optimization of CSMA (with directional and omni-directional antennas) with respect to the carrier sense detection threshold P_{cs}. The result of this study is presented in Figure 7.5.6. The density of successful transmissions is increased by a factor of 1.94 when $\beta = 1.5$ and by a factor of 1.95 when $\beta = 3$.

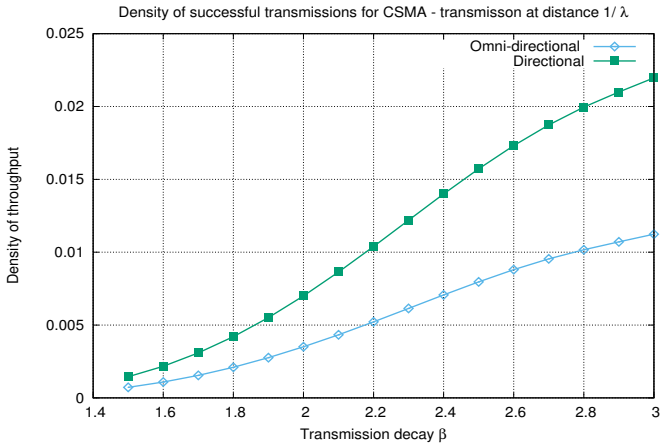

Figure 7.5.6: Density of successful transmissions when the carrier sense detection threshold is optimized versus β ($\lambda = 0.1$, $r = 10$, $T = 10$).

In Figure 7.5.7, we study the density of successful transmission (when CSMA is optimized with respect to P_{cs}) with respect to the capture threshold T. We observe that the gain when we use directional antennas rather than of omni-directional antennas is 2.01 when $T = 1$ and only 1.97 when $T = 10$.

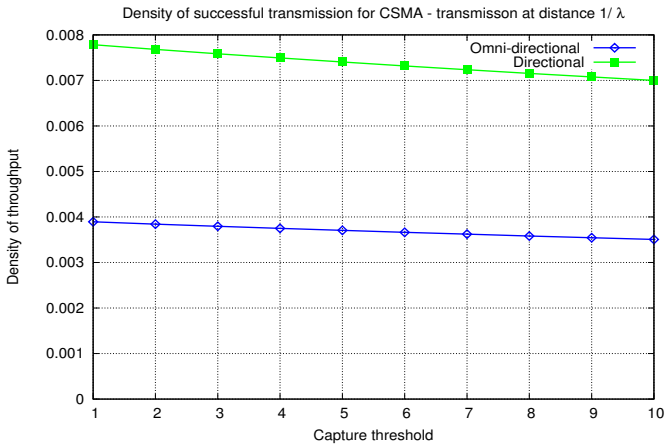

Figure 7.5.7: Density of successful transmissions when the carrier sense detection threshold is optimized versus T. ($\lambda = 0.1$, $r = 10$, $T = 10$ and $\beta = 2$).

7.6 Conclusion

In this chapter, we present a simple stochastic model based on the Signal-to-Interference Ratio (SIR) to evaluate the gain when we use directional antennas instead of omni-directional antennas in a VANET. We assume that the vehicles in our VANET are located according to a homogeneous Poisson Point Process of density λ. The decay of the transmission signal follows a power law and we assume that there is also Rayleigh fading. We compute the density of successful transmissions from a given node to a neighbor node at distance r. In our numerical results, r is chosen to be the average distance from one node to its closest neighbor.

We adopt Aloha (slotted and non-slotted) and CSMA as access schemes. For Aloha we have obtained simple closed formulas. We have also obtained explicit formulas for CSMA but which require more intensive computation. For any given transmission probability p, Aloha with directional antennas has a significantly larger density of successful transmissions than Aloha with omni-directional antennas. When optimized in p, the gain in density of successful transmissions of Aloha when we use directional instead of omni-directional antennas is exactly 2. In CSMA, we also have a gain close to 2.0 whatever are the values of the parameters of the model: β and T. This model can be reused with more complex assumptions: presence of noise, other fading laws, random distance between the transmitter and the receiver, adaptive coding techniques, 2D networks, etc. Our model can be adapted to these new assumptions but this will require more intensive numerical computation.

Chapter 8

Conclusion and Perspectives

Contents

8.1 Synthesis

Improving the safety of roads vehicle users represents the main objective of the design of Vehicular Ad-hoc NETworks (VANETs). Through V2V and V2R communications, VANETs can support a wide range of road safety applications such as cooperative collision warning, emergency braking, cooperative driving, and accident detection. Most of these applications, if not all, require an efficient and reliable broadcast mechanism in order to inform neighboring drivers about a dangerous situation in a timely manner. Medium Access Control (MAC) protocols play a primary role in providing efficient delivery while minimizing data packet loss. However, one of the major challenges of vehicular networks is designing an efficient MAC protocol which can cope with the high speed of the vehicles, the frequent changes in netawork topology, and the lack of an infrastructure. The introductory part of this thesis (Chapter 2) summarizes the general aspect of VANETs and points out the regulation aspect worldwide and different projects targeting this area.

Whereas other studies have chosen to investigate TDMA access, the focus of this thesis is to analyze and improve the current IEEE 802.11p standard which uses a CSMA-based protocol very close to the widespread WiFi access. This thesis studies

two aspects of the IEEE 802.11p. The first aspect delat with in Chapter 4, considers the MAC scheme of IEEE 802.11p, namely the back-off technique and the inter-frame spacing. The second aspect of the IEEE 802.11p is the CSMA behavior with its key tuning parameter: the carrier-sense threshold. This is developed in Chapters 5, 6 and 7.

In a first part of this thesis we have not considered the spatial effect on the performance but we have assumed that all the nodes are within range of each other. With this assumption, we were able to compute the probability of successful transmissions given the size of the collision window. We could derive performance evaluation of the IEEE 802.11p access protocol with respect to various network parameters, such as the mean distance between two vehicles, the number of lanes, etc. We also have studied different variants in the access protocol such as: acknowledgment, acknowledgment with binary exponential, etc., and we have found the best approach to obtain the highest packet delivery ratio. We have shown that the simplest access with no packet acknowledgment is actually the strategy which maximizes the probability of success and thus which is the best for safety issues in VANETs. In fact the use of acknowledgments incurs an overhead which is not counterbalanced by the gain of reliability. The use of binary exponential backoff when the packet is not acknowledged does not improve the performance.

We have then studied the effect of varying inter-frames to obtain different classes of traffic in an IEEE 802.11p access and we have built a Markov model for access with different inter-frame spacings and different collision windows. We have shown that using different inter-frame spacings can be very efficient to maintain a high probability of successful transmissions when two classes of traffic offer an input load that exceeds the channel throughput.

In the second part of this thesis we have adopted a complementary approach to that used in the first part. We consider the global performance of VANETs and thus the spatial density of successful transmissions, which is the key parameter in our VANETs. We have also shown that the important factor is the transmission from nodes to their neighbors. Using this new spatial model with transmissions from nodes to their neighbors, we were able to derive an analytical model to compute the density of successful transmissions with respect to all the important network parameters. The model confirms the conjecture that the carrier sense threshold is a key parameter of

the CSMA access. The model shows that the carrier sense threshold must be tuned according to the network parameters and primarily the density of nodes. The model allows the maximum density of the successful transmissions to be computed and the influence of the other parameters (signal decay, capture threshold, etc.) on this maximum density. We have compared the results of our analytical model with results of simulation and the matching is rather good.

We then studied how the carrier-sense threshold can be automatically tuned according to the density of nodes. We started this study by re-using our CSMA analytical model. We observed (and then proved) that the optimal CSMA transmission probability does not depend on the density of nodes in our VANETs. Thus an algorithm which tunes the carrier threshold to reach this optimal transmission value will be a successful scheme. Since the transmission probability is directly linked to the average delay of a node, we can build your tuning scheme on the average delay to send a packet. Another approach is to adapt the carrier sense threshold so that the Channel Busy Ratio is close to 1. If the Channel Busy Ratio is too large, the carrier sense threshold must be increased otherwise it must be decreased. We have conducted various studies about these stabilization algorithms and the simulations confirm that the two approaches proposed work well to tune the carrier sense threshold. Finally an experimental validation has been set up to test the proposed algorithm under real conditions.

In the last chapter of this thesis, we investigated how using directional antennas can improve the performance in terms of the density of successful transmissions. We adapted and re-used the model developed for the CSMA modeling. We showed that the gain of directional can be very significant, a gain from 50% to 100% can be reached.

8.2 Perspectives

We have studied how the current IEEE 802.11p standard can be used to support safety applications. We have developed several algorithms and estimated their benefit with given assumptions. More general assumptions (other signal decay functions, other fading laws, more advanced reception model [variable rate]) could be handled at the price of more complex formulas. Estimating performance under these new conditions will lead to more intensive computation but it is still within reach.

We can also combine the schemes we have developed (e.g. enhanced back-off technique

and adaptive carrier sense threshold). The performance of such a combination is for sure possible by simulation but building analytical model could be difficult.

Fair comparisons between the optimized IEEE 802.11p we have proposed and other TDMA-based techniques [173–181] should also prove very challenging and interesting. The main difficulty in such a comparison lies in the design of the evaluation scenarios which should represent the most probable situations in vehicular networks.

Chapter 9

Résumé de Thèse

9.1 Introduction générale

L'évolution annuelle des nombres des accidents sur les routes dans le monde entier a motivé le développement de systèmes de transport intelligents (STI) et d'autres applications pour améliorer la sécurité routière et donner aux conducteurs et passagers une sensation de confort. Dans ce contexte, un réseau de communication, appelé Vehicular Ad hoc NETwork (VANET), dans lequel les véhicules sont équipés de dispositifs sans fil a été développé pour rendre possibles ces applications. Actuellement, la technologie Vehicle to Vehicle communication (V2V) est devenue une technologie émergente qui peut réduire le nombre des accidents en permettant à chaque véhicule de fournir en temps réel des avertissements dans le cas de la conduite dangereuse, excès de vitesses ou lorsqu'un événement critique est prévu. L'avertissement dans les réseaux véhiculaires peut être soit par un affichage d'un message sur le tableau de bord, un signal sonore, ou par vibration du siège. Les VANETs connaissent de plus en plus d'intérêt en recherche et dans l'industrie en raison de la grande variété de services qu'ils peuvent fournir. Grâce à des équipements informatiques embarqués, les véhicules peuvent communiquer les uns avec les autres et avec des équipements fixes le long des routes. Les applications des VANETs sont nombreuses notamment la gestion de trafic, l'aide à la conduite, la détection d'embouteillage, la signalisation d'accident ou de congestion de trafic, et, l'obtention d'informations via Internet pendant que les véhicules sont en mouvement. Ces applications peuvent être divisées en trois catégories en fonction de leurs importances: des applications de sécurité, des applications de gestion du trafic et des applications de confort.

Les applications des réseaux VANETs varient considérablement dans leurs exigences de qualité de service. En effet, les applications de sécurité ont des exigences très strictes en termes de délai de transmission et le taux de perte. Par contre, les applications de confort ont des exigences strictes en termes de débit. Par conséquent, un protocole de communication dans ce réseau, doit être en mesure de répondre aux diverses exigences de Qualité de Service (QdS) des différents types de trafic qui circulent dans le réseau. Le protocol Medium Access Control (MAC) joue un rôle important dans la satisfaction de ces exigences. Dans les VANETs, les véhicules partagent un canal de transmission commun en utilisant une même fréquence radio et donc une mauvaise exploitation du canal peut conduire à des collisions et peut engendrer aussi un gaspillage de la bande passante. Un protocol MAC doit être alors conçu pour partager le canal entre les différents nœuds d'une manière efficace et équitable. Toutefois, en raison des caractéristiques particulières des VANETs, les protocoles MAC traditionnels ne sont pas adaptés aux besoins des réseaux VANETs, ce qui conduit soit, à l'adaptation de ces protocoles MAC, soit à la conception de nouveaux mécanismes d'accès optimisés pour les VANETs. Par conséquent, le contrôle d'accès au support de transmission dans le réseau VANET reste un vrai défi lorsque nous cherchons à fournir un service de haute qualité.

Comme les applications de sécurité dans VANETs ont des exigences de QdS strictes, un protocole de contrôle d'accès au support (MAC) qui peut fournir un service de diffusion avec des délais d'accès bornées et un taux de collision minimum est requis. Cependant, de nombreux problèmes se posent en raison de la forte mobilité des véhicules dans VANETs et de la variation de la densité des véhicules (passage à l'échelle) et ceci affecte les performances du standard 802.11p.

9.2 Analyses des Contributions de la thèse

9.2.1 État de l'art : Les réseaux VANET

La recherche dans les réseaux véhiculaires (VANET) a suscité un intérêt croissant au cours des dernières années en raison de sa capacité à améliorer la sécurité routière en utilisant la communication inter-véhicule. Cependant, la mobilité élevée des réseaux VANET provoque des changements fréquents dans la topologie du réseau et entraîne des interruptions fréquentes dans la communication, ce qui présente un vrai défi lors

de la conception de protocoles de communication dans les VANET. Dans ce chapitre, nous nous avons décrit les caractéristiques des VANET et leurs différents types de communications véhiculaires. Nous avons classé les applications de véhicules dans trois catégories principales en fonction de leur amélioration de la sécurité sur la route et de leurs exigences en termes de délai et de débit. De plus, nous avons présenté les différentes normalisations existantes, ainsi que les différents projets et activités de recherche sur les deux plans Européen et international.

9.2.2 État de l'art : La gestion de la congestion

L'un des défis les plus importants auquel fait face aujourd'hui le déploiement des systèmes de transport intelligents est le problème de gestion de congestion du canal radio. Ainsi, nous avons présenté un état de l'art de la gestion de congestion dans les réseaux VANET. Nous avons expliqué les trois principales causes de congestion dans les réseaux CSMA appliqués aux réseaux VANET. Nous avons ensuite présenté une étude par simulation qui montre la corrélation qui existe entre la dégradation des performances de la technologie IEEE 802.11p et l'augmentation de la charge réseau. De plus, nous avons présenté les approches fondamentales de gestion de congestion ainsi que leurs métriques. Nous avons par la suite présenté l'état de l'art des solutions existantes qui sont en cours de standardisation par l'ETSI, ainsi que les éventuelles pistes d'exploration.

9.2.3 Analyse et amélioration de la diffusion dans la norme IEEE 802.11

Nous avons montré que des modèles analytiques simples permettent d'analyser les performances réseau de IEEE 802.11p à analyser. Si nous sommes en mesure d'estimer les paramètres importants d'un VANET: taux de génération de paquets, la longueur des paquets, la distance entre les véhicules, le nombre de voies, la portée des sens des porteurs, nous pouvons facilement évaluer le taux de réussite d'une transmission aléatoire. Nous avons étudié diverses techniques de transmission, à la fois avec et sans retransmission. Nous avons montré que l'utilisation d'accusés de réception entraine un surcout qui dégrade les performances globales du réseau en termes de paquets transmis avec succès alors qu'il améliore le taux de réussite des paquets effectivement transmis. Une solution possible pourrait être d'utiliser le schéma simple sans aucun accusé de réception, mais quelques transmissions aveugles supplémentaires du même

paquet pourraient être effectué lorsque le paquet contient des informations vitales. De cette façon, nous obtiendrions le même gain qu'avec une transmission avec une seule demande d'accusé de réception.

Nous avons ensuite développé un modèle analytique pour étudier l'effet de la variation de l'espacement entre trames les A et la fenêtre de collision W. Nous avons montré que la différenciation des performances obtenues lorsque nous modifions l'espacement entre trames (même pour une faible différence) est très importante et peut donc être utilisée pour protéger le trafic urgent contre des informations moins vitales.

9.2.4 Optimisation de la technique CSMA pour un réseau 1D et 2D

Nous avons présenté un modèle simple de la technique d'accès CSMA et nous avons montré l'importance de l'optimisation de celle-ci en fonction de la densité des noeuds. Nous avons montré que l'optimisation du seuil de détection de porteuse permet d'obtenir une densité de transmissions réussies qui croit linéairement avec la densité des noeuds si nous évaluons la transmission . Nous avons observé que l'utilisation d'un seuil de détection de porteuse constant entraîne une perte très importante dans le débit global du réseau. Cet effet est beaucoup plus pénalisant lorsque la densité des noeuds dans le réseau est sous-estimée que lorsqu'il est surestimée. Les calculs numériques que nous avons réalisés montrent que la meilleure performance du réseau n'est pas atteinte lorsque les transmissions sont presque toujours réussies mais quand il y a un taux de réussite d'environ $0,6$. Nous avons également étudié l'influence de la paramètres du modèle: μ, T et β. Le taux de du fading n'influence pas le performances du réseau s'il est optimisé correctement. Nous montrons que T (le seuil de capture) et β (le taux de décroissance du signal ont un impact plus important sur les réseaux 2D que sur les réseaux 1D. Les résultats de cette étude ont été validés par des résultats de la simulation et nous avons une bonne concordance entre les résultats des deux approches.

Nous étudions aussi le passage à l'échelle du protocole Aloha et nous montrons que si l'on s'intéresse aux transmissions dans son voisinage, le taux de transmission optimal d'Aloha p ne dépend pas de la densité des noeuds dans le réseau. Nous évaluons également le gain obtenu par CSMA sur Aloha. Nous notons que si CSMA est optimisé le gain est important (autour de 100%) mais si CSMA n'est pas optimisé, Aloha peut présenter de meilleures performances.

9.2.5 CSMA dynamique

Nous utilisons ici les modèles développés pour l'optimisation des réseaux CSMA. Nous observons, puis démontrons, que lorsque le réseau est optimisé (pour la densité de transmission réussie), la valeur optimale de la probabilité de transmission (la probabilité moyenne de transmission pour un noeud indiquée par p dans notre modèle) ne dépend pas de la densité des véhicules λ. Par ailleurs, p est directement lié au délai d'accès moyen D de CSMA. Ainsi, nous pouvons concevoir un algorithme de transmission adaptatif qui met à jour P_{cs} pour atteindre la valeur optimale de D: D_{target}. Nous avons testé notre algorithme adaptation du seuil détection de porteuse à la fois pour les réseaux 1D et 2D. Nous avons étudié l'influence des paramètres du modèle (taux de décroissance du signal, taux de capture) et nous avons montré que des erreurs d'appréciation de ces paramètres ne modifiaient pas significativement l'adaptation de l'agorithme en fonction de la densité.

Nous avons ensuite validé par simulation deux versions de l'algorithme : une première version qui se base sur le délai, et une deuxième version qui se base sur le CBR (le taux de congestion du canal). L'algorithme basé sur le CBR à montré des meilleures performances sur tous les scénarios. Cela peut Ã^{a}tre du au fait que l'algorithme basé sur le CBR utilise une métrique globale, alors que l'algorithme basé sur le délai utilise une métrique moins préciseÂ : le délai local.

Nous avons finalement validé le principe de l'algorithme basé sur le CBR par des expérimentations réelles réalisés avec des vrais systèmes embarqués dans des véhicules. Les expérimentations en eux lieux sur les pistes expérimentales de Satory, et les résultats obtenus sont très encourageants.

9.2.6 CSMA et antennes directionnelles

Nous avons utilisé le modè développé au chapitre 5 pour étudier le gain obtenu par l'utilisation d'antennes directionnelles. Nous avons dévelopé des formules closes pour Aloha, Aloha non-slotté et CSMA. Les calculs montrent que ce gain est très significatif et peut varier entre 50% et 100% en fonction des paramètres de propagation et de capture.

9.3 Conclusion et Perspectives

Il serait intérressant de poursuivre les investigations de cette thèse en utilisant d'autres hypothèses: autres types de fading, codage adaptatif, etc. Les outils mathématiques introduits dans cette thèse pourraitent fonctionner au prix de formules plus complexes conduisant à des calculs numériques plus consommateurs en ressource.

Un autre travail plus ambitieux serait de mener une comparaison objective et équitable entre le standard IEEE 802.11p avec les améliorations apportées dans ce travail et les méthodes d'accès de type TDMA. Pour ce faire il convient de mener la difficile tache de construire les éléments de comparaison et les scénarios les plus probable dans un réseau véhiculaire.

Bibliography

[1] Q. Tse, *Improving message reception in vanets*, in International Conference on Mobile Systems, Applications and Services (MobiSys), Krakow, Poland, Jun. 2009.

[2] H. Hartenstein and K. Laberteaux, *A tutorial survey on vehicular ad hoc networks*, IEEE Communications Magazine, vol. 46, no. 6, pp. 164-171, Jun. 2008.

[3] Y. Toor, P. Muhlethaler, and A. Laouiti, *Vehicle ad hoc networks: applications and related technical issues*, Communications Surveys Tutorials, vol. 10, no. 3, pp. 74-88, Third Quarter 2008.

[4] F. Ye, R. Yim, J. Zhang, and S. Roy, *Congestion control to achieve optimal broadcast efciency in vanets*, in IEEE International Conference on Communications (ICC), Cape Town, South Africa, May 2010, pp. 1-5.

[5] H. Moustafa and Y. Zhang, *Vehicular networks: Techniques, Standards, and Applications*, CRC Press, Apr. 2009.

[6] B. Hofmann-Wellenho, H. Lichtenegger and J. Collins, *Global Positioning System: Theory and Practice*, 4th ed., Springer-Verlag, 1997.

[7] E.D. Kaplan, *Understanding GPS: Principles and Applications*, Artech House, 1996.

[8] R. Kumar and M. Dave, *Mobile Agent as an Approach to Improve QoS in Vehicular Ad Hoc Network*, International Journal of Computer Applications, no. 2, pp. 67-72, 2010.

[9] M. Fiore, J. Harri, F. Filali and C. Bonnet, *Vehicular Mobility Simulation for VANETs*, IEEE Annual Simulation Symposium (ANSS), pp. 301-309, Washington, DC, USA, Mar. 2007.

[10] D. Jiang, V. Taliwal, A. Meier, W. Holfelder and R. Herrtwich, *Design of 5.9 GHz DSRC based vehicular safety communication*, IEEE Wireless Communication, vol. 13, no. 5, pp. 36-43, Oct. 2006.

[11] M. Shulman and R. Deering, *Safety Communications in the United States*, Ford Motor Company, General Motors Corporation, United States, no. 07-0010, 2006.

[12] Chai K Toh, *Ad Hoc Mobile Wireless Networks: Protocols and Systems*, Pearson Education, Dec 3, 2001.

[13] The U.S. Department Transportation: *www.its.dot.gov*

[14] Y. Kudoh, *DSRC standards for multiple applications*, 11th world congress on ITS, Nagoya, Japan, Oct. 2009.

[15] K. Bilstrup, *Vehicular communication standards-DSRC, CALM M5, WAVE and 802.11p*, SAFER Seminar, Gothenburg, Sweden, Jan. 2009.

[16] J. Yin, T. Elbatt and S. Habermas, *Performance evaluation of safety applications over DSRC vehicular ad hoc networks*, ACM international workshop on Vehicular ad hoc networks, pp. 1-9, New York, USA, Oct. 2004.

[17] Y. J. Li, *An overview of the DSRC/WAVE technology*, International Conference on Heterogeneous Networking for Quality, Reliability, Security and Robustness in Heterogeneous Networks, Vol. 74, pp. 544-558, Houston, TX, USA, Nov. 2010.

[18] Federal Communications Commission, *FCC 99-305, FCC Report and Order*, FCC 99-305, FCC Report and Order, Oct. 1999.

[19] 802.11p-2010, *IEEE standard for information technology-Telecommunications and information exchange between systems-local and metropolitan area networks-specific requirements part 11: Wireless LAN medium access control (MAC) and physical layer (PHY) and physical layer (PHY) specifications amendment 6: Wireless access in vehicular environments*, 2010.

[20] 802.11-2007, *The institute of electrical and electronics engineers IEEE standard for information technology-telecommunications and information exchange*

between systems-local and metropolitan area networks-specific requirements. Part 11: Wireless LAN medium access and metropolitan area networks-specific requirements part 11: Wireless LAN medium access control (MAC) and and physical layer (PHY) specifications, 2007.

[21] R. Uzcátegui and G. Acosta-Marum, *WAVE: A Tutoriat*, IEEE Communications Magazine, vol. 47, no. 5, pp. 126-133, May. 2009.

[22] IEEE1609.4, *IEEE 1609.4-2006*, Wireless Access in Vehicular Environments (WAVE) Multi-Channel Operation, Draft Standard, 2006.

[23] Q. Chen, D. Jiang and L. Delgrossi, *IEEE 1609.4 DSRC Multi-Channel Operations and Its Implications on Vehicle Safety Communications*, IEEE Vehicular Networking Conference (VNC), pp. 1-8, Tokyo, Japan, Oct. 2009.

[24] Task Group p. IEEE 802.11p, *Wireless Access in Vehicular Environments (WAVE)*, Draft Standard, 2007.

[25] ISO 21217:2010, *Intelligent transport systems - Communications access for land mobiles (CALM) - Architecture*, 2010.

[26] ISO 21215:2010, *Intelligent Transport Systems - Communications access for land mobiles (CALM) - M5*, 2010.

[27] ISO 29281:2011, *Intelligent Transport Systems - Communications access for land mobiles (CALM) - Non-IP networking*, 2011.

[28] The CALM Forum Ltd, *The CALM handbook*, pp. 1-64, 2010.

[29] J. E. Hakegard, B. Holter, I. Tardy and T. Moen, *Assesssment of wireless technologies*, SINTEF, European commission DG Information Society and Media, 2011.

[30] ETSI TC ITS: http://www.etsi.org.

[31] S. Hess, G. Segarra, K. Evensen, A. Festag, T. Weber, S. Cadzow, M. Arndt and A. Wiles, *Towards Standards for Sustainable ITS in Europe*, 16th ITS World Congress and Exhibition, pp. 1-8, Stockholm, Sweden, Sep. 2009.

[32] ISO-21217-CALM-Arch, *Intelligent transport systems - Communications access for land mobiles (CALM) - Architecture*, 16th ITS World Congress and Exhibition, pp. 1-64, Apr. 2010.

[33] ETSI EN 302 665 V1.1.1 (2010-09), *Intelligent Transport Systems (ITS) - Communications Architecture*, Apr. 2010.

[34] COMeSafety Project, "COMeSafety European ITS Communication Architecture", Munchen, Germany, October 2008.

[35] COOPERS project: http://www.coopers-ip.eu.

[36] Geonet project (Geo-addressing and Geo-routing for Vehicular Communications): http://www.geonet-project.eu.

[37] E-safety Vehicle Intrusion Protected Applications (EVITA): http://www.evita-project.org.

[38] T. Leinmuller, L. Buttyan, J. P. Hubaux, F. Kargl, R. Kroh, P. Papadimitratos, M. Raya and E. Schoch, *Sevecom - secure vehicle communication*, IST Mobile Summit, Mykonos, Greece, Jun, 2006.

[39] D. Reichardt, M. Miglietta, L. Moretti, P. Morsink and W. Schulz, *Cartalk 2000: safe and comfortable driving based upon inter-vehicle communication*, IEEE Intelligent Vehicle Symposium, Vol. 2, pp. 545-550, Versailles, France, Jun. 2002.

[40] COMeSAFETY Project (COMmunication for eSafety): http://www.comesafety.org.

[41] Car 2 car communication consortium manifesto, overview of the c2c-cc system (C2CCC): http://www.car-to-car.org/fileadmin/downloads/C2C-CC_manifesto_v1.1.pdf.

[42] ETSI TC ITS: http://www.etsi.org.

[43] SafeSpot (Cooperative vehicles and road infrastructure for road safety): http://www.safespot-eu.org/.

[44] EstiNet Network Simulator and Emulator (NCTUns 5.0): http://nsl.csie.nctu.edu.tw/nctuns.html.

[45] IETF (Internet Engineering Task Force): http://www.ietf.org.

[46] FleetNet-Internet on the road: http://www.et2.tu-harburg.de/fleetnet.

[47] CAR 2 CAR Communication Consortium: http://www.car-to-car.org.

[48] O. Shagdar, *Evaluation of Distributed Congestion Control -Reactive DCC*, Inria, Research Report, Dec. 2014.

[49] M. Sepulcre, J. Mittag, P. Santi, H. Hartenstein, and J. Gozalvez, *Congestion and awareness control in cooperative vehicular systems*, Proceedings of the IEEE, vol. 99, pp. 1260-1279, 2011.

[50] Y. Zang, L. Stibor, X. Cheng, H.-J. Reumerman, A. Paruzel, and A. Barroso, *Congestion control in wireless networks for vehicular safety applications*, Proceedings of the 8th European Wireless Conference, 2007.

[51] M. R. Jabbarpour, R. M. Noor, R. H. Khokhar, and C.-H. Ke, *Cross-layer congestion control model for urban vehicular environments*, Journal of Network and Computer Applications, vol. 44, pp. 1-16, 2014.

[52] M. Y. Darus and K. Abu Bakar, *A review of congestion control algorithm for event-driven safety messages in vehicular networks*, International Journal of Computer Science Issues, vol. 8, pp. 49-53, 2011.

[53] M. S. Bouassida and M. Shawky, *On the congestion control within VANET*, Wireless Days, 2008. WD'08. 1st IFIP, pp. 1-5, 2008.

[54] J. He, H.-H. Chen, T. M. Chen, and W. Cheng, *Adaptive congestion control for DSRC vehicle networks*, IEEE communications letters, vol. 14, pp. 127-129, 2010.

[55] X. Shen, X. Cheng, R. Zhang, B. Jiao, and Y. Yang, Distributed congestion control approaches for the IEEE 802.11 p vehicular networks, IEEE Intelligent Transportation Systems Magazine, vol. 5, pp. 50-61, 2013.

[56] F. Ye, R. Yim, S. Roy, and J. Zhang, Efficiency and reliability of one-hop broadcasting in vehicular ad hoc networks, IEEE Journal on Selected Areas in Communications, vol. 29, pp. 151-160, 2011.

[57] J. He, H.-H. Chen, T. M. Chen, and W. Cheng, Adaptive congestion control for DSRC vehicle networks " IEEE communications letters, vol. 14, pp. 127-129, 2010.

[58] L. Wischhof and H. Rohling, Congestion control in vehicular ad hoc networks, IEEE International Conference on Vehicular Electronics and Safety, pp. 58-63, 2005.

[59] M. Torrent-Moreno, P. Santi, and H. Hartenstein, Fair sharing of bandwidth in VANETs, Proceedings of the 2nd ACM international workshop on Vehicular ad hoc networks, 2005, pp. 49-58

[60] Internet ITS consortium: http://www.internetits.org.

[61] PReVENTive and Active Safety Applications: http://www.prevent-ip.org.

[62] EuroFOT EU project: http://www.eurofot-ip.eu.

[63] PRE-DRIVEC2X EU project: http://www.pre-drive-c2x.eu.

[64] FCC DSRC (Dedicated Short Range Communications): http://wireless.fcc.gov/services/its/dsrc.

[65] ISO (International Standard Organization): http://www.iso.org/iso.

[66] IEEE (Institute of Electrical and Electronics Engineers): http://www.ieee.org/index.html.

[67] S. Zeadally, R. Hunt, Y. Chen, A. Irwin and A. Hassan, *Vehicular Ad Hoc Networks (VANETs): Status, Results, and Challenges*, Telecommunication Systems, Vol. 51, no. 4, pp. 217-241, Aug. 2012.

[68] M. A. Abu-Rgheff, G.M. Abdalla and S. M. Senouci, *SOFTMAC: Space-orthogonal frequency-time medium access control for VANET*, IEEE Global Information Infrastructure Symposium (GIIS), pp. 1-8, Hammamet, Tunisia, Jun. 2009.

[69] Y. C. Yao Ni, Y. Tseng and J. P. Sheu, *The broadcast storm problem in a mobile ad hoc network*, ACM/IEEE international conference on Mobile computing and networking (MOBICOM), pp. 151-162, Seattle, Washington, Aug. 1999.

[70] Z. Wang and M. Hassan, *How much of DSRC is available for non-safety use?*, ACM international workshop on VehiculAr Inter-NETworking, systems, and applications, pp. 23-29, Lake District, United Kingdom, Jun. 2012.

[71] J. Harding, G. R. Powell, R. Yoon, J. Fikentscher, C. Doyl, D. Sade, M. Lukuc, J. Simons and J. Wang, *Vehicle-to-vehicle communications: Readiness of V2V technology for application*, National Highway Traffi Safety Administration, no. DOT HS 812 014, Washington, DC, Aug. 2014.

[72] M. Shulman and R. Deering, *Safety Communications in the United States*, Ford Motor Company, General Motors Corporation, no. 07-0010, United States, 2006.

[73] M. Gramaglia, C. J. Bernardos and M. Calderon, *Seamless internet 3G and opportunistic WLAN vehicular connectivity*, EURASIP Journal on Wireless communications and Networking, Vol. 2011, no.1, pp. 1-20, 2011.

[74] M. Guo, M.H. Ammar and E.W. Zeguran, *V3: a vehicle-to-vehicle live video streaming architecture*, Pervasive Mobile Computing, Vol. 1, no.4, pp. 404-424, 2005.

[75] ETSI TR 101 612, Intelligent Transport Systems (ITS), *Cross Layer DCC Management Entity for operation in the ITS G5A and ITS G5B medium*, Report on Cross layer DCC algorithms and performance evaluation. V1.1.1, 2014-09.

[76] Kenney, J.B., Bansal, G., Rohrs, C.E, *Limeric: a linear message rate control algorithm for vehicular DSRC systems*, The 8th ACM Int. Workshop on Vehicular Inter-networking, VANET. pp. 21-30, 2011.

[77] Jacobson, V., *Congestion Avoidance and Control*, Symposium on Communications Architectures and Protocols, SIGCOMM pp. 314-329, 1988.

[78] ETSI TS 103 175; Intelligent Transport Systems (ITS), *Cross Layer DCC Management Entity for operation in the ITS G5A and ITS G5B medium*, V1.1.1, 2015-06.

[79] R. Stanica, E. Chaput and A. L. Beylot, *Physical Carrier Sensing in Vehicular Ad-Hoc Networks*, IEEE International Conference on Mobile Ad-hoc and Sensor Systems (MASS), pp. 580-589, Valencia, Spain, Oct. 2011.

[80] R. Stanica, E. Chaput and A. L. Beylot, *Local Density Estimation for Contention Window Adaptation in Vehicular Networks*, IEEE International Symposium on Personal, Indoor and Mobile Radio Communications (PIMRC), pp. 730-734, Toronto, Canada, Sep. 2011.

[81] V. Pereira and T. Sousa, *Evolution of Mobile Communications: from 1G to 4G*, Department of Informatics Engineering of the University of Coimbra, Portugal 2004.

[82] J. So and N. Vaidya, *Multi-Channel MAC for Ad Hoc Networks: Handling Multi-Channel Hidden Terminals Using A Single Transceiver*, ACM international symposium on Mobile ad hoc networking and computing (MobiHoc), pp. 222-233, Tokyo, Japan, May. 2004.

[83] R. Lasowski, C. Scheuermann, F. Gschwandtner and C. Linnhoff-Popien, *Evaluation of Adjacent Channel Interference in Single Radio Vehicular Ad-Hoc Networks*, IEEE Consumer Communications and Networking Conference (CCNC), pp. 267-271, Las Vegas, USA, Jan. 2011.

[84] J. Yeh, *Simulation of local computer networks - a case study*, Computer Networks, Vol. 3, no. 6, pp. 401-417, Dec. 1979.

[85] C. K. Park, M. W. Ryu and K. H. Cho, *Survey of MAC Protocols for Vehicular Ad Hoc Networks*, Smart Computing Review, Vol. 12, no. 4, pp. 286-295, Aug. 2012.

[86] J. Kakarla and S. S. Sathya, *A Survey and Qualitative Analysis of Multi-channel MAC Protocols for VANET*, International Journal of Computer Applications, Vol. 38, no. 6, pp. 0975-8887, Jan. 2012.

[87] M. J. Booysena, S. Zeadallyb and G. J. V. Rooyena, *Survey of media access control protocols for vehicular ad hoc networks*, IET Communications, Vol. 5, no. 11, pp. 1619-1631, Jul. 2011.

[88] H. Menouar, F. Filali and M. Lenardi, *A survey and qualitative analysis of MAC protocols for vehicular ad hoc networks*, IEEE Wireless Communications, Vol. 13, no. 5, pp. 30-35, Oct. 2006.

[89] E. Shih, S. H. Cho, N. Ickes, R. Min, A. Sinha, A. Wang and A. Chandrakasan, *Physical layer driven protocol and algorithm design for energy-efficient wireless sensor networks*, ACM Annual International Conference on Mobile Computing and Networking (SIGMOBILE), pp. 272-287, Rome, Italy, Jul. 2001.

[90] F. Borgonovo, A. Capone, M. Cesana and L. Fratta, *RR-ALOHA, a Reliable R-ALOHA broadcast channel for ad-hoc inter-vehicle communication networks*, IEEE IFIP Annual Mediterranean Ad Hoc Networking Workshop (Med-Hoc-Net), Baia Chia, Italy, 2002.

[91] M. A. Abu-Rgheff, G.M. Abdalla and S. M. Senouci, *SOFTMAC: Space-orthogonal frequency-time medium access control for VANET*, IEEE Global Information Infrastructure Symposium (GIIS), pp. 1-8, Hammamet, Tunisia, Jun. 2009.

[92] N. Lu, Y. Ji, F. Liu and X. Wang, *DMMAC : A dedicated multi-channel MAC protocol design for VANET with adaptive broadcasting*, IEEE Wireless Communications and Networking Conference (WCNC), pp. 1-6, Sydney, Australia, Apr. 2010.

[93] F. Borgonovo, A. Capone, M. Cesana and L. Fratta, *RR-ALOHA, a Reliable R-ALOHA broadcast channel for ad-hoc inter-vehicle communication networks*, IEEE IFIP Annual Mediterranean Ad Hoc Networking Workshop (Med-Hoc-Net), Baia Chia, Italy, Apr. 2002.

[94] F. Borgonovo, A. Capone, M. Cesana and L. Fratta, *ADHOC MAC: new MAC architecture for ad hoc networks providing efficient and reliable point-to-point and broadcast services*, Wireless Networks, Vol. 10, no. 4, pp. 359-366, 2004.

[95] W. Zhuang, H. A. Omar and L. Lio, *VeMAC: A novel multichannel MAC protocol for vehicular ad hoc networks*, IEEE Conference on Computer Communications Workshops (INFOCOM WKSHPS), pp. 413-418, Shanghai, China, Aug. 2011.

[96] H. A. Omar, W. Zhuang and L. Li, *Evaluation of VeMAC for V2V and V2R Communications under Unbalanced Vehicle Traffic*, IEEE Vehicular Technology Conference (VTC Fall), pp. 1-5, Québec City, Canada, Sep. 2012.

[97] H. A. Omar, W. Zhuang and L. Li, *VeMAC: A TDMA-Based MAC Protocol for Reliable Broadcast in VANETs*, IEEE Transactions on Mobile Computing, Vol. 12, no. 9, pp. 1724-1736, Sep. 2013.

[98] H. A. Omar, W. Zhuang and L. Lio, *On Multihop Communications For In-Vehicle Internet Access Based On a TDMA MAC Protocol*, IEEE Conference on Computer Communication (INFOCOM), pp. 1770-1778, Toranto, Canada, Apr. 2014.

[99] Y. Weidong, L. Pan, L. Yan, Z. Hongsong, *Adaptive TDMA slot assignment protocol for vehicular ad-hoc networks*, Journal of China Universities of Posts and Telecommunications, Vol. 20, no. 1, pp. 11-18, Feb. 2013.

[100] W. Yang, W. Liu, P. Li and L. Sun, *TDMA-Based Control Channel Access for IEEE 802.11p in VANETs*, International Journal of Distributed Sensor Networks, Vol. 2014, no. 4, pp. 1-9, Aug. 2014.

[101] W. Ke and Y. Weidong and L. Pan and Z. Hongsong, *A Decentralized Adaptive TDMA Scheduling Strategy for VANET*, IEEE Wireless Communications and Networking Conference Workshops (WCNCW), pp. 216-221, Shanghai, China, Apr. 2013.

[102] R. Zou, Z. Liu, L. Zhang and Muhammad Kamil, *A near collision free reservation based MAC protocol for VANETs*, IEEE Wireless Communications and Networking Conference (WCNC), pp. 1538-1543, Istanbul, Turkey, Apr. 2014.

[103] L. Zhang, Z. Liu, R. Zou, J. Guo and Y. Liu *A Scalable CSMA and Self-Organizing TDMA MAC for IEEE 802.11 p/1609.x in VANETs*, Wireless Personal Communications, Vol. 74, no. 4, pp. 1197-1212, Feb. 2014.

[104] D. N. M. Dang, H. N. Dang, V. Nguyen, Z. Htike and C. S. Hong, *HER-MAC: A Hybrid Efficient and Reliable MAC for Vehicular Ad Hoc Networks*, IEEE 28th International Conference on Advanced Information Networking and Applications (AINA), pp. 186-193, Victoria, Canada, May. 2014.

[105] K. Bilstrup, E. Uhlemann, E. G. Strï¿½m and U. Bilstrup, *On the Ability of the 802.11p MAC Method and STDMA to Support Real-Time Vehicle-to-Vehicle Communication*, EURASIP Journal on Wireless Communications and Networking, pp. 1-13, 2009.

[106] H. Yu, Z. He and K. Niu, *STDMA for Vehicle-to-Vehicle Communication in A Highway Scenario*, International Symposium on Microwave, Antenna, Propagation and EMC Technologies for Wireless Communications (MAPE), pp. 133-138, Chengdu, China, Oct. 2013.

[107] *Recommendations ITU-R M.1371-1*, Technical characteristics for universal shipborne automatic identification system using time division multiple access in the VHF maritime mobile band, 2006.

[108] F. Yu and S. Biswas, *A Self Reorganizing MAC Protocol for Inter-vehicle Data Transfer Applications in Vehicular Ad Hoc Networks*, International Conference on Information Technology (ICIT), pp. 110-115, Orissa, Dec. 2007.

[109] T. Wu and S. Biswas, *Reducing Inter-cluster TDMA Interference by Adaptive MAC Allocation in Sensor Network*, IEEE International Symposium on a World of Wireless Mobile and Multimedia Networks (WoW-MoM), pp. 507-511, Taormina, Giardini Naxos, Jun. 2005.

[110] Y. Gùnter, B. Wiegel and H. Grossmann, *Cluster-based medium access scheme for vanets*, IEEE Intelligent Transportation Systems Conference (ITSC), pp. 343-348, Washington, USA, Oct. 2007.

[111] J. So and N. Vaidya, *Multi-channel MAC for ad hoc networks: Handling multi-channel hidden terminals using a single transceiver*, ACM International Symposium on Mobile Ad Hoc Networking and Computing (MobiHoc), pp. 222-233, Tokyo, Japan, May. 2004.

[112] H. Su and X. Zhang, *Clustering-based multichannel MAC protocols for QoS provisionings over vehicular ad hoc networks*, IEEE Transactions on Vehicular Technologyg, Vol. 56, no. 6, pp. 3309-3323, Nov. 2007.

[113] H. Su, X. Zhang and H. H. Chen, *Cluster-based multi-channel communications protocols in vehicle ad hoc networks*, IEEE Journals on Wireless Communications, Vol. 13, no. 5, pp. 44-51, Oct. 2006.

[114] S. Bharati and W. Zhuang, *CAH-MAC: Cooperative ADHOC MAC for Vehicular Networks*, IEEE Journal on Selected Areas in Communications, Vol. 31, no. 9, pp. 470-479, Sept. 2013.

[115] S. Bharati and W. Zhuang, *Performance analysis of cooperative ADHOC MAC for vehicular networks*, IEEE Global Communications Conference (GLOBECOM), pp. 5482-5487, California, USA, Dec. 2012.

[116] T. L. Sheu and Y. H. Lin, *A Cluster-based TDMA System for Inter-Vehicle Communications*, Journal Of Information Science, Vol. 30, no. 1, pp. 213-231, Jan. 2014.

[117] M.S. Almalag, S. Olariu and M.C. Weigle, *TDMA cluster-based MAC for VANETs (TC-MAC)*, International Symposium on a World of Wireless, Mobile and Multimedia Networks (WoWMoM), pp. 1-6, San Francisco, California, USA, Jun. 2012.

[118] L. Miao, F. Ren, C. Lin and A. Luo, *A-ADHOC: An adaptive real-time distributed MAC protocol for Vehicular Ad Hoc Networks*, International Conference on Communications and Networking (ChinaCOM), pp. 1-6, Xi'an, China, Aug. 2009.

[119] R. Ding and Q. A. Zeng, *A clustering-based multi-channel vehicle-to-vehicle (V2V) communication system*, International Conference on Ubiquitous and Future Networks (ICUFN), pp. 83-88, Hong Kong, China, Jun. 2009.

[120] M. S. Almalag and M. C. Weigle, *Using Traffic Flow for Cluster Formation in Vehicular Ad-hoc Networks*, IEEE International Conference on Communications (ICC), pp. 631-636, Denver, Colorado, USA, Oct. 2010.

[121] Y. Günter and H.P. Groβmann and W.H. Khalifa and M. Salah and O.H. Karam, *Simulator for Inter-Vehicle Communication Based on Traffic Modeling*, IEEE Intelligent Vehicles Symposium, pp. 99-104, Parma, Italy, Jun. 2004.

[122] W. Guo and L. Huang and L. Chen and H. Xu and C. Miao, *R-MAC: Risk-Aware Dynamic MAC Protocol for Vehicular Cooperative Collision Avoidance System*, International Journal of Distributed Sensor Networks, Vol. 2013, Apr. 2013.

[123] VanetMobiSim: http://vanet.eurecom.fr/.

[124] *Basic Set of Applications; Part 2: Specification of Cooperative Awareness Basic Service Cooperative Awareness (CAM): ETSI TS 102 637-2 V1.2.1 Intelligent Transport Systems (ITS); Vehicular Communications*, ETSI EN 302 637-2.

[125] *Intelligent Transport Systems (ITS); Vehicular Communications; Basic Set of Applications; Part 3: Specifications of Decentralized Environmental Notification Basic Service*, ETSI EN 302 637-2.

[126] Xu, Changchun and Yang, Zongkai, *Non-saturated Throughput Analysis of IEEE 802.11 Ad Hoc Networks*, IEICE - Trans. Inf. Syst, May 2006, vol = E89-D, pp 1676–1678

[127] Wang, JC-P and Abolhasan, Mehran and Franklin, Daniel R and Safaei, Farzad *Characterising the Behaviour of IEEE 802.11 Broadcast Transmissions in Ad Hoc Wireless LANs*, Communications, 2009. ICC'09. IEEE International Conference on, pp 1–5, 2009.

[128] , G. Bianchi *Performance Analysis of the IEEE 802.11 Distributed Coordination Function*, IEEE Journal of Selected Areas in Communications, vol = 18, N = 3, March 2000, pp 535–547.

[129] Hafeez, Khalid Abdel and Zhao, Lian and Ma, Bobby Ngok-Wah and Mark, Jon W, *Performance Analysis and Enhancement of the DSRC for VANET's Safety Applications*, IEEE T. Vehicular Technology, volume = 62, number =7, pp 3069-3083, 2013

[130] Ghahramani, S.A.A.G. and Hemmatyar, A.M.A., *A new hybrid model for performance evaluation of IEEE 802.11p broadcast mode in vehicular ad hoc networks: A numerical*, Connected Vehicles and Expo (ICCVE), 2013 International Conference on, 2013, pp 719-725

[131] Fred Daneshgaran and Massimiliano Laddomada and Fabio Mesiti and Marina Mondin, *Unsaturated Throughput Analysis of IEEE 802.11 in Presence of Non Ideal Transmission Channel and Capture Effects*, CoRR, volume = abs/0710.5235 ,2007.

[132] Kleinrock, L. and F. Tobagi, *Packet Switching in Radio Channels: Part I — Carrier Sense Multiple-Access Modes and Their Throughput-Delay Characteristics*, IEEE Transactions on Communications, 1975, COM-23, 12, pp 1400-1416, December.

[133] S. Ghez and S. Verdu and S. Schartz, *Stability Properties of Slotted Aloha with Multipacket Reception Capability*, IEEE Trans. Automat. Contr., vol 7, 1988, pp - 640 -648.

[134] Baccelli, F. and Blaszczyszyn, B. and Muhlethaler, P. *An Aloha protocol for multihop mobile wireless networks*, Information Theory, IEEE Transactions on, 2006, vol 52, n 2, pp 421 - 436.

[135] Jacquet, P. and Muhlethaler, P, *Mean number of transmissions with CSMA in a linear network*, 2010 IEEE 72nd Vehicular Technology Conference: VTC2010-Fall. 6-9 September 2010, Ottawa, Canada

[136] Dietrich Stoyan and W. S. Kendall and Joseph Mecke, *Stochastic geometry and its applications. 2nd edition* Wiley, pp 1-436, 1995

[137] Muhlethaler, P. and Najid, Abdellah, *Throughput optimization in multihop CSMA mobile ad hoc networks*, EW 2004. The 5th European Wireless Conference, February 24 - 27. Barcelona.

[138] Busson, A. and Chelius, G , *Point Processes for Interference Modeling in CSMA/CA Ad-Hoc Networks*, Conference: Proceedings of the 6th ACM International Workshop on Performance Evaluation of Wireless Ad Hoc, Sensor, and Ubiquitous Networks, PE-WASUN 2009, October 28-29 2009, Tenerife, Canary Islands, Spain.

[139] F. Baccelli and B. Blaszczyszyn, *Stochastic Geometry and Wireless Networks, Volume II Applications*, NoW Publishers, Foundations and Trends in Networking, pp 1-312 ,volume 4, No 1-2,2009.

[140] Ramachandran, I. and Roy, S., *On the Impact of Clear Channel Assessment on MAC Performance*, GLOBECOM 06. IEEE, 27 Nov -1 Dec 2006, San Francisco, California USA

[141] Ramachandran, I. and Roy, S, *Analysis of throughput and energy efficiency of p-persistent CSMA with imperfect carrier sensing*, GLOBECOM 05. IEEE, 2-4 Dec 2005, St Louis, MO USA

[142] M. Hadded, P. Muhlethaler, A. Laouiti, R. Zagrouba and L. A. Saidane, *Tdma-based mac protocols for vehicular ad hoc networks a survey, qualitative analysis and open research issues*, IEEE Communications Surveys Tutorials, Vol. 17, no. 4, pp. 2461-2492, Jun. 2015.

[143] B. Blaszczyszyn, A. Laouiti, P. Muhlethaler and Y. Toor, *Opportunistic broadcast in VANETs (OB-VAN) using active signaling for relays selection*, IEEE International Conference on ITS Telecommunications (ITST08), pp. 384-389, Oct. 2008.

[144] J. Qian, T. Jing, Y. Huo, Y. Li, W. Zhou and Z. Li, *A next-hop selection scheme providing long path lifetime in VANETs*, IEEE 26th International Symposium on Personal, Indoor and Mobile Radio Communications (PIMRC), pp. 1929-1933, Aug. 2015.

[145] C. E. Perkins and E. M. Royer, *Ad hoc on demand distance vector routing*, Second IEEE Workshop on Mobile Computing Systems and Applications, pp. 90-100, Feb. 1999.

[146] B. Karp and H. Kung, *GPSR: greedy perimeter stateless routing for wireless networks*, in international conferences on Mobile Computing and Networking (MobiCom), Boston, Massachusetts, USA, 2000, pp. 243-254.

[147] F. Karnadi, Z. Mo, and K. chan Lan, *Rapid generation of realistic mobility models for VANET*, in IEEE WCNC, Hong Kong, China, Mar. 2007, pp. 2506-2511.

[148] I. Rhee, A. Warrier, J. Min, and L. Xu, *DRAND: Distributed randomized tdma scheduling for wireless ad hoc networks*, in ACM MobiHo, New York, USA, May 2006, pp. 190-201.

[149] Y. B. Ko and N. H. Vaidya, *Flooding-based geocasting protocols for mobile ad hoc networks*, Mobile Networks and Applications, vol. 7.

[150] SUMO Simulator: http://sumo.sourceforge.net.

[151] M. Lacage and T. R. Henderson, "Yet another network simulator," in *Proceeding from the 2006 Workshop on Ns-2: The IP Network Simulator*, WNS2 '06. New York, NY, USA: ACM, 2006. [Online]. Available: http://doi.acm.org/10.1145/1190455.1190467

[152] Nadjib Achir, Younes Bouchaala, Paul Muhlethaler, and Oyunchimeg Shagdar, *Optimisation of spatial CSMA using a simple stochastic geometry model for 1D and 2D networks*, IWCMC 2016 September 5-9th, 2016, Paphos, Cyprus

[153] Jing Zhu, Benjamin Metzler, Xingang Guo, and York Liu *Adaptive CSMA for Scalable Network Capacity in High-Density WLAN: a Hardware Prototyping Approach* in Proc. of IEEE Infocom 2006, April 23-29 Barcelona Spain.

[154] J. Zhu, X. Guo, L. Lily Yang, W. Steven Conner, *Leveraging spatial reuse in 802.11 mesh networks with enhanced physical carrier sensing, ICC 2004* IEEE International Conference on Communications, vol. 27, no. 1, June 2004 pp. 4004-4011

[155] X. Yang and N. H. Vaidya, *On the Physical Carrier rSense in WirelessAd-hoc Networks*, in Proc. IEEE INFOCOM 2005, March 13 - 15 2005 Miami

[156] P. Muhlethaler, Y. Bouchaala, O. Shagdar, N. Achir, A simple stochastic geometry model to test a simple adaptive CSMA protocol: Application for VANETs,,

The International Conference on Performance Evaluation and Modeling in Wired and Wireless Networks - PEMWN 2016, pp. 1-6, 2016.

[157] Baccelli, F. and Blaszczyszyn, B. and Muhlethaler, P. *An Aloha protocol for multihop mobile wireless networks, IEEE Transactions on Information Theory, Vol 52 No 2, pp. 421-436*

[158] Nadjib Achir, Younes Bouchaala, Paul Muhlethaler, and Oyunchimeg Shagdar , Optimisation of spatial CSMA using a simple stochastic geometry model for 1D and 2D networks IWCMC 2016, September 5-9th, 2016, Paphos, Cyprus

[159] B. Blaszczyszyn and P. Muhlethaler, *Stochastic analysis of non-slotted aloha in wireless ad-hoc networks Proceedings IEEE INFOCOM 2010, March 2010, pp. 1–9*

[160] P. Gupta and P. R. Kumar, "The capacity of wireless networks," IEEE Transactions on Information Theory*, vol. 46, no. 2, pp. 388–404, Mar 2000.*

[161] S. Yi, Y. Pei, and S. Kalyanaraman, "On the capacity improvement of ad hoc wireless networks using directional antennas," in Proceedings of the 4th ACM International Symposium on Mobile Ad Hoc Networking &Amp; Computing*, ser. MobiHoc '03. New York, NY, USA: ACM, 2003, pp. 108–116. [Online]. Available: http://doi.acm.org/10.1145/778415.778429*

[162] R. L. Jesch, "Measured vehicular antenna performance," IEEE Transactions on Vehicular Technology*, vol. 34, no. 2, pp. 97–107, May 1985.*

[163] L. Reichardt, T. Fugen, and T. Zwick, "Influence of antennas placement on car to car communications channel," in 2009 3rd European Conference on Antennas and Propagation*, March 2009, pp. 630–634.*

[164] A. Kwoczek, Z. Raida, J. Lacik, M. Pokorny, J. Puskely, and P. Vagner, "Influence of car panorama glass roofs on car2car communication (poster)," in 2011 IEEE Vehicular Networking Conference (VNC)*, Nov 2011, pp. 246–251.*

[165] S. Ghez, S. Verdu, and S. Schartz, "Stability properties of slotted Aloha with multipacket reception capability," IEEE Trans. Automat. Contr., vol 7*, pp. 640–648, 1988.*

[166] P. Jacquet and P. Muhlethaler, "Mean number of transmissions with csma in a linear network," in 2010 IEEE 72nd Vehicular Technology Conference: VTC2010-Fall*, 6-9 September 2010, Ottawa, Canada 2010.*

[167] P. Muhlethaler and A. Najid, "Throughput optimization in multihop csma mobile ad hoc networks," in EW 2004. The 5th European Wireless Conference*, February 24 - 27. Barcelona 2004.*

[168] D. Stoyan, W. S. Kendall, and J. Mecke, Stochastic geometry and its applications. 2nd edition. *Wiley, 1995.*

[169] A. Busson and G. Chelius, "Point processes for interference modeling in CSMA/CA ad-hoc networks," in Conference: Proceedings of the 6th ACM International Workshop on Performance Evaluation of Wireless Ad Hoc, Sensor, and Ubiquitous Networks, PE-WASUN 2009*, October 28-29 2009, Tenerife, Canary Islands, Spain, 2009.*

[170] F. Baccelli and B. Błaszczyszyn, Stochastic Geometry and Wireless Networks, Volume II — Applications*, ser. Foundations and Trends in Networking. NoW Publishers, 2009, vol. 4, No 1–2.*

[171] P. Muhlethaler, Y. Bouchaala, O. Shagdar, and N. Achir, "A simple stochastic geometry model to test a simple adaptive csma protocol: Application for VANETS," in 2016 International Conference on Performance Evaluation and Modeling in Wired and Wireless Networks (PEMWN)*, Nov 2016, pp. 1–6.*

[172] F. Baccelli and B. Błaszczyszyn, Stochastic Geometry and Wireless Networks, Volume I — Theory*, ser. Foundations and Trends in Networking. NoW Publishers, 2009, vol. 3, No 3–4.*

[173] M. Hadded, P. Muhlethaler, A. Laouiti, R. Zagrouba and L. A. Saidane, Tdma-based mac protocols for vehicular ad hoc networks a survey, qualitative analysis and open research issues*, IEEE Communications Surveys Tutorials, Vol. 17, no. 4, pp. 2461-2492, Jun. 2015.*

[174] M. Hadded, P. Muhlethaler and A. Laouiti, Performance evaluation of a TDMA-based multi-hop communication scheme for reliable delivery of warning messages in vehicular networks*, International Wireless Communications & Mobile Computing Conference (IWCMC 2015), Valence, Espagne, June 2017.*

[175] M. Hadded, P. Muhlethaler, A. Laouiti and L. A. Saidane, TDMA-aware Routing Protocol for Multi-hop Communications in Vehicular Ad Hoc Networks*, IEEE Wireless Communications and Networking Conference WCNC, San Francisco, USA, Mar 2017.*

[176] M. Hadded, A. Laouiti, P. Muhlethaler and L. A. Saidane, An Infrastructure-Free Slot Assignment Algorithm for Reliable Broadcast of Periodic Messages in Vehicular Ad hoc Networks*, Vehicular Technology Conference VTC-Fall, Montreal, Canada, Sep 2016.*

[177] M. Hadded, P. Muhlethaler, A. Laouiti and L. A. Saidane, A Centralized TDMA based Scheduling Algorithm for Real-Time Communications in Vehicular Ad Hoc Networks*, The* 24^{th} *International Conference on Software, Telecommunications and Computer Networks (SoftCOM 2016), Split, Croatia, Sep 2016.*

[178] M. Hadded, P. Muhlethaler, A. Laouiti and L. A. Saidane, A Novel Angle-based Clustering Algorithm for Vehicular Ad Hoc Networks*, Second International Workshop on Vehicular Adhoc Networks for Smart Cities (IWVSC'2016), Kuala Lumpur, Malaysia, August 2016.*

[179] M. Hadded, R. Zagrouba, P. Muhlethaler, A. Laouiti and L. A. Saidane, A Multi-Objectif Genetic Algorithm-Based Adaptive Weighted Clustering Protocol in VANET*, The annual IEEE Congress on Evolutionary Computation (IEEE CEC 2015), pp. 994-1002, Sendai, Japan, May 2015 .*

[180] M. Hadded, P. Muhlethaler, R. Zagrouba, A. Laouiti and L. A. Saidane, Using Road IDs to Enhance Clustering in Vehicular Ad hoc Networks*, International Wireless Communications & Mobile Computing Conference (IWCMC 2015), pp. 285-290, Dubrovnik, Croatia, Aug 2015.*

[181] M. Hadded, R. Zagrouba, A. Laouiti, P. Muhlethaler and L. A. Saidane, An Optimal Strategy for Collision-Free Slot Allocation in Vehicular Ad Hoc NETworks*, Advances in Intelligent Systems and Computing. 306, IWVSC'2014, Kuala Lumpur, Malaysia.*